Generating Recombinant Affinity Reagents by Phage- and Ribosome-Display

BY

MICHAEL KIERNY
B.S., Iowa State University, 2006

THESIS

Submitted as partial fulfillment of the requirements
for the degree of Doctor of Philosophy in
Biological Sciences in the Graduate College of the
University of Illinois at Chicago, 2014

Chicago, Illinois

Defense Committee:

Pete Okkema, Chair
Brian K. Kay, Advisor
Teresa Orenic
Lawrence Miller, Department Of Chemistry
David Eddington, Department of Bioengineering

ACKNOWLEDGEMENTS

I would foremost like to thank Dr. Brian Kay for everything he has done for me. I would not have survived graduate school if not for his motivation, generosity, and incredible patience. Any of future accomplishments in my science career will have been made possible by the time I spent in his lab. I can't begin to think of a way to appropriately thank him. I hope to repay him by making a positive impact in the field and doing great science. I wish him and his family the best.

I would also like to thank Dr. Thomas Cunningham who was a great secondary mentor and friend in the lab. I will never forget our visit to Cambridge, England where we became snow-bound through Christmas.

On that note I want to thank Dr. John McCafferty and his wonderful family for welcoming us into his lab and then his home after we became snow induced refugees in London.

Drs. Andreas Plückthun and Birgit Dreier deserve a nod for teaching me the valuable method of ribosome-display over six weeks at the University of Zurich, which eventually led to an internship at Roche Diagnostics.

I want to thank the other graduate students in my program, especially Dr. Hsiao-Lei Lai and Nicholas Waszczak for being fantastic friends, for helping deal with the stress of a Ph. D program, and for getting me into running for fitness.

ACKNOWLEDGEMENTS (continued)

I really want to acknowledge my good friend and lab mate Dr. Renhua Huang. Our discussions about science, politics, philosophy, fishing, and China, will be greatly missed. I know no other who is devoted to science as much as he is.

Finally I would like to thank my committee for their suggestions, encouragement, and positive influence on my time at UIC. Dr. Peter Okkema was a great chairperson and I thank him for listening to my concerns.

MRK

TABLE OF CONTENTS

TABLE OF CONTENTS (continued)

LIST OF TABLES

LIST OF FIGURES

LIST OF ABBREVIATIONS

CACNA1F	Calcium Channel Voltage-Dependent, L-type, Alpha 1 subunit
Cb	Carbenicillin
CDR	Complementarity Determining Region
cDNA	complementary DNA
cccDNA	closed-circular complementary DNA
Cm	Chloroamphenicol
CNGA3	Cyclic Nucleotide Gated Channel Alpha 3
DNA	Deoxyribonucleic Acid
E. coli	*Escherichia coli*
EDTA	Ethylenediaminetetraacetic acid
ELISA	Enzyme-Linked Immunosorbent Assay
Fab	Antigen binding fragment
Fc	Fragment crystallizable
FDA	Food and Drug Administration
FHA	Fork-Head Associated Domain
FN3	Fibronectin III
FPLC	Fast Protein Liquid Chromatography
GBB5	Guanine Nucleotide-Binding Protein Beta 5
HRP	Horse Radish Peroxidase
IgG	Immunoglobulin G
ITC	Isothermal Titration Calorimetry

IVTT	*In vitro* transcription and translation
Kan	Kanamycin
MBP	Maltose Binding Protein
MS	Mass Spectrometry
NCBI	National Center for Biotechnology Information
PCR	Polymerase Chain Reaction
PD	Phage-display
PExSR	Primer Extension for Selection Recovery
PSA	Prostate Specific Antigen
RD	Ribosome-display
RGS9	Regulator of G-protein Signaling 9
scFv	single-chain Fragment of variable regions
SDS-PAGE	Sodium Dodecyl Sulfate-Polyacrylamide Gel Electrophoresis
SPR	Surface Plasmon Resonance

SUMMARY

Biological recognition molecules have become of increasing importance in the past two decades. The fields of therapeutics, biological identification, and basic biology have seen a demand for new reagents to aide in their advancement. Naturally derived monoclonal antibodies have answered some of these demands. However, the complexity, cost, and time required to generate them, is sometimes prohibitive in their ability to reach the life sciences marketplace where a real impact can be felt. Because of these limitations, we have looked to recombinant techniques. Recombinant reagents can be generated in tubes instead of animals, expressed in large amounts in bacteria, and renewed indefinitely. They can be engineered using various scaffolds to tackle specific problems, include tags and modifications of chemicals, enzymes, or protein, and have their sequences synthesized anywhere in the world. These reagents have their own current limitations in quality and general acceptance within the scientific community. This is slowly changing as chemical drug libraries are becoming exhausted, early diagnosis of disease is crucial for patient health outcomes, and public criticism of animal research is coming to a tipping point.

Many areas in medicine would be better served by early detection. Biomarkers are typically specific proteins or DNA that if detected in a bodily fluid can be indicative of a certain disease state or injury. Discovery of the biomarker is the initial step, followed by constructing a detection assay using antibodies or aptamers to recognize the aforementioned molecules. We have attempted to engineer scFv antibodies to detect

proteins from retinal injury caused by laser exposure. Four putative biomarkers were chosen and antibodies generated against short peptide sequences known to be present in blood serum after injury incursion. One of these antibodies generated by phage-display was able to detect the endogenous protein in retinal lysates of three animals. We attempted to improve the binding affinities through affinity maturation, however we were plagued by technical issues and a propensity to isolate weak binding but high expressing clones. To make the antibody more useful in an alternative approach, we dimerized the recognition epitopes to get an increase in sensitivity due to avidity.

Considering the shortcomings we experienced attempting to increase the utility of recombinant antibodies, we have developed a novel process to obtain high quality reagents in a high throughput manner. This process has combined two protein display technologies in a novel way that allows us to utilize the advantages of both. We first constructed a large library in a format intended for an *in vitro* display technology called ribosome-display. Using this library for the initial selection, we then converted the format to an *E. coli* dependent technology called phage-display in a process we have dubbed, Primer Extension for Selection Recovery or PExSR. Phage-display is both faster and less labor intense; hence the remainder of the selection process was conducted using this technique. In practice, PExSR resulted reagents with equilibrium dissociation constant (K_D) in the picomolar range. These were 100-fold better than we have ever seen in our lab in the past using solely phage-display. The procedure also took about a third of the time.

Multiplexing the method has enhanced the benefits of the technique further where multiple targets can be mixed in the initial selection and separated downstream. This extends the stock of library aliquots and saves tremendous amounts of time. Experiments using three targets simultaneously yielded single-digit nanomolar K_D binders. We anticipate this method to be attractive to industry because the initial libraries are simpler to generate, have very large starting libraries (1x10^13), and quickly result in reagents that have requisite specificity and affinity for various biological applications.

CHAPTER 1

INTRODUCTION

Michael R. Kierny, T. Cunningham, and B. K. Kay

Figures have been published in *Nano Reviews* (2012), doi:10.3402/nano.v3i0.17240

1.1 The scope of recombinant affinity reagents

After the completion of the human genome project in 2001 (1,2), it has become increasingly apparent that the next challenge is the elucidation of the much more complex proteome (3). The immense complexity arises for many reasons such as: 1.) alternative splicing variants of the 20,500 genes (4) in the genome; 2.) the dynamics of post-translational modifications; 3.) degradation products or site-specific cleavage; 4.) tissue and temporally specific expression patterns. Therefore, the thorough study of cells, tissues, and whole organisms will require an equal number of reagents that recognize every variation of protein in many model organisms as well as humans. Further, there will be demand for reagents customized for each investigator's application whether it is tracking locations of proteins, determining expression levels, or inhibiting interactions.

Although there is an incalculable amount of research left to be done, the understanding of the proteome's role in organism development, homeostasis, cell signaling, or response to stress are crucial to advancement in treatments for human ailments like congenital defects, diseases such as cancer or Multiple Sclerosis, infections by bacteria or viruses, and injuries to organs and tissues. Obviously the easing of the effects of illness would greatly improve human quality of life and extend the time humans are healthy and productive.

To generate the large number and diversity of tools to tackle such an endeavor, recombinant affinity reagents, made by biotechnological protein display methods, have

become increasingly popular as alternatives to traditional antibodies made by animal immunizations (5). These reagents can be made cheaply, quickly, and in a high-throughput manner that would be necessary to meet the demand for the myriad of applications and experiments mentioned above (6). With our current technology, these tools are our best route to achieve a full understanding of the workings of a living organism.

1.2 Advantages of recombinant affinity reagents

The term “recombinant affinity reagent” is a broad categorization of a diverse set of protein scaffolds from many different organisms. Some of these reagents are fragments taken from immunoglobulin antibodies that have regions of amino acid diversity which will recognize certain shaped or charged epitopes of antigen proteins with varying degrees of specificity and affinity (**Fig. 1**). Other affinity reagents are derived from proteins that naturally have an unrelated function but have been engineered to behave like antibody fragments. Short regions of diversity can be added, while the remainder, or scaffold, is held constant. These are in contrast to “traditional antibodies” that are generated from the adaptive immune system by eliciting a natural immune response of an animal, usually a mouse or rabbit, and then immortalizing the B-cells in hybridoma technology (7). These immune system derived antibodies have natural limitations on important characteristics such as affinity (8), tissue penetration (9), and the ability to target ubiquitous small post-translational modifications (10) .

Recombinant reagents have many advantages over traditional immunoglobulin antibodies. First, recombinant reagents are generated using *in vitro* techniques or by bacteria, yeast, or bacteriophage and therefore do not require harm to research animals. Second, their sequences can be recovered, cloned, manipulated, and sent physically or electronically throughout the world. Third, because the sequence is preserved, the reagent is essentially immortalized when deposited in GenBank. Traditional antibodies have either a finite amount or source, or require an expensive hybridoma fusion procedure to allow longer term production (7). Fourth, modifications to the reagents can add purification tags, identification epitopes, fusion proteins or enzymes (11), fluorescent molecules (12), nanoparticles (13), or therapeutic agents (14), all site specifically to avoid interference with antigen recognition. Fifth, incorporation of unnatural amino acids expands the set of components available for interaction (15). Fifth, specific scaffolds can be chosen to ensure the best chance for binding to desired regions of the target protein whether it's a concave or convex epitope, a cleft, or a post-translational modification like a phosphorylation (16). Sixth, the DNA can be cloned and the antibody expressed inside cells to perturb protein functions (17,18). Finally, many of the methods used to generate the reagents can be automated with robotics and performed in high-throughput manner.

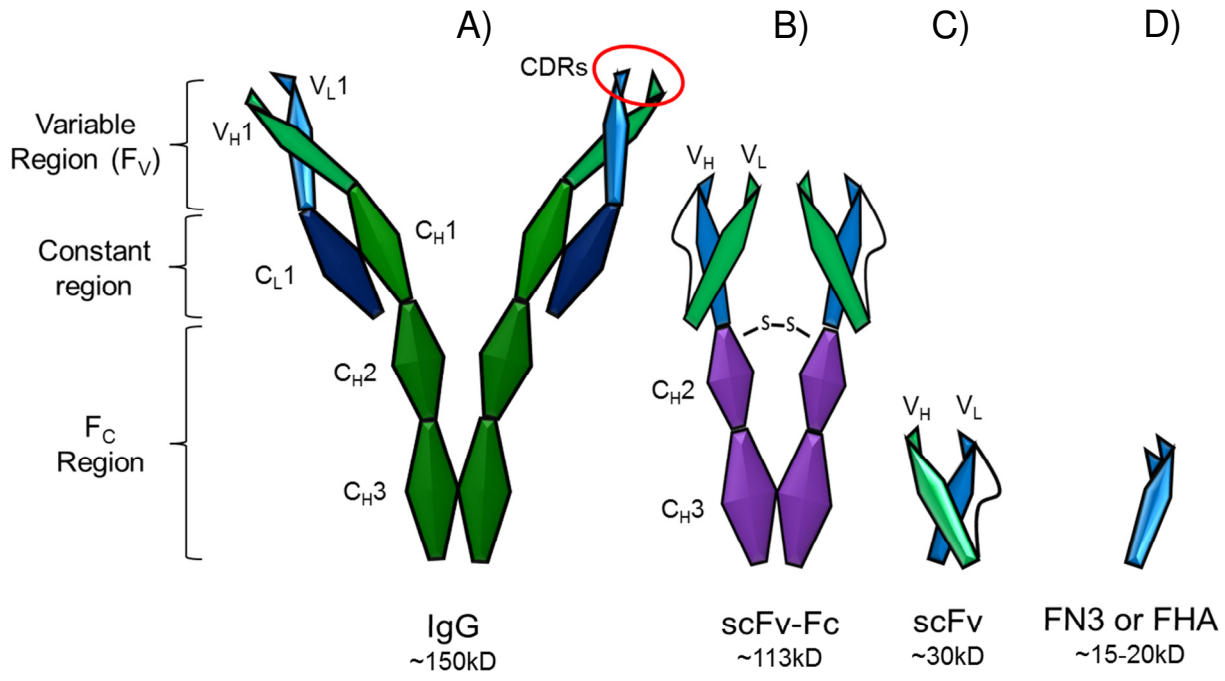

Figure 1. Schematic comparison of antibodies. A general cartoon of natural and engineered antibodies. A) A natural Immunoglobulin G antibody. B) A single-chain Fragment of variation dimerized by a Fragment crystallizable region. C) An engineered single-chain Fragment of variation. D) An engineered scaffold such as a FN3 or FHA.

1.3 Types of affinity reagent scaffolds

There are many different scaffolds originating from various organisms and polypeptides. To mention a few, Camelids are single domain antibodies derived from the immune systems of camels (19), Affibodies originate from the cell wall protein A of *Staphylococcus aureus* (20), DARPins are engineered Ankyrin repeat proteins (21), and anticalins from the family of cup-shaped β-barrel lipocalins (22). Here, I will go further into depth on two that generally recognize most protein epitopes, and one that is

designed to be specific for epitopes containing phosphorylated tyrosine residues. The first is a single-chain fragment of variation (scFv) (**Fig. 1C**) that originates from cloned regions of an immunoglobulin G (IgG) repertoire and is fused together by a linker amino acid chain (*23,24*). The second is an alternative scaffold affinity reagent of the human fibronectin III protein known as the FN3 monobody where the scaffold is held constant but 2-3 loops of 5-10 amino acids each are varied (25). The third is the Fork-head associated domain engineered to recognize motifs containing phosphothreonines (16) (**Fig. 1D**).

1.3.1 Single-chain fragment of variation

Of the most extensively used recombinant affinity reagents is the single-chain fragment of variation or scFv (23,24) (**Fig. 1C, 2A**). This reagent is comprised of two components, the variable light chain (V_L) and the variable heavy (V_H) chain of an immunoglobulin G that are cloned from the germline of B-cells or spleen from animal or human donors and linked together by an engineered Glycine-Serine rich sequence (26). Each chain has three complementarity determining regions (CDRs) to give a total of six variable loops that can interact with a target protein. Their molecular weights are about 30 kDa but because the V_L can be from 16 different subfamilies of the Vκ and $V_λ$, and the V_H from seven families, *E. coli* expression yields can vary widely (27).

ScFvs have been used for a diverse set of targets and applications. For example they have been developed against Hepatitis B virus surface antigens (28), can target and inhibit brain tumor cell proliferation (29), can bind tightly to short peptides (30) and

prions (31), carbohydrates (32), gold (33) and have been generated against neurotransmitter receptors (34). They have been expressed inside frog embryos to inhibit developmental pathways (35), been attached to nickel coated carbon nanotubes to detect the colorectal cancer biomarker Carcinoembryonic Antigen (36), and have been coupled to quantum dots to image a breast cancer tumor in a living mouse (37).

Of the more recent high-profile examples of the utility of scFvs comes from the pharmaceutical industry. Benlysta (Belimumab) is an antibody drug developed for the treatment of Systemic Lupus Erythematosus (SLE). This inhibitor of B-lymphostat stimulator was originally discovered through scFv library selections and affinity maturation where the strongest inhibiting clone was grafted onto a full IgG (38). This was the first treatment for SLE approved by the FDA in over 50 years (39), demonstrating that the new class of monoclonal antibody drugs has the potential to make headway in human disease where chemical drugs have failed.

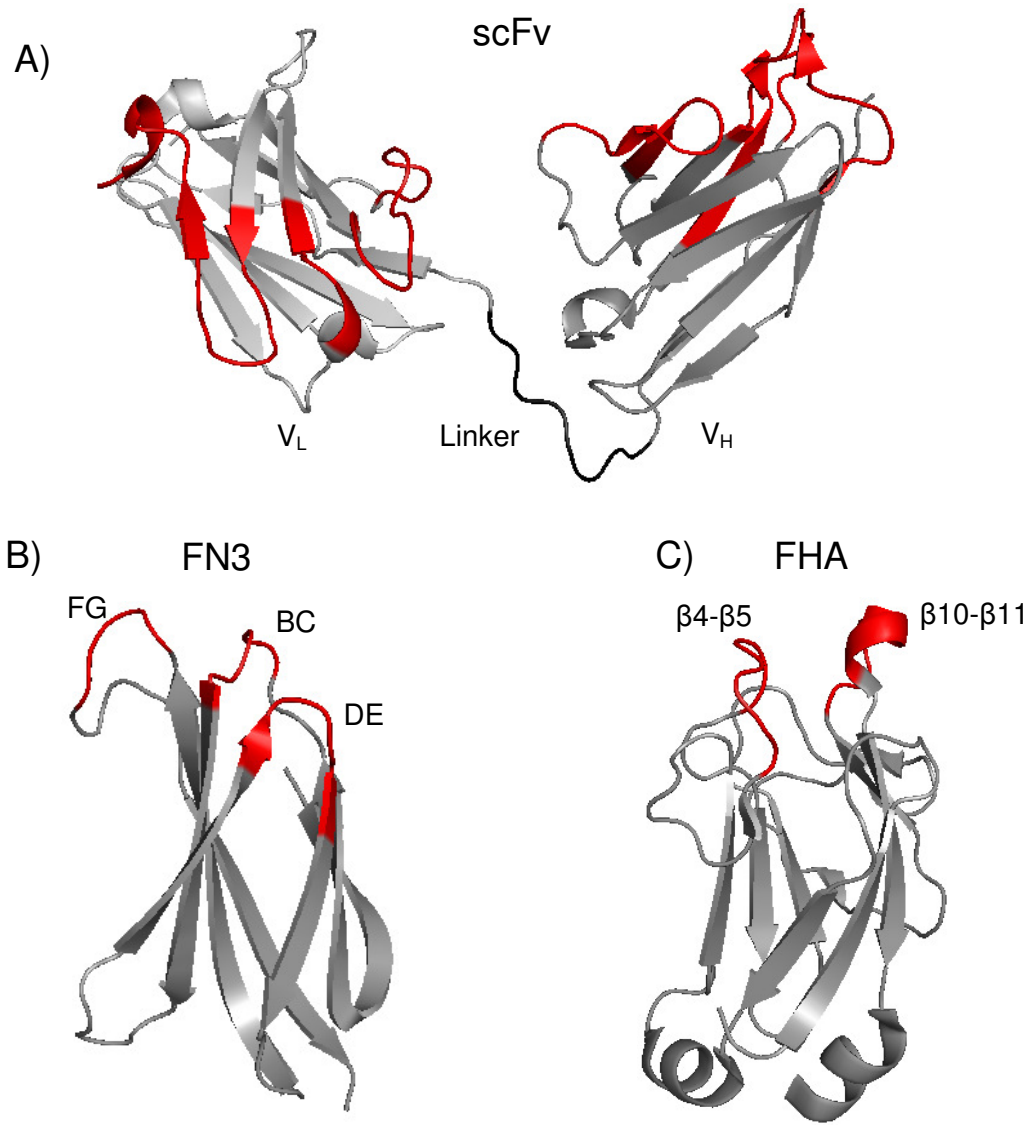

Figure 2. Structures of affinity reagent scaffolds. Three-dimensional reconstructions of x-ray crystallography using PyMol Molecular graphics system. In grey are the scaffold regions. In red are the variable recognition domains. A) Single-chain Fragment of variation (PDB: 1MOE). B) Fibronectin III monobody (PDB: 1FNA). C) Forkhead-Associated domain (PDB: 1G6G). Proteins are not drawn to scale.

1.3.2 Fibronectin type III monobody

One of the more popular alternative scaffold affinity reagents is derived from the tenth domain of the human fibronectin type III, known as the FN3 monobody (40) (**Fig. 2B**). This reagent scaffold is about the size of one of the variable chains of the scFv at about 94 amino acids and contains no disulfide bonds (41). The protein structure contains three loops, the BC, FG, and DE loops, of which can be diversified analogously to the CDRs of antibodies (25). It is normally found in the extracellular matrix and is involved in the interactions between cells (42) and, therefore, has a natural binding surface.

FN3 monobodies have been used against protein targets as common as Maltose Binding Protein (43) and streptavidin (44), but also against clinically relevant targets like Tumor Necrosis Factor-α (45). Interestingly monobodies have been developed as specific inhibitors of protein interaction domains of the Src Homology 2 (SH2) Abl Kinase (46) and the SH3 domain of the Fyn tyrosine kinase (47). They have successfully inhibited the replication of the virus causing severe acute respiratory syndrome (SARS) by binding to the nucleocapsid protein when the monobody is expressed intercellularly (48). FN3 monobodies have also been generated against alternate conformations of the estrogen receptor-α to discriminate between different ligands bound to the ligand binding domain (49).

In the pharmaceutical industry, this scaffold has also gone as far as phase II clinical trials in the development of a Vascular Endothelial Growth Factor Receptor 2

(VEGFR-2) agonist, called Angiosept, or CT-322 (50). The trials for treatment of Glioblastoma Multiforme showed that the monobody could slow down tumor growth by limiting blood flow to the tissue; however, the therapeutic has not yet been approved by the FDA (Clincaltrials.gov).

1.3.3 Forkhead associated domain

A more specialized scaffold has been engineered to recognize domains containing phosphorylations of the amino acid, threonine. The Rad53 protein from *Saccharomyces cerevisiae* has been demonstrated to bind to the region of the Rad9 protein containing a phosphothreonine when regulating the cell cycle (51). The domain associated with this recognition is known as the Forkhead associated domain (FHA) (**Fig. 2C**) which has been identified in many kinases and transcription factors (52). Pershad, Wypisniak, and Kay (16) used directed evolution of the FHA1 domain to become more promiscuous in its recognition but retain the ability to specifically bind regions containing phosphorylated residues. They showed that by varying residues surrounding residues conserved for phospho-recognition, they could select for variants from a large library that bound to phosphopeptides that differed in sequence from the original Rad9 protein, but would not bind the non-phosphorylated version of the peptide. The libraries were generated by randomizing two loops in the protein, the β4-β5 and β10-β11 that had been identified as crucial for FHA1 binding the Rad9 phosphothreonine. Although the binding affinity was relatively modest, FHA domains

from the newly created libraries were selected that bound phosphorylated peptides of the transcription factors MAPK3, MAPK1, JunD and JunB. The reagents were satisfactory for ELISA but had insufficient binding characteristics for more informative assays like cell staining or western blot. There is promise that these limitations will be overcome with reports in the literature of naturally occurring FHAs binding at an equilibrium dissociation constant of 100 nM (53).

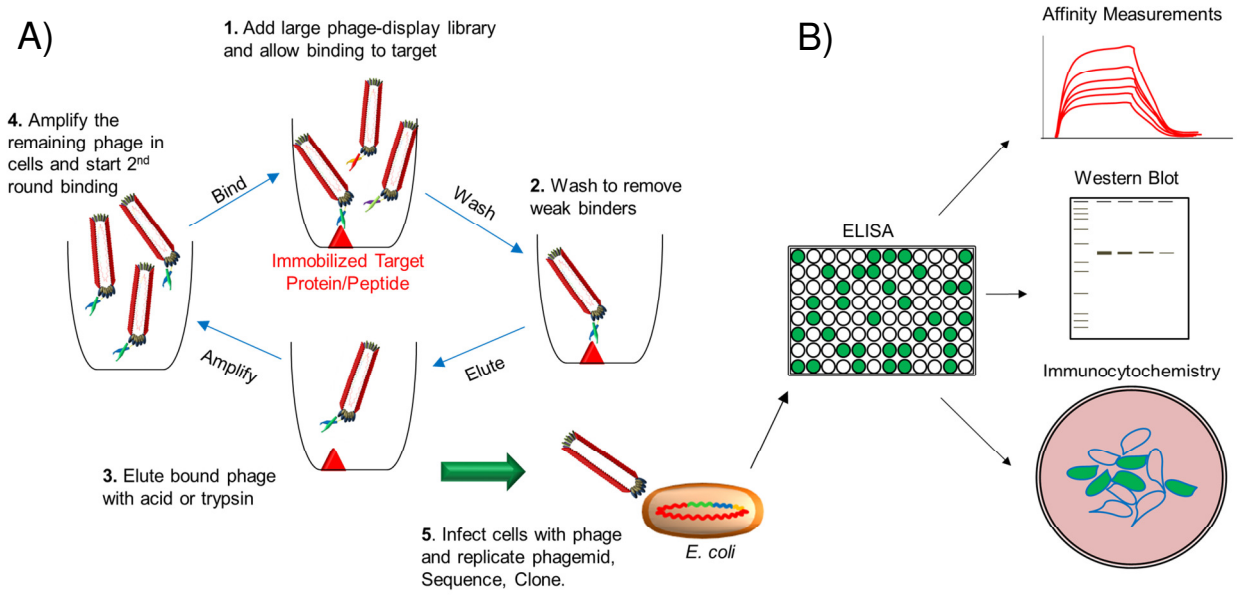

Figure 3. Phage-display selection procedure and binder characterization. A) Selection scheme. 1) A typical phage-display selection starts with a large library of affinity reagent displayed phage particles. These are added to the target in solution or immobilized on a microtiter plate, and allowed to bind. 2) The target is washed to remove any weak binding reagents. 3) The remaining tightly binding reagents are denatured by acid or trypsin and added to *E.coli* cells for infection. 4) The enriched phage are expressed and purified to start a second round where stringencies are

increased. 5) After 3-4 rounds of selection, the remaining phage infect *E. coli* and are plated for isolated colonies. B) Binder characterization. Single colonies are picked for monoclonal phage ELISA to determine specificity. The isolates with the highest absorbance signal over background are cloned into a bacterial expression vector and purified. Characterization of binding affinities by SPR or ITC identifies the most promising candidates. These are then used for biological applications in immunoassays such as western blot and immunocytochemistry.

1.4 Phage-display of affinity reagents

To generate recombinant affinity reagents, a platform for directed evolution is required that in some way links the protein with its cognate nucleic acid sequence. Of the most commonly used technologies to provide a means to preserve sequence data and probe the function of its protein is by displaying it on a M13 filamentous bacteriophage particle (54). In this fashion, libraries containing billions of variations of an affinity reagent class can be exposed to an antigen of interest where through a stringent selection procedure, the reagents with the desired characteristics (affinity, specificity, stability in high or low pH, thermal stability) can be enriched and recovered (55)(**Fig. 3**). The technique is partly conducted *in vivo* within bacterial cells that contain a DNA phagemid encoding for the affinity reagent library in frame with sequence for the pIII minor coat protein of the phage particle, and an M13 origin of replication. Phage production is induced with infection of the *E. coli* by a helper phage that provides the 13 necessary coat proteins (56). As the phage particle is assembled, the pIII coat protein fused to the affinity reagent is incorporated into the phage capsid and monovalently displayed as a functional protein (57). The single-stranded DNA phagemid is

encapsulated thereby linking the genotype with the phenotype (**Fig. 4**). After recovery of the selected binder, the phage can infect TG-1 *E. coli* containing an F^+ pilus and the phagemid isolated for sequencing and cloning (58,59).

This technology was invented by George Smith et. al.(54) in the mid 1980's and was first used for selecting from a library of recombinant antibody fragments by John McCafferty et. al. in 1990 (60). Since then, it has been used to generate untold numbers of reagents. For almost 30 years, libraries of phage have been displaying peptides (61,62), antibody fragments such as Fabs (63) and scFvs (60), other scaffolds like FN3s (25), DARPins (64) and even the immunoglobulins found in nurse sharks (65). It has led to the development of one of the world's best-selling therapeutic, Adalimumab (Humira®), a TNF-alpha antagonist for inflammatory diseases like rheumatoid arthritis or Crohn's disease (66,67). Phage-display has also produced reagents that allow for tumor imaging of breast cancer (68), reagents that can detect biological threat agents like the Botulism toxin (69), and reagents that neutralize pathogenic viruses like the Ebola virus (70). It is clear from these examples that the technology is an extremely powerful tool for protein engineering. Considering all this progress, up until very recently, much of the commercial side of research has been seriously hampered by patent issues and expensive licensing fees. Now that many of the patents covering phage-display and scFvs are expiring or have expired (71), we anticipate an explosion of new commercial recombinant antibodies against a multitude of antigens as companies freely ramp up their production pipelines or start them for the first time.

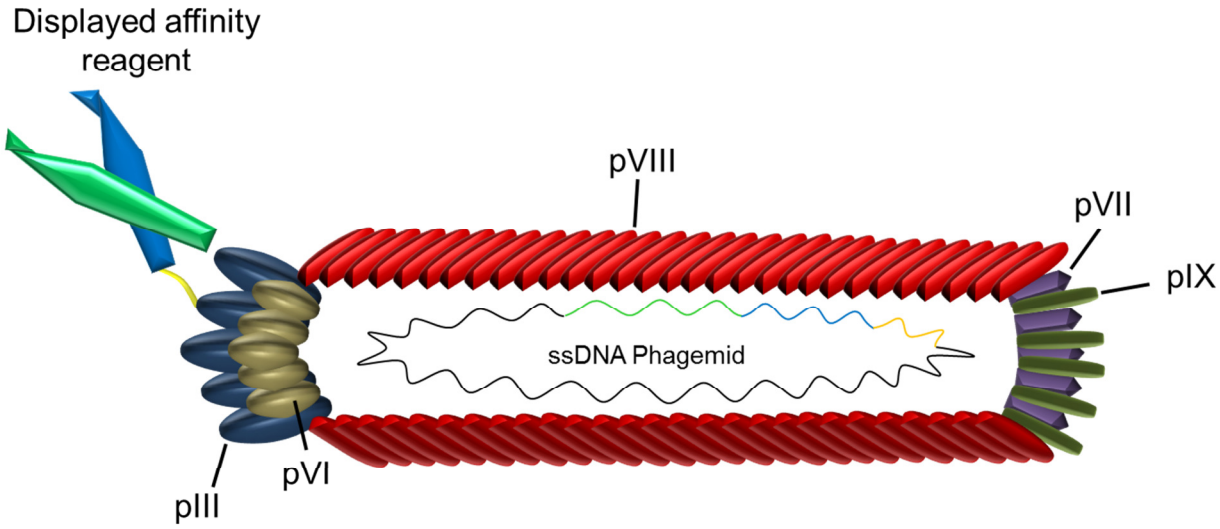

Figure 4. M13 Bacteriophage displaying an affinity reagent. A single M13 phage particle is shown displaying one affinity reagent in fusion to the pIII minor coat protein through a linker (yellow). The genotype of the affinity reagent, linker, and a pIII protein are included in the ssDNA phagemid within the capsid. The coat proteins shown pVI, pVII, pVIII, pIX and the non-fused pIII are provided by a second "Helper" phage.

1.5 Ribosome-display of affinity reagents

Ribosome-display is a completely *in vitro* technology that links the genotype with phenotype through stalled ribosomal translation by forming a complex of the nascent affinity reagent, the ribosome, and the reagent's mRNA (72,73)(**Fig. 5**). One of the key aspects of this display technology is seamless integration of affinity maturation into the selection procedure. Error-prone or mutagenic PCR is applied after each round to further diversify the enriched sequences. This attribute allows "Darwinian evolution" to take place (74).

The ribosome-display library is constructed and stored as plasmid DNA where the template is made by PCR amplification and then transcribed and translated immediately before the presentation to the antigen. The transcript consists of a T7 promoter, a ribosome binding site, a 5' and 3' stem loop to reduce RNase degradation, the open reading frame of the affinity reagent, and a tether allowing the complete protein to exit the ribosomal tunnel, which also lacks a stop codon. The missing stop codon causes the ribosome to stall during translation. With adequate amounts of Mg^{2+} present, the mRNA-Protein-Ribosome will remain stalled in complex while incubated with antigen (**Fig. 6**). After the selection pressure, the mRNA can be recovered with addition of the metal-ion chelator EDTA to release the complex, and subsequent reverse-transcription and PCR of the cDNA. The PCR product is then cloned back into the original vector for further rounds of selection or into a bacterial expression vector for expression and characterization (75).

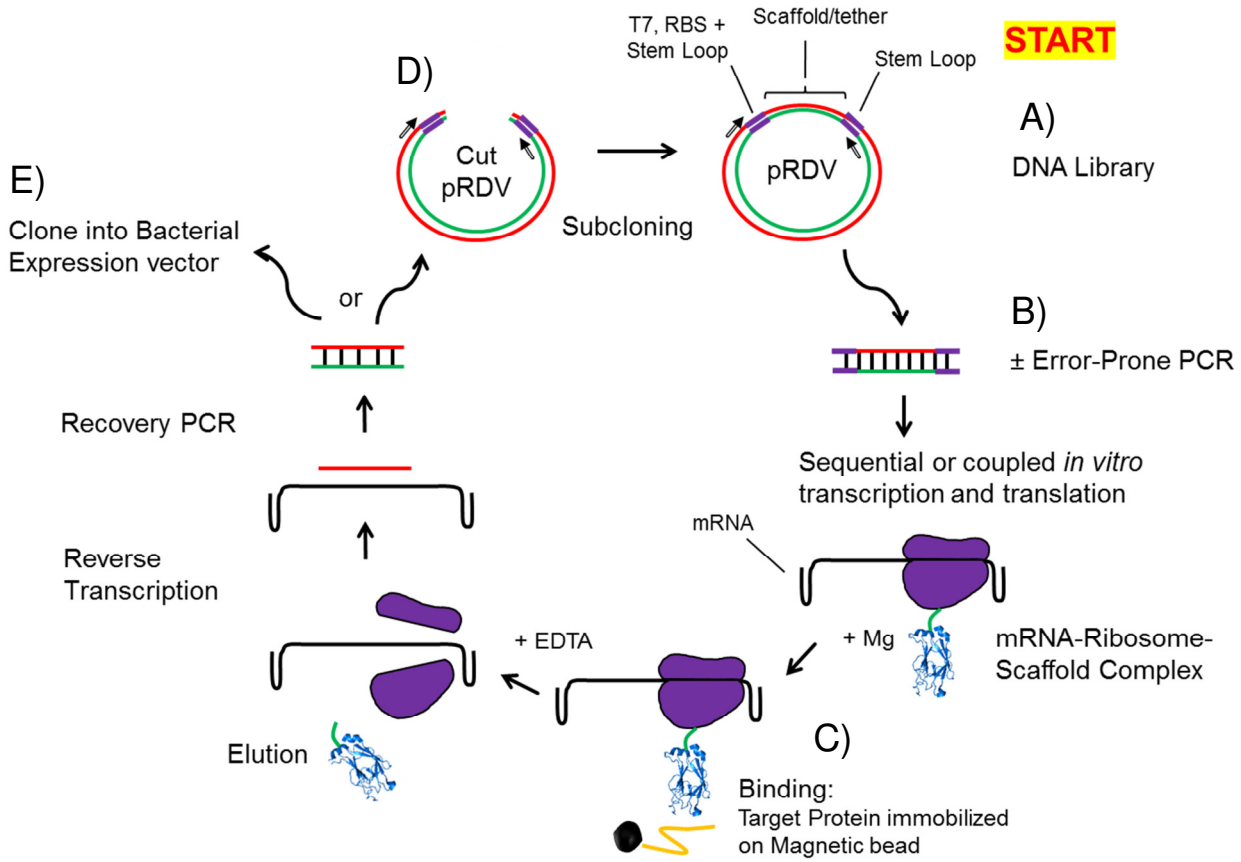

Figure 5. Ribosome-display selection. A) The selection starts with a large DNA library of > 1x10^12 variants in the pRDV plasmid. The template contains a T7 promoter, Ribosome Binding Site, and a 5' stem loop upstream of the scaffold of interest fused to the TolA tether region. Also a 3' stem loop is added during the initial PCR. B) The primary PCR can be used to amplify the library or add diversity through error-prone PCR. The template is then used for *in vitro* transcription followed by translation where the complex is formed. C) The complex is mixed with the target protein and then captured on a magnetic bead. After washing, the complex is eluted by chelation of the Mg^{2+} with EDTA. The mRNA is reverse transcribed and then amplified by PCR using the inside primers. From this point, the selection can continue (D) with subcloning the recovered product into the original pRDV to add the regulation elements back (purple) or the recovered product can be sub-cloned directly into an *E. coli* expression vector for characterization (E). This diagram was adapted from Dreier et. al.(76)

This technology has been instrumental in directed evolution and protein engineering since its conception in the mid 1990's (73,77). Even though one laboratory has dominated this landscape, important discoveries have been made. The *in vitro* nature has allowed studies to be done that have been limited in other systems. One example along these lines is the expression of mammalian receptors that aggregate in every other system except when displayed as a complex with ribosomes. Study of some of these receptors has been impossible up until this discovery (78). Ribosome-display has been used to generate antibodies against prions as a potential diagnostic (31), it has been used to build reagents that helped elucidate the mechanism of dynamic instability of tubulin (79), and it's been used for tumor diagnostics by targeting the Human Epidermal Growth Receptor 2 (HER2) related to breast cancer (80). Finally, a ribosome-display developed DARPin affinity reagent against Vascular Endothelial Growth Factor (VEGF) is showing promise in clinical trials as a treatment of vision loss that is associated with diabetic macular degeneration (81).

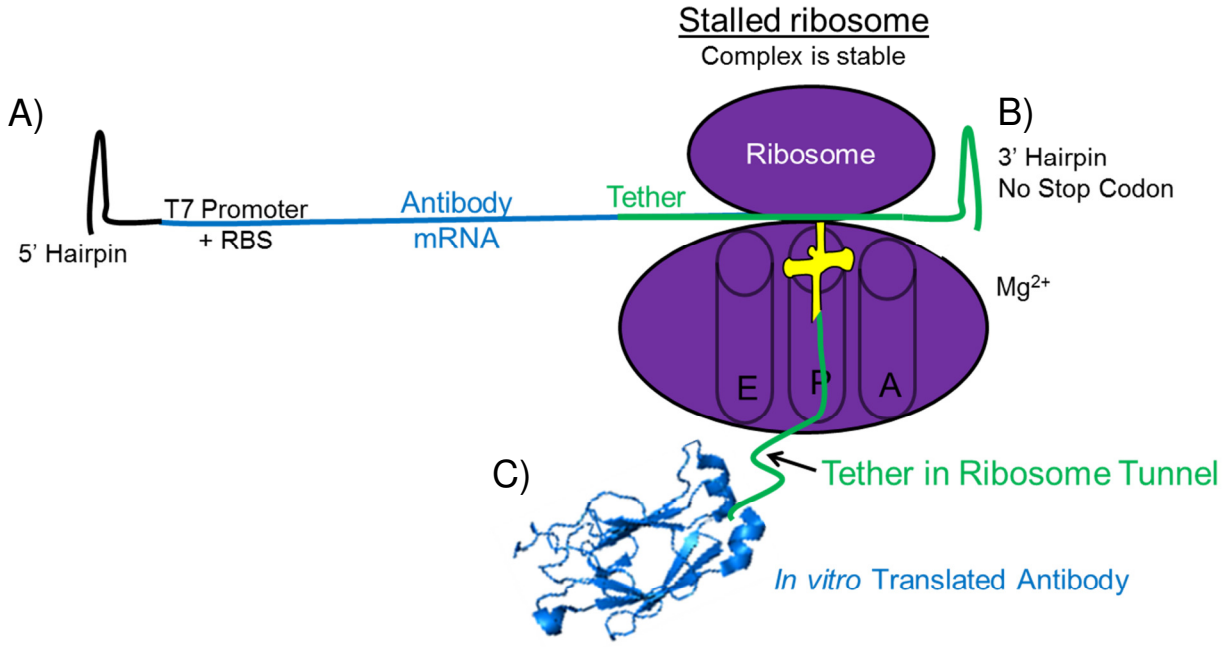

Figure 6. Complex formation of the essential selection unit in ribosome-display. A) The mRNA transcript containing the antibody sequence (blue) and the tether (green) is translated by the ribosome as a single polypeptide until it nears the end of the sequence at which point it stalls when no stop codon is present (B) leaving the A site empty. The fully functional polypeptide (C) has emerged from the ribosomal tunnel via the tether and is covalently linked to the peptidyl-tRNA in the P-site, which in turn is locked into the ribosome. The complex remains tightly packed together in the presence of high concentrations of Mg^{2+}. The 5' and 3' hairpins help to prevent nuclease digestion of the mRNA until it can be recovered through reverse transcription, post-selection.

1.6 Selections and affinity maturation

With our current understanding of biochemistry, we cannot fully predict protein folding or protein interactions (82). Therefore, we cannot design proteins *de novo* to carry out our preferred function. Although advances have been made in computational

biology for the design of binding interfaces (83), we still commonly look to naturally occurring proteins for a starting point in which we can improve with small modifications to functionally important regions. To isolate proteins that have a desired characteristic, libraries of billions of variants are constructed. A selection procedure on this library is performed that applies a pressure, eliminates variants that fail to meet the criteria, and enriches the ones that survive (84). If it is possible to apply a specified selection pressure in the laboratory, the protein can be tailored to meet the requirements of the investigator. Many times the characteristic of interest to select for is specific affinity to a biomolecule.

Primary affinity selections usually start with a library with a large diversity typically around $1x10^{10}$ for phage-display or a $1x10^{12}$ library for ribosome-display (55,73). Displayed variants, at 10 to100-fold of the diversity of the library (amplified by phage expression or PCR respectively) are then applied to a Biotinylated target in solution or immobilized on a surface (85). Adding excess library ensures that each member of the library will be represented 1 to 10 times in the first round. After allowing sufficient time for binding, the weaker binders are removed through a series of washes with buffer containing detergent. The remaining binders are eluted from their targets, recovered, and amplified in preparation for additional rounds. The second and third rounds include increased stringencies through more washing steps, reduction in target concentrations, or competition with excess free target. Besides selecting for affinity, one could also use these techniques to select for thermal stable clones by gradually increasing temperature during target incubations throughout each round (86) or for

generating an intermolecular disulfide dependent protein void of disulfide bonds by increasing reducing agent in each round (74).

Affinity maturation is the process by which a set of candidate reagents, recovered after the above primary selection, are enhanced in a secondary selection to bind at a greater affinity (87,88). This is accomplished with introducing additional variation, usually provided by error-prone PCR (89), generation of a large secondary library, and finally a competition selection with a large excess of non-biotinylated target, to favor those with longer off-rates. This can be repeated for as many cycles as desired until the binding characteristics are satisfactory. The secondary library random mutagenesis and selections make it possible to survey effectively a much larger number of potential binders than would ever be feasible to intelligently construct in a single library. If cell transformation were not an issue, we could likely still randomize only 12 residues assuming we wanted get every combination possible. If we wanted a library with 20 randomized residues including every combination of the 20 amino acids, the amount of protein required would be greater than the mass of a grand piano, at 200 kg. Forty residues with the same parameters and the library would be 10,000 times more massive than the earth. It quickly becomes apparent that it would be impossible to construct a primary library with diversity equal to the diversity seen in affinity maturation.

It has been demonstrated that the off-rate selection is crucial to obtaining the tightest binders possible (90). The equilibrium dissociation constant (K_D) of a protein to a ligand is measured as a ratio between the association rate (k_a or on-rate) and the

dissociation rate (k_d or off-rate) where the $K_D = \frac{K_d}{k_a}$. Biophysical studies of antibody interactions show that the association rate does not change more than 10-fold whether the overall affinity is high or low. There appears to be a physical limitation of diffusion for most large molecules (91). Increasing affinity therefore can only be achieved through improvement of the dissociation rate (58,72). After the secondary library members have been added to the target and allowed to reach equilibrium, 10 to 1,000- fold excess competitor is used to remove reagents with weak affinities. Reagents with high affinities have long off-rates and would more likely remain bound with the original target. Reagents with low affinities have short off-rates and would likely dissociate from the original target and re-associate with the free competitor target since it is in much greater concentration. Long washes and dilutions do not have the same effect on selecting high affinity binders. Counterintuitively, it has also been shown that long incubations with the competitor is detrimental to obtaining tight binders since equilibrium would be reached and therefore selection pressure on all binders would be the same (90). Shorter times with higher concentrations of competitor are preferred.

1.7 Dimerization for avidity

An alternative strategy for improving a reagent's usefulness is by increasing the apparent affinity through avidity. Avidity is achieved by dimerizing a known binding reagent into a single molecule that provides two sites to simultaneously bind to target (92). This is known as bivalency and is mimicking immunoglobulins of the immune

system (93). This increases the apparent affinity where two binding sites in equilibrium will likely have at least one site interacting at any given time and, therefore, will maintain a high local concentration. This reduces the chance the reagent will diffuse away. These can be homodimers or heterodimers. Homodimers are useful if the target is a homodimer as well (has two recognition sites for the binding reagent). They can also exhibit affinity through avidity by binding to a monomer target that is immobilized in a high concentration where the antigenic epitopes are of sufficient distance for the two recognition regions of the affinity reagent to span and bind simultaneously (94,95). Heterodimers of affinity reagents will recognize two separate domains of a single target protein, forming a sort of clamp (96). Normally, they are generated separately as monomers, determined to recognize separate epitopes, and are then dimerized. These reagents are more applicable to investigating biological questions since proteins of interest in the cell are often soluble.

A common means to dimerize two reagents is through a Fragment crystallizable (Fc) hinge region of an IgG (**Fig. 1B**) that acts as a stable linker by forming a disulfide bond between two identical units (97). This is done by standard sub-cloning into a vector containing the CH2 and CH3 regions flanked by multiple cloning sites. Previous investigations have reported a 100-fold increase in functional affinity when converting from an scFv to an scFv-Fc (98). Additionally, where the scFv format is degraded and cleared quickly from the *in vivo* system (99), the Fc has been shown to extend the half-life 12-fold (100). This has enhanced the reagents enough to be potential therapeutics for rheumatoid arthritis (101) and a prophylactic for the West Nile Virus (98).

1.8 Biomarkers of disease and injury

Upon disease or injury to a complex organism, the cells that have been affected respond by releasing proteins into the surrounding fluids specific to their tissue expression profile. If the presence or change in concentration of these proteins can be linked to an event, then the detection of the proteins can yield important data on the state of the organism. These proteins that have been discovered to be indicative of disease or injury are called biomarkers (102) . The sensitive measurements of biomarkers will help with early diagnosis, as well as with monitoring disease progression and remission. This is seen as indispensable in the future of medicine where a patient's complete physical condition can be evaluated in a single visit. Eventually the assays will be miniaturized to the size of smart phones where they will have a presence at the point-of-care in hospitals and sold commercially as common glucose meters carried by diabetics are available today (103).

The first step towards these ambitious projections is the discovery process by which a condition is associated with a set of biomarkers. This is no easy task considering the thousands of proteins released into the five liters of circulating blood serum that is degrading and filtering them constantly. Additionally, the patient population is diverse, each releasing unique amounts of protein at varying rates in their distinct situations. Finding a single "smoking gun" protein for diagnosis is ideal, panels of 4-8 biomarkers are more likely to give a confident answer, with less possibility of a false-positive or false-negative result.

The biomarker discovery process starts with a set of patients presenting a common clinically diagnosed condition (**Fig. 7**). A fluid is collected, usually the blood serum, that is fractionated and subjected to trypsin enzymatic cleavage. The treated fractions are analyzed by liquid chromatography coupled with the very sensitive tandem mass spectrometry (LC/MS/MS) that results in the sequences of short amino acid of thousands of protein fragments (104,105). The fragmented sequences can then be matched to their full length protein version through a GenBank database search.

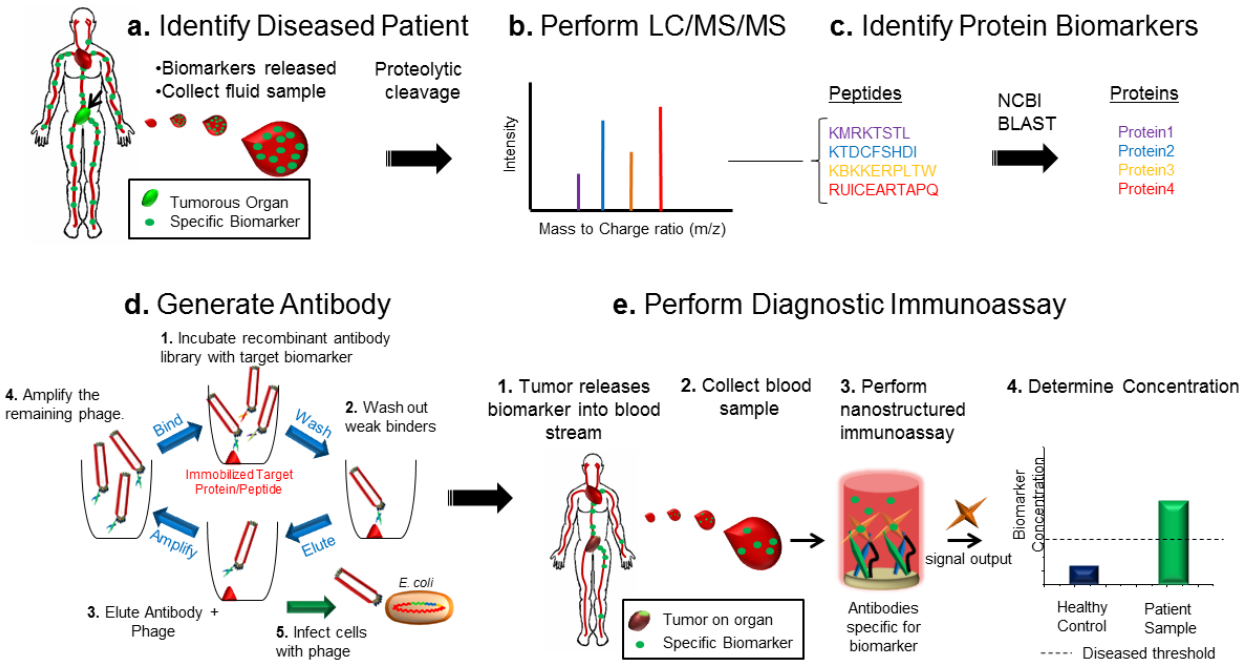

Figure 7. From biomarker discovery to disease diagnostics. A) A diseased patient or population of patients with the same condition, has fluid collected from various sources that potentially contain an indicative protein. Generally, the blood serum is the most common and lease intrusive. B) The serum is fractionated and cleaved into small peptides that are analyzed by Liquid Chromatography and tandem Mass Spectrometry. C) The peptide sequences are queried in a protein sequence database to identify the putative biomarkers. These are contrasted to a healthy control group and qualified as indicators of a disease through extensive biological testing. D) Antibodies are generated through a process like phage-display. E) The validated diagnostic is performed by

assaying the blood of a high-risk patient. The concentration is determined and compared to the healthy control. Disease diagnosis, progression, or remission, is assessed.

The quintessential example of a biomarker is Prostate Specific Antigen, or PSA, that is used to diagnose prostate cancer (106). Although the validity of the test has been called into question in the past several years (107), it still is the gold standard for protein biomarker detection. Men over the age of 55 have their blood tested for levels of PSA. There is a basal level that varies among men but generally a high concentration leads to cancer diagnosis and a prostate biopsy for confirmation (108). This biomarker is also a good example of the effects of false positive results which occurs frequently with this test. It is now being debated on whether the cost of a false positive result or over-diagnosis to a patient's psychological well-being outweighs the benefit of detecting the cancer (109). This underscores the complexities involved in biomarker discovery, validation, and sensitive detection.

Diagnostics that attempt to help alleviate some of these concerns by providing a more comprehensive analysis is exemplified by a test in trials for traumatic brain injury or (TBI). This test uses a panel of biomarkers including the proteolytic products of α-Spectrin Breakdown product to diagnose (110,111) TBI and was popularized by its use with American servicemen who have experienced concussions from roadside explosive devices in the combat zones of Iraq and Afghanistan (112).

In addition to these, a number of cancers are routinely screened for with FDA approved biomarker assays. Some of the more common are: Carcinoembryonic Antigen

(CEA) for Colon and rectal carcinoma (113), Cancer Antigen 125 (CA125) for ovarian cancer (114), and Alpha-Fetoprotein (AFP) for liver cancer (115).

Further discovery of protein biomarkers will warrant the necessity for the development of custom recombinant affinity reagents for validation, qualification, and diagnosis of diseases. Recombinant affinity reagents will also be recruited to treat the diseases through inhibition, neutralization, or drug-targeting. Considering the recent achievement of the “$1,000” genome sequence (116), the future of personalized medicine is rapidly approaching.

1.9 Conclusion

Using technologies like phage- and ribosome-display we have generated affinity reagents against a range of target proteins. We have selected for scFv antibodies that recognize putative biomarker peptides of retinal proteins implicated in injury from laser exposure. One of these antibodies was shown to bind to the endogenous protein from mammalian retinal lysates in western blotting. This antibody was then converted into a bivalent format to enhance its functional affinity through avidity and we show the improvements in lower detection limits. We also incorporated some of the retinal binding scFvs into an electrochemical detection platform that would produce an electrical current upon antigen binding in an automated immunoassay.

In addition, we have shown for the first time that the Forkhead-associated domain is amenable to ribosome-display. Affinity maturation through the error-prone PCR successfully improved the binding affinity of a phospho-recognizing anti-Myc FHA. Although the increase in affinity is modest, a route to further enhancement is outlined. Modification of the ribosome-display method by use of commercially available kits has shortened and simplified the procedure. With this change, we believe we have made ribosome-display more accessible to small labs.

A second theme is the development of a novel technology that combines ribosome-display and phage-display to more efficiently generate affinity reagents. We term this method: Primer Extension for Selection Recovery (PExSR) where the first round of selection takes advantage of the large naïve library sizes possible with ribosome-display. The next step is format conversion to phage-display through primer annealing and extension to a single-stranded DNA phagemid. The following rounds of selection are then conducted with increasing concentrations of competitor using phage-display which is less time consuming, cheaper, and less labor intense. We also modified some of the steps to lower some initial barriers in establishing the technique in a molecular biology laboratory. We envision the PExSR method as an attractive option for industrial antibody production and also as a way to encourage the adoption of the ribosome-display technique, which has yet to experience wide spread acceptance.

1.10 References

1. Venter JC, Adams MD, Myers EW, Li PW, Mural RJ, et al. The sequence of the human genome. *Science* 291: 1304-1351. (2001).

2. Lander ES, Linton LM, Birren B, Nusbaum C, Zody MC, et al. Initial sequencing and analysis of the human genome. *Nature* 409: 860-921. (2001).

3. Hanash S. HUPO initiatives relevant to clinical proteomics. *Mol Cell Proteomics* 3: 298-301. (2004).

4. Clamp M, Fry B, Kamal M, Xie X, Cuff J, et al. Distinguishing protein-coding and noncoding genes in the human genome. *Proc Natl Acad Sci U S A* 104: 19428-19433. (2007).

5. Dubel S, Stoevesandt O, Taussig MJ, Hust M. Generating recombinant antibodies to the complete human proteome. *Trends Biotechnol* 28: 333-339. (2010).

6. Colwill K, Graslund S. A roadmap to generate renewable protein binders to the human proteome. *Nat Methods* 8: 551-558. (2011).

7. Kohler G, Milstein C. Continuous cultures of fused cells secreting antibody of predefined specificity. *Nature* 256: 495-497. (1975).

8. Batista FD, Neuberger MS. Affinity dependence of the B cell response to antigen: A threshold, a ceiling, and the importance of off-rate. *Immunity* 8: 751-759. (1998).

9. Jain RK. Transport of molecules across tumor vasculature. *Cancer Metastasis Rev* 6: 559-593. (1987).

10. Kehoe JW, Velappan N, Walbolt M, Rasmussen J, King D, et al. Using phage display to select antibodies recognizing post-translational modifications independently of sequence context. *Mol Cell Proteomics* 5: 2350-2363. (2006).
11. Muller BH, Chevrier D, Boulain JC, Guesdon JL. Recombinant single-chain Fv antibody fragment-alkaline phosphatase conjugate for one-step immunodetection in molecular hybridization. *J Immunol Methods* 227: 177-185. (1999).

12. Morino K, Katsumi H, Akahori Y, Iba Y, Shinohara M, et al. Antibody fusions with fluorescent proteins: a versatile reagent for profiling protein expression. *J Immunol Methods* 257: 175-184. (2001).

13. Qian X, Peng XH, Ansari DO, Yin-Goen Q, Chen GZ, et al. In vivo tumor targeting and spectroscopic detection with surface-enhanced Raman nanoparticle tags. *Nature Biotechnology* 26: 83-90. (2008).

14. Lewis Phillips GD, Li G, Dugger DL, Crocker LM, Parsons KL, et al. Targeting HER2-positive breast cancer with trastuzumab-DM1, an antibody-cytotoxic drug conjugate. *Cancer Res* 68: 9280-9290. (2008).

15. Liu CC, Mack AV, Tsao ML, Mills JH, Lee HS, et al. Protein evolution with an expanded genetic code. *Proc Natl Acad Sci U S A* 105: 17688-17693. (2008).

16. Pershad K, Wypisniak K, Kay BK. Directed evolution of the forkhead-associated domain to generate anti-phosphospecific reagents by phage display. *J Mol Biol* 424: 88-103. (2012).

17. Cardinale A, Biocca S. The potential of intracellular antibodies for therapeutic targeting of protein-misfolding diseases. *Trends Mol Med* 14: 373-380. (2008).

18. Kummer L, Parizek P, Rube P, Millgramm B, Prinz A, et al. Structural and functional analysis of phosphorylation-specific binders of the kinase ERK from designed ankyrin repeat protein libraries. *Proc Natl Acad Sci U S A* 109: E2248-2257. (2012).

19. Hamers-Casterman C, Atarhouch T, Muyldermans S, Robinson G, Hamers C, et al. Naturally occurring antibodies devoid of light chains. *Nature* 363: 446-448. (1993).

20. Nord K, Nilsson J, Nilsson B, Uhlen M, Nygren PA. A combinatorial library of an alpha-helical bacterial receptor domain. *Protein Eng* 8: 601-608. (1995).

21. Kohl A, Binz HK, Forrer P, Stumpp MT, Pluckthun A, et al. Designed to be stable: crystal structure of a consensus ankyrin repeat protein. *Proc Natl Acad Sci U S A* 100: 1700-1705. (2003).

22. Gebauer M, Skerra A. Anticalins small engineered binding proteins based on the lipocalin scaffold. *Methods Enzymol* 503: 157-188. (2012).

23. Huston JS, Levinson D, Mudgett-Hunter M, Tai MS, Novotny J, et al. Protein engineering of antibody binding sites: recovery of specific activity in an anti-digoxin single-chain Fv analogue produced in Escherichia coli. *Proc Natl Acad Sci U S A* 85: 5879-5883. (1988).

24. Bird RE, Hardman KD, Jacobson JW, Johnson S, Kaufman BM, et al. Single-chain antigen-binding proteins. *Science* 242: 423-426. (1988).

25. Koide A, Bailey CW, Huang X, Koide S. The fibronectin type III domain as a scaffold for novel binding proteins. *J Mol Biol* 284: 1141-1151. (1998).

26. Marks JD, Griffiths AD, Malmqvist M, Clackson TP, Bye JM, et al. By-passing immunization: building high affinity human antibodies by chain shuffling. *Biotechnology (N Y)* 10: 779-783. (1992).

27. Schofield DJ, Pope AR, Clementel V, Buckell J, Chapple S, et al. Application of phage display to high throughput antibody generation and characterization. *Genome Biol* 8: R254. (2007).

28. Zhang JL, Gou JJ, Zhang ZY, Jing YX, Zhang L, et al. Screening and evaluation of human single-chain fragment variable antibody against hepatitis B virus surface antigen. *Hepatobiliary Pancreat Dis Int* 5: 237-241. (2006).

29. Zhu X, Bidlingmaier S, Hashizume R, James CD, Berger MS, et al. Identification of internalizing human single-chain antibodies targeting brain tumor sphere cells. *Mol Cancer Ther* 9: 2131-2141. (2010).

30. Zahnd C, Spinelli S, Luginbuhl B, Amstutz P, Cambillau C, et al. Directed in vitro evolution and crystallographic analysis of a peptide-binding single chain antibody fragment (scFv) with low picomolar affinity. *J Biol Chem* 279: 18870-18877. (2004).

31. Luginbuhl B, Kanyo Z, Jones RM, Fletterick RJ, Prusiner SB, et al. Directed evolution of an anti-prion protein scFv fragment to an affinity of 1 pM and its structural interpretation. *J Mol Biol* 363: 75-97. (2006).

32. Ravn P, Danielczyk A, Jensen KB, Kristensen P, Christensen PA, et al. Multivalent scFv display of phagemid repertoires for the selection of carbohydrate-specific antibodies and its application to the Thomsen-Friedenreich antigen. *J Mol Biol* 343: 985-996. (2004).

33. Watanabe H, Nakanishi T, Umetsu M, Kumagai I. Human anti-gold antibodies: biofunctionalization of gold nanoparticles and surfaces with anti-gold antibodies. *J Biol Chem* 283: 36031-36038. (2008).

34. Koduvayur SP, Gussin HA, Parthasarathy R, Hao Z, Kay BK, et al. Generation of recombinant antibodies to rat GABAA receptor subunits by affinity selection on synthetic peptides. *PLoS One* 9: e87964. (2014).

35. Abler LL, Sheets MD. Expression of scFv antibodies in Xenopus embryos to disrupt protein function: implications for large-scale evaluation of the embryonic proteome. *Genesis* 35: 107-113. (2003).

36. Lo YS, Nam DH, So HM, Chang H, Kim JJ, et al. Oriented immobilization of antibody fragments on Ni-decorated single-walled carbon nanotube devices. *ACS Nano* 3: 3649-3655. (2009).

37. Balalaeva IV, Zdobnova TA, Brilkina AA, Krutova IM, Stremovskiy OA, et al. Whole-body imaging of HER2/neu-overexpressing tumors using scFv-antibody conjugated quantum dots. *Proc SPIE* 7575: 757510. (2010).

38. Stohl W, Hilbert DM. The discovery and development of belimumab: the anti-BLyS-lupus connection. *Nature Biotechnology* 30: 69-77. (2012).

39. FDA approves Benlysta to treat lupus. US Food and Drug Adminstration. (2011)
40. Lipovsek D. Adnectins: engineered target-binding protein therapeutics. *Protein Eng Des Sel* 24: 3-9. (2011).

41. Main AL, Harvey TS, Baron M, Boyd J, Campbell ID. The three-dimensional structure of the tenth type III module of fibronectin: an insight into RGD-mediated interactions. *Cell* 71: 671-678. (1992).

42. Potts JR, Campbell ID. Fibronectin structure and assembly. *Curr Opin Cell Biol* 6: 648-655. (1994).

43. Koide A, Gilbreth RN, Esaki K, Tereshko V, Koide S. High-affinity single-domain binding proteins with a binary-code interface. *Proc Natl Acad Sci U S A* 104: 6632-6637. (2007).

44. Garcia-Ibilcieta D, Bokov M, Cherkasov V, Sveshnikov P, Hanson SF. Simple method for production of randomized human tenth fibronectin domain III libraries for use in combinatorial screening procedures. *Biotechniques* 44: 559-562. (2008).
45. Xu L, Aha P, Gu K, Kuimelis RG, Kurz M, et al. Directed Evolution of High-Affinity Antibody Mimics Using mRNA Display. *Chemistry & Biology* 9: 933-942. (2002).
46. Wojcik J, Hantschel O, Grebien F, Kaupe I, Bennett KL, et al. A potent and highly specific FN3 monobody inhibitor of the Abl SH2 domain. *Nat Struct Mol Biol* 17: 519-527. (2010).

47. Huang R, Fang P, Kay BK. Isolation of monobodies that bind specifically to the SH3 domain of the Fyn tyrosine protein kinase. *N Biotechnol* 29: 526-533. (2012).

48. Liao H-I, Olson CA, Hwang S, Deng H, Wong E, et al. mRNA Display Design of Fibronectin-based Intrabodies That Detect and Inhibit Severe Acute Respiratory Syndrome Coronavirus Nucleocapsid Protein. *Journal of Biological Chemistry* 284: 17512-17520. (2009).

49. Koide A, Abbatiello S, Rothgery L, Koide S. Probing protein conformational changes in living cells by using designer binding proteins: Application to the estrogen receptor. *Proceedings of the National Academy of Sciences* 99: 1253-1258. (2002).

50. Tolcher AW, Sweeney CJ, Papadopoulos K, Patnaik A, Chiorean EG, et al. Phase I and pharmacokinetic study of CT-322 (BMS-844203), a targeted Adnectin inhibitor of VEGFR-2 based on a domain of human fibronectin. *Clin Cancer Res* 17: 363-371. (2011).

51. Liao H, Yuan C, Su MI, Yongkiettrakul S, Qin D, et al. Structure of the FHA1 domain of yeast Rad53 and identification of binding sites for both FHA1 and its target protein Rad9. *J Mol Biol* 304: 941-951. (2000).

52. Hofmann K, Bucher P. The FHA domain: a putative nuclear signalling domain found in protein kinases and transcription factors. *Trends Biochem Sci* 20: 347-349. (1995).

53. Pennell S, Westcott S, Ortiz-Lombardia M, Patel D, Li J, et al. Structural and functional analysis of phosphothreonine-dependent FHA domain interactions. *Structure* 18: 1587-1595. (2010).

54. Smith GP. Filamentous Fusion Phage - Novel Expression Vectors That Display Cloned Antigens on the Virion Surface. *Science* 228: 1315-1317. (1985).

55. Griffiths AD, Duncan AR. Strategies for selection of antibodies by phage display. *Curr Opin Biotechnol* 9: 102-108. (1998).

56. Vieira J, Messing J. Production of single-stranded plasmid DNA. *Methods Enzymol* 153: 3-11. (1987).

57. Lowman HB, Bass SH, Simpson N, Wells JA. Selecting high-affinity binding proteins by monovalent phage display. *Biochemistry* 30: 10832-10838. (1991).

58. Winter G, Griffiths AD, Hawkins RE, Hoogenboom HR. Making antibodies by phage display technology. *Annu Rev Immunol* 12: 433-455. (1994).

59. Kehoe JW, Kay BK. Filamentous phage display in the new millennium. *Chem Rev* 105: 4056-4072. (2005).

60. McCafferty J, Griffiths AD, Winter G, Chiswell DJ. Phage antibodies: filamentous phage displaying antibody variable domains. *Nature* 348: 552-554. (1990).

61. Scott JK, Smith GP. Searching for peptide ligands with an epitope library. *Science* 249: 386-390. (1990).

62. Devlin JJ, Panganiban LC, Devlin PE. Random peptide libraries: a source of specific protein binding molecules. *Science* 249: 404-406. (1990).

63. Hoogenboom HR, Griffiths AD, Johnson KS, Chiswell DJ, Hudson P, et al. Multi-subunit proteins on the surface of filamentous phage: methodologies for displaying antibody (Fab) heavy and light chains. *Nucleic Acids Res* 19: 4133-4137. (1991).

64. Steiner D, Forrer P, Pluckthun A. Efficient Selection of DARPins with Sub-nanomolar Affinities using SRP Phage Display. *Journal of Molecular Biology* 382: 1211-1227. (2008).

65. Dooley H, Flajnik MF, Porter AJ. Selection and characterization of naturally occurring single-domain (IgNAR) antibody fragments from immunized sharks by phage display. *Mol Immunol* 40: 25-33. (2003).

66. Rau R. Adalimumab (a fully human anti-tumour necrosis factor alpha monoclonal antibody) in the treatment of active rheumatoid arthritis: the initial results of five trials. *Ann Rheum Dis* 61 Suppl 2: ii70-73. (2002).

67. den Broeder A, van de Putte L, Rau R, Schattenkirchner M, Van Riel P, et al. A single dose, placebo controlled study of the fully human anti-tumor necrosis factor-alpha antibody adalimumab (D2E7) in patients with rheumatoid arthritis. *J Rheumatol* 29: 2288-2298. (2002).

68. Karasseva N, Glinsky V, Chen N, Komatireddy R, Quinn T. Identification and Characterization of Peptides That Bind Human ErbB-2 Selected from a Bacteriophage Display Library. *Journal of Protein Chemistry* 21: 287-296. (2002).

69. Emanuel P, O'Brien T, Burans J, DasGupta BR, Valdes JJ, et al. Directing antigen specificity towards botulinum neurotoxin with combinatorial phage display libraries. *J Immunol Methods* 193: 189-197. (1996).

70. Maruyama T, Rodriguez LL, Jahrling PB, Sanchez A, Khan AS, et al. Ebola Virus Can Be Effectively Neutralized by Antibody Produced in Natural Human Infection. *Journal of Virology* 73: 6024-6030. (1999).

71. Storz U IP Issues in the Therapeutic Antibody Industry. In: Kontermann R, Dübel S, editors. Antibody Engineering: Springer Berlin Heidelberg. pp. 517-581.(2010)

72. Pluckthun A. Ribosome display: a perspective. *Methods Mol Biol* 805: 3-28. (2012).

73. Hanes J, Pluckthun A. In vitro selection and evolution of functional proteins by using ribosome display. *Proc Natl Acad Sci U S A* 94: 4937-4942. (1997).

74. Jermutus L, Honegger A, Schwesinger F, Hanes J, Pluckthun A. Tailoring in vitro evolution for protein affinity or stability. *Proc Natl Acad Sci U S A* 98: 75-80. (2001).

75. Dreier B, Pluckthun A. Ribosome display: a technology for selecting and evolving proteins from large libraries. *Methods Mol Biol* 687: 283-306. (2011).

76. Dreier B, Plückthun A Rapid Selection of High-Affinity Binders Using Ribosome Display. In: Douthwaite JA, Jackson RH, editors. Ribosome Display and Related Technologies: Springer New York. pp. 261-286.(2012)

77. Mattheakis LC, Bhatt RR, Dower WJ. An in vitro polysome display system for identifying ligands from very large peptide libraries. *Proc Natl Acad Sci U S A* 91: 9022-9026. (1994).

78. Schimmele B, Grafe N, Pluckthun A. Ribosome display of mammalian receptor domains. *Protein Eng Des Sel* 18: 285-294. (2005).

79. Pecqueur L, Duellberg C, Dreier B, Jiang Q, Wang C, et al. A designed ankyrin repeat protein selected to bind to tubulin caps the microtubule plus end. *Proc Natl Acad Sci U S A* 109: 12011-12016. (2012).

80. Zahnd C, Pecorari F, Straumann N, Wyler E, Pluckthun A. Selection and characterization of Her2 binding-designed ankyrin repeat proteins. *J Biol Chem* 281: 35167-35175. (2006).

81. Campochiaro PA, Channa R, Berger BB, Heier JS, Brown DM, et al. Treatment of Diabetic Macular Edema With a Designed Ankyrin Repeat Protein That Binds Vascular Endothelial Growth Factor: A Phase I/II Study. *American Journal of Ophthalmology* 155: 697-704.e692. (2013).

82. Schreier B, Stumpp C, Wiesner S, Höcker B. Computational design of ligand binding is not a solved problem. *Proceedings of the National Academy of Sciences* 106: 18491-18496. (2009).

83. Tinberg CE, Khare SD, Dou J, Doyle L, Nelson JW, et al. Computational design of ligand-binding proteins with high affinity and selectivity. *Nature* 501: 212-216. (2013).

84. Marks JD, Hoogenboom HR, Bonnert TP, McCafferty J, Griffiths AD, et al. By-passing immunization. Human antibodies from V-gene libraries displayed on phage. *J Mol Biol* 222: 581-597. (1991).

85. Parmley SF, Smith GP. Antibody-selectable filamentous fd phage vectors: affinity purification of target genes. *Gene* 73: 305-318. (1988).

86. Pershad K, Kay BK. Generating thermal stable variants of protein domains through phage display. *Methods* 60: 38-45. (2013).

87. Low NM, Holliger P, Winter G. Mimicking Somatic Hypermutation: Affinity Maturation of Antibodies Displayed on Bacteriophage Using a Bacterial Mutator Strain. *Journal of Molecular Biology* 260: 359-368. (1996).

88. Hawkins RE, Russell SJ, Winter G. Selection of phage antibodies by binding affinity. Mimicking affinity maturation. *J Mol Biol* 226: 889-896. (1992).

89. Zaccolo M, Williams DM, Brown DM, Gherardi E. An approach to random mutagenesis of DNA using mixtures of triphosphate derivatives of nucleoside analogues. *Journal of Molecular Biology* 255: 589-603. (1996).

90. Zahnd C, Sarkar CA, Pluckthun A. Computational analysis of off-rate selection experiments to optimize affinity maturation by directed evolution. *Protein Eng Des Sel* 23: 175-184. (2010).

91. Northrup SH, Erickson HP. Kinetics of protein-protein association explained by Brownian dynamics computer simulation. *Proc Natl Acad Sci U S A* 89: 3338-3342. (1992).

92. Pluckthun A, Pack P. New protein engineering approaches to multivalent and bispecific antibody fragments. *Immunotechnology* 3: 83-105. (1997).

93. Kaufman EN, Jain RK. Effect of Bivalent Interaction upon Apparent Antibody Affinity: Experimental Confirmation of Theory Using Fluorescence Photobleaching and Implications for Antibody Binding Assays. *Cancer Research* 52: 4157-4167. (1992).

94. Crothers DM, Metzger H. The influence of polyvalency on the binding properties of antibodies. *Immunochemistry* 9: 341-357. (1972).

95. Pack P, Muller K, Zahn R, Pluckthun A. Tetravalent miniantibodies with high avidity assembling in Escherichia coli. *J Mol Biol* 246: 28-34. (1995).

96. Huang J, Koide A, Makabe K, Koide S. Design of protein function leaps by directed domain interface evolution. *Proc Natl Acad Sci U S A* 105: 6578-6583. (2008).

97. Andrade EV, Albuquerque FC, Moraes LM, Brigido MM, Santos-Silva MA. Single-chain Fv with Fc fragment of the human IgG1 tag: construction, Pichia pastoris expression and antigen binding characterization. *J Biochem* 128: 891-895. (2000).

98. Gould LH, Sui J, Foellmer H, Oliphant T, Wang T, et al. Protective and therapeutic capacity of human single-chain Fv-Fc fusion proteins against West Nile virus. *J Virol* 79: 14606-14613. (2005).

99. Huston JS, George AJ, Adams GP, Stafford WF, Jamar F, et al. Single-chain Fv radioimmunotargeting. *Q J Nucl Med* 40: 320-333. (1996).

100. Powers DB, Amersdorfer P, Poul M, Nielsen UB, Shalaby MR, et al. Expression of single-chain Fv-Fc fusions in Pichia pastoris. *J Immunol Methods* 251: 123-135. (2001).

101. Murray KM, Dahl SL. Recombinant human tumor necrosis factor receptor (p75) Fc fusion protein (TNFR:Fc) in rheumatoid arthritis. *Ann Pharmacother* 31: 1335-1338. (1997).

102. Gutman S, Kessler LG. The US Food and Drug Administration perspective on cancer biomarker development. *Nat Rev Cancer* 6: 565-571. (2006).

103. Newman JD, Turner AP. Home blood glucose biosensors: a commercial perspective. *Biosens Bioelectron* 20: 2435-2453. (2005).

104. Link AJ, Eng J, Schieltz DM, Carmack E, Mize GJ, et al. Direct analysis of protein complexes using mass spectrometry. *Nat Biotechnol* 17: 676-682. (1999).

105. Washburn MP, Wolters D, Yates JR, 3rd. Large-scale analysis of the yeast proteome by multidimensional protein identification technology. *Nat Biotechnol* 19: 242-247. (2001).

106. Stamey TA, Yang N, Hay AR, Mcneal JE, Freiha FS, et al. Prostate-Specific Antigen as a Serum Marker for Adenocarcinoma of the Prostate. *New England Journal of Medicine* 317: 909-916. (1987).

107. Hayes JH, Barry MJ. Screening for prostate cancer with the prostate-specific antigen test: a review of current evidence. *JAMA* 311: 1143-1149. (2014).

108. Stenman UH, Leinonen J, Zhang WM, Finne P. Prostate-specific antigen. *Semin Cancer Biol* 9: 83-93. (1999).

109. Heijnsdijk EA, Wever EM, Auvinen A, Hugosson J, Ciatto S, et al. Quality-of-life effects of prostate-specific antigen screening. *N Engl J Med* 367: 595-605. (2012).

110. Ringger NC, O'Steen BE, Brabham JG, Silver X, Pineda J, et al. A novel marker for traumatic brain injury: CSF alphaII-spectrin breakdown product levels. *J Neurotrauma* 21: 1443-1456. (2004).

111. Siman R, Toraskar N, Dang A, McNeil E, McGarvey M, et al. A panel of neuron-enriched proteins as markers for traumatic brain injury in humans. *J Neurotrauma* 26: 1867-1877. (2009).

112. Burton TM. New Test for Brain Injury on Horizon. *Wall Street Journal*. (2010).

113. Gold P, Freedman SO. Demonstration of Tumor-Specific Antigens in Human Colonic Carcinomata by Immunological Tolerance and Absorption Techniques. *J Exp Med* 121: 439-462. (1965).

114. Bast RC, Jr., Feeney M, Lazarus H, Nadler LM, Colvin RB, et al. Reactivity of a monoclonal antibody with human ovarian carcinoma. *J Clin Invest* 68: 1331-1337. (1981).

115. Malaguarnera G, Giordano M, Paladina I, Berretta M, Cappellani A, et al. Serum markers of hepatocellular carcinoma. *Dig Dis Sci* 55: 2744-2755. (2010).

116. Sheridan C. Illumina claims [dollar]1,000 genome win. *Nat Biotech* 32: 115-115. (2014).

CHAPTER 2

GENERATING AFFINITY REAGENTS AGAINST RETINAL BIOMARKERS

Portions of this research have been submitted for publication

Michael R. Kierny, Thomas D. Cunningham, Rachida A. Bouhenni, Deepak Edward, and Brian K. Kay. Submitted for review to *PLOS One* (October 2014).

2.1 Abstract

Candidate biomarkers, indicative of disease and injury, are beginning to overwhelm the process of validation through immunological means. Recombinant antibodies developed through phage-display can help alleviate this build up faster and more efficiently than traditional immunizations of animals. Peptide fragments of putative biomarkers of laser induced injury, discovered through mass spectrometry, were used as targets for a selection against a library of phage-displayed human single-chain fragment of variation recombinant antibodies. One single-chain antibody of Fragment variable regions (scFv) against the retinal protein GBB5, had an affinity of ~300 nM and recognized the full length endogenous protein in western blot. Alanine scanning of the peptide identified 3 charged and 1 hydrophobic amino acid as the critical binding residues. To enhance the utility of the reagent, the antibody was dimerized through a Fragment crystallizable hinge region and expressed in mammalian tissue culture. This increased functional affinity through avidity and allowed a 25-fold lower detection limit in western blot. To show the possibility of using the reagents in a miniaturized diagnostic, we deposited scFvs on the surface of electrodes and recorded electrical current generated upon antigen binding in an electrochemical reaction.

2.2 Introduction

The discovery of biomarkers that are indicative of disease or injury and their sensitive detection is the future of preventive medicine. Biomarkers are biological molecules released by cells into the serum or surrounding fluid in response to a biological state. Detection of certain biomarker proteins that are associated with a condition and are at abnormal concentrations, can aid in prevention, diagnosis, and regression monitoring. Although biomarkers can be of any biological composition, the proteome has the greatest potential for insight into the diseased state of a patient. Recognizing specific proteins at low concentrations can be challenging when thousands of different proteins can be present in a complex sample.

Currently there are many biomarkers used routinely for diagnostics. Some examples of injury biomarkers are: Neutrophil Gelatinase Associated Lipocalin (NGAL) for acute kidney injury(1,2), Troponin I (cTnI) for mycoradial infarction (3), and a panel of biomarkers including α-Spectrin II Breakdown products for traumatic brain injury (4). For diseases, biomarkers of cancers are predominant since early diagnosis has long been known to improve patient outcome (5). Typical biomarkers of cancer are: prostate specific antigen (PSA) for prostate cancer (6,7), CA 125 for Ovarian cancer (8), and Carcinoembryonic Antigen (CEA) for colorectal cancer (9).

Traditional antibodies made by animal immunizations and hybridoma immortalization (10) have been the best tool so far to identify the enormous numbers of

medically relevant proteins, however there are not nearly enough to cover the proteome, many of the antibodies that are available are not specific (11), and they take a lot of effort to generate (12). Therefore, to continue to advance preventative medicine and quality of life, newer technologies must be employed to meet the rising need for custom antibodies of newly discovered biomarkers.

Recombinant affinity reagents developed through technologies like phage-display provides a better means to develop diagnostics for disease (13). This technology allows for libraries of antibody fragments to be co-expressed with the M13 bacteriophage coat protein pIII during phage assembly where it is available to bind an antigen of interest (14). After a selection procedure that increases in stringency through three rounds of antibody-antigen incubation, washing, and amplification of the tightest binding sequences, the DNA sequence encoding the selected antibody can be recovered. The key to this technology is the linking of the genotype with the phenotype where the DNA for the displayed antibody is encapsulated within the phage particle (15).

Laser illuminations of commercial and military aircraft pose a serious threat to pilot's vision and the safety of the passengers on board. The events are most often to occur near airports where human population is most dense and planes are at the lowest altitude. This is also the point when a pilot is performing the most complex operational procedures that require the greatest concentration and visual acuity (16). When the laser enters through the pupil, the beam is focused onto the retina up to 100,000 times

(17) and causes damage by thermal and mechanical means (18) (**Fig. 8**). There were nearly 4,000 unauthorized laser illumination events reported in 2013 (19). This can have temporary effects of flash-blindness, afterimage, and distraction, or cause more severe retinal burns (20,21). The degree of retinal damage and the effects to the pilot's ability to fly the aircraft can vary by situation. Currently, pupil dilation with an exam by an ophthalmologist is the only way to determine the extent of the damage (22), but leaves the pilot unable to fly for 4-8 hours. A low-invasive diagnostic, probing for biomarkers in serum or tear duct fluid of an exposed pilot to confirm the degree of damage, would be invaluable to the aviation industry.

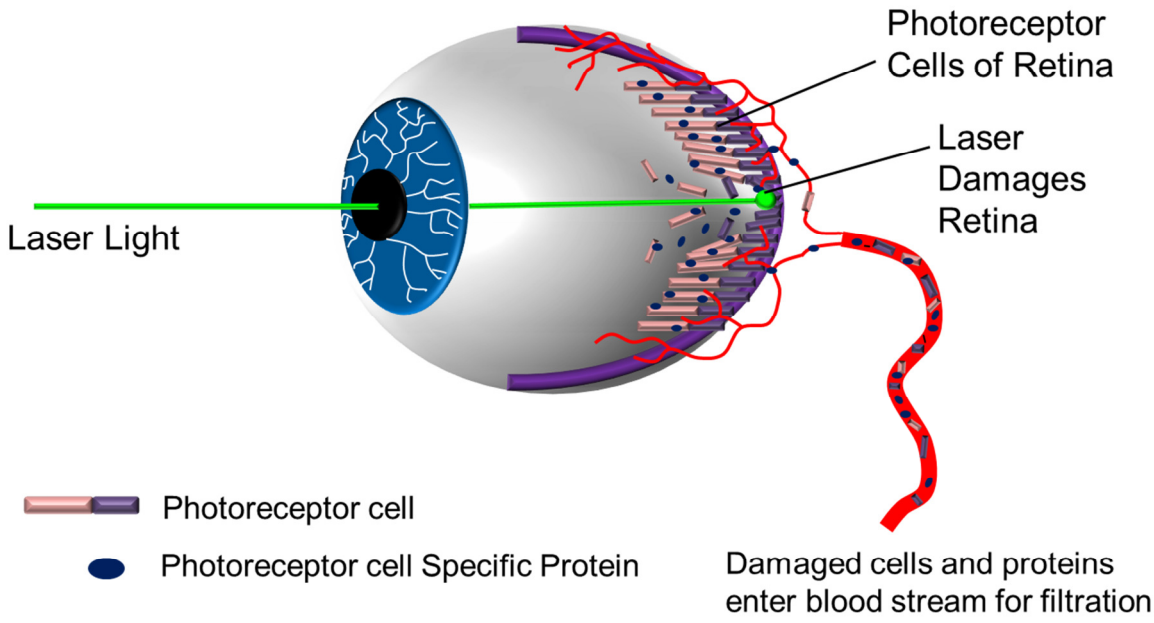

Figure 8. Diagram of retinal injury from laser exposure. As the laser enters the pupil, it is focused by the lens onto the retina. Depending on the intensity and duration of exposure, the cellular layers of the retina can be damaged. Photoreceptor cells are specialized and therefore express specific proteins. The damaged cells and components are cleared from the area of injury and enter the serum where they can be detected as biomarkers and correlated with the laser exposure.

Here we have generated single-chain variable fragment antibodies against four putative biomarkers of laser induced retinal injury using phage-display. One scFv antibody, against the retinal protein GBB5, was carried further to demonstrate a method to characterize antibodies generated from peptide fragments identified by Mass Spectrometry of serum samples. The scFv was shown to have a ~300 nM affinity and could recognize the full length endogenous protein in western blot. To increase the usefulness of the reagent, the scFv was homodimerized through a Fragment crystallizable hinge region of an IgG. This gave a 25-fold lower detection limit in western blot and a 4.5-fold improvement in ELISA signal. Investigation of the critical residues for contact was determined through alanine scanning.

We also wanted to incorporate our scFvs into a diagnostic platform that would be amenable to miniaturization and automation. An electrochemical detection microchip, originally intended for DNA microarrays, was explored for this purpose. Deposited scFvs were observed to capture antigen and return a concentration dependent electrical current generated by a redox reaction on the surface of electrodes.

2.3 Materials and methods

2.3.1 Peptide synthesis

Putative biomarker peptides were identified through liquid chromatography tandem mass spectrometry (LC-MS/MS) by collaborators Drs. Deepak Edward and Rachida Bouhenni at SUMMA Health Systems (Akron, Ohio) using methods described previously (23) and IRB #10-039 (Northeast Ohio Medical Universities, NEOMED. Peptides were synthesized by the protein core facility of the Research Resources Center at the University of Illinois-Chicago. The N-terminus contains a biotin molecule followed by a four amino acid linker composed of Glycine-Serine-Glycine-Serine. The identified peptide of 9-14 amino acids follows the linker and ends with a C-terminal amidation. Peptides were dissolved into sterile phosphate buffered saline (PBS: 137 mM NaCl, 3 mM KCl, 8 mM NaH_2PO_4, 1.5 mM KH_2PO_4) and stored at -20°C. The peptides synthesized are named after the full length biomarker. Calcium Channel Voltage-Dependent, L-type, Alpha 1 subunit: CACNA1F#1 (IRWFSHSTR) and CACNA1F#3 (TEGNLEQANQELRIVIK); Cyclic Nucleotide Gated Channel Alpha 3: CNGA3 (RLTRLESQMNRRCCGFSPDRE); Guanine Nucleotide-Binding Protein Beta 5: GBB5 (KLHDVELHQVAERV); and Regulator of G-protein Signaling 9: RGS9 (KLVEVPTKMRV).

2.3.2 Phage-display selection

The scFv phage-display library was a gift from Dr. Mark Sullivan (University of Rochester, Rochester, NY) (24). The wells of a Nunc Maxisorp 96-well microtiter plate (Nunc) were coated with 50 ng NeutrAvidin™ (Thermo Fisher Scientific) in PBS and incubated at 4°C overnight. The plate was blocked with 1% casein (Thermo Fisher Scientific) for 1 h and then washed 3 times with PBS with 0.5% Tween 20 (PBST). The scFv phage-display library ($1x10^9$ sequence diversity, and titer of $1x10^{12}$ phage/mL) was added in 50 µL volumes to four blocked wells and incubated for 1 h to deselect casein and NeutrAvidin™ binders. The unbound phage were transferred to wells containing 50 ng of biotinylated-peptide and incubated for 2 h at room temperature with shaking. The wells were washed 5 times with PBST. The bound virions were recovered using 50 µL of 100 mM Glycine-HCl, pH 2.0 for 10 min. The eluted phage were neutralized with 3 µL of 2 M Tris, pH 10. The eluted virions were neutralized with 3 µL of 2 M Tris, pH 10. This was used to infect 750 µL of TG-1 *Escherichia coli* growing to mid-log phase, with an optical density at 600 nm (OD_{600}) of 0.4, and incubated at 37°C without shaking for 1 h. The cells were spread on a Luria Bertani (LB) agar plate (10 g/L tryptone, 5 g/L yeast extract, 10 g/L NaCl, 15 g/L Agar) containing 50 µg/mL Carbenicillin (Cb), and incubated overnight at 30°C.

The following day, the lawn of colonies was scraped into 15 mL of LB/Cb. To 40 mL of LB/Cb, was added 100 µL of the scraped cells, and then grown to mid-log phase at

37°C (250 rpm shaking). One mL of cells were removed and infected with M13K07 helper phage (New England BioLabs), at a multiplicity of infection (MOI) of 10, for 1 h at 37°C, with 150 rpm shaking. This mixture was added to 30 mL of LB/Cb/Kanamycin (Kan, 50 µg/mL), and grown overnight at 30°C, 250 rpm shaking, to allow for phage particle production.

To precipitate the secreted virions for the second round of selection, the overnight culture was spun down and ~30 mL supernatant adjusted to a final concentration of 500 mM NaCl, 4% PEG_{8000}, and incubated on ice for 1 h. This tube was spun at 12,000 rpm for 15 min. The precipitated virions was suspended in 1 mL of 0.5% casein in PBS. This was used for the second round of affinity selection.

Rounds #2 and #3 of affinity selection were performed the same as round #1, except that the target was now reduced to 5 ng in a single well and the washes of PBST were increased to 7 times, with harsh vigorous pipetting up and down in between.

After the final round of infection and plating of clones, 94 colonies were used to inoculate wells of a 96-well deep plate containing 100 µL of LB/Cb and grown to mid-log phase (OD_{600} =0.4). To these cultures, 200 µL of M13K07 helper phage in LB/Cb and were added without shaking for 1 h at 37°C. Plates were spun down, supernatant discarded, and 400 µL of LB/Cb/Kan added for overnight phage expression at 30°C with 250 rpm shaking.

2.3.3 Monoclonal phage enzyme linked immunosorbent assay (ELISA

Two 96-well microtiter plates were coated overnight with 50 ng/well NeutrAvidin™ in PBS. The wells were blocked with 1% casein in PBS for 1 h. To one plate was added the target biotinylated peptide at 50 ng/well and incubated for 1 h. After washes in PBS and PBST, 50 µL of supernatant from each well of the overnight culture of expressed phage was added to the corresponding well of the coated target or background no-target plate, and incubated for 1 h. Washes of PBST and PBS followed. For detection of the bound phage particles, 50 µL of anti-M13-Horse Radish Peroxidase (HRP; GE Healthcare), diluted to 1:5,000 in PBS, was added to all wells. Following washes of PBST and PBS, 50 µL of 2,2'-azino-bis (3-ethylbenzothiazoline-6-sulphonic acid (ABTS) (Sigma-Aldrich) in 50 mM Sodium Citrate pH 4 with 0.03% H_2O_2 was added, and color change recorded at absorbance wavelength 405 nm using a FluoStar OPTIMA (BMG Labtech) spectrophotometer micro-titer plate reader. Specific binders were identified by comparing the absorbance of corresponding wells on background and target plates.

2.3.4 Cloning and bacterial expression

The positive clones were grown up overnight and the plasmid DNA was prepared using a MiniPrep DNA purification column (Wizard MiniPrep, Promega). The scFv

regions were sequenced using forward primer ompA (CTGTCATAAAGTTGTCACGGCCGA) and reverse primer 266 (CCCCTTATTAGCGTTTGCCATCTT). Unique clones were then sub-cloned using the *HindIII* and *SalI* restriction sites (New England Biolabs) into a low phosphate promoter (Alkline Phospotase- PhoA) *E. coli* expression plasmid pKP300DIIIDAP (25), with an in-frame N-terminal FLAG tag, C-terminal 6x poly-Histidine tag, and an OmpA signal sequence targeting to the periplasm . Expression is performed in low phosphate modified C.R.A.P. media (26) (3.57 g ammonium sulfate, 0.71 g sodium citrate dihydrate, 1.07 g potassium chloride, 5.36 g Yeast Extract, 5.36 g Hycase SF Casein hydrolysate, pH adjusted with potassium hydroxide to 7.3, deionized H_2O added to 872 mL and autoclaved; added 7 mL 1 M magnesium sulfate and 14 mL 1 M glucose) with 50 µg/mL Cb overnight at 30°C (250 rpm shaking).

For small scale expression, the infected bacterial cells were spun down and resuspended in a lysis solution consisting of Bugbuster in PBS (Novagen) and Benzonase Nuclease HC (Novagen) for 20 min. After pelleting the cell debris, the scFv was purified from the supernatant by immobilized metal affinity chromatography (IMAC) using His·Mag Agarose Magnetic beads (Novagen) and a Kingfisher mL robot (ThermoScientific). Antibodies were eluted into 500 mM Imidazole, 500 mM NaCl, and 20 µM Tris-HCl (EB), and stored at 4°C, or at -20°C in 15% Glycerol.

For large scale expression, infected cells were added to 200 mL of low phosphate media, 50 µg/mL Cb, and allowed to grow 22-24 h at 30°C with 250 rpm shaking. Cultures were spun down and prepared for sonication by resuspending the cell pellet in 25 mL of filter sterilized equilibration buffer (50 mM sodium phosphate, 300 mM sodium chloride, pH 7.4) on ice. The cOmplete EDTA free protease Inhibitor cocktail (Roche Applied Science) was added and performed sonication on ice with 10 sec on sonication, 10 sec off for a total of 10 min, with 50% amplitude using a SonicDismemberator (Branson inc. Model 500). The lysate was spun at 15,000 rpm for 15 min. Supernatant was transferred to a 50 mL centrifuge tube. Agarose was prepared by washing 200-300 µL of Clontech His60 Ni Superflow™ resin (60 mg/mL binding capacity, Clontech Laboratories, inc.) twice with equilibration buffer. Added resin to cleared lysate and incubated at 4°C for 2 h while tumbling. Lysate was spun down for 2 min at 1,000 rpm. The supernatant removed and resuspend in 1 mL wash buffer containing 50 mM sodium phosphate, 300 mM sodium chloride, 10 mM Imidazole, pH 7.4. This was spun and wash buffer removed. Washes were repeated three more times. Elution occurred in 250 µL filter sterilized Elution buffer (50 mM sodium phosphate, 300 mM sodium chloride, pH 7.4, 300 mM Imidazole) for 10 min. The supernatant was spun down and saved. The elution was repeated with additional 250 µL elution buffer. Concentration was determined by NanoDrop A280 (ThermoScientific). The purity was determined by SDS-PAGE.

2.3.5 Soluble scFv ELISA

Plates were coated with 50 ng/well NeutrAvidin™ or BSA, overnight at 4°C. The plates were washed in PBST and 50 µL of 50 ng/well biotinylated peptide was added and incubated for 1 h. After washing, 200 µL of 5% Non-Fat Dried Milk in PBST was added to block the wells for 1 h. This was followed by washing in PBST and PBS, and addition of 50 µL of the purified scFv antibody in PBS for 1 h with shaking. Wells were washed with PBST and 50 µL of ABTS in 50 mM Sodium Citrate pH 4, 0.03% Hydrogen Peroxide, was added to all wells. The color change was recorded at 405 nm with the microtiter plate reader.

2.3.6 Western blot of retinal lysates

Retinal lysates from rabbit (*Ortolagus cuniculus)* and mouse (*Mus musculus*) were obtained from Dr. Edward (SUMMA Health Systems) IRB #10-039 (Northeast Ohio Medical Universities, NEOMED). Chicken eyes (*Gallus gallus*) were purchased from a local Amish butcher (Alliance Poultry Farms (1636 W Chicago Ave, Chicago, IL.). Retinas and eyeballs were homogenized in 10 mM Tris-HCl, pH 7.4, 1 mM EDTA, and 200 mM Sucrose. Lysate was spun down and 5 µL of the supernatant used for SDS-PAGE and western blotting. Gel electrophoresis was performed in Tris-Glycine-SDS buffer on a 12% precast Mini-Protean TGX polyacrylamide gel (Bio-Rad), at 12 mA for 1.5 h. The protein was then transferred to PVDF membrane (Millipore) overnight at 25 V

in Tris-Glycine-SDS buffer with 20% Methanol. The membrane was blocked with 5% Non-Fat Dried Milk in PBST for 1 h. One PBST and one PBS wash was done for 5 min each. The anti-GBB5-H9 scFv was added at a concentration of 1 µg/mL in 25 mL PBS and incubated with shaking for 2 h. Blot was washed once with PBST and PBS for 5 min each The secondary antibody, anti-Flag-HRP M2 (Sigma-Aldrich), was diluted 1:5000 in PBS was incubated with blots for 1 h, with shaking. The blots were washed once with PBST and PBS for 5 min each. Detection was performed using ECL Plus reagent (GE) and imaged using a Storm 860 Phosphorimager (Molecular Dynamics).

2.3.7 Alanine scanning of GBB5 peptide

Thirteen versions of the GBB5 peptide were synthesized with alanine replacing each consecutive position, one at a time, in the peptide. The N-terminus contains a biotin molecule followed by a four amino acid linker composed of Gly-Ser-Gly-Ser. Of each peptide, 250 ng was immobilized in triplicate on a NeutrAvidin™ coated Nunc 96-well Maxisorp plate. The ELISA was conducted similar to the soluble ELISA above. After blocking with 1% casein (ThermoScientific), 50 ng of anti-GBB5-H9 scFv or anti-GBB5-A1 scFv was added in PBST for 1 h. The secondary antibody at 1:5,000 anti-FLAG-HRP in PBST was added for 1 h. The signal was detected with ABTS and read at 405 nm in the microtiter plate reader.

2.3.8 scFv-FC expression

The plasmid pBIOCAM5 (27) containing the Fragment crystallizable sequence (Fc) of the human Immunoglobulin G was a gift from Dr. John McCafferty (University of Cambridge, UK). This construct contained a CMV promoter for expression in HEK-293 Freestyle cells, the constant C_{H2}-C_{H3} regions of the human Fc followed by a six histidine tag and a C-terminal tri-FLAG Tag. The H9 scFv was sub-cloned upstream of the Fc through the *NcoI* and *NotI* restriction sites. The Fc contains cysteine residues to form homodimers through disulfide bond formation.

Using standard cell culturing techniques, HEK-293 F' (Invitrogen) cells were grown as a 50 mL suspension in Freestyle™ 293 serum-free media (Gibco) to a density of 1x10^6 cells/mL at 37°C, in 10% CO_2,140 rpm rotation. After 2 passages, the cells were transiently transfected using 20 µg of 0.2 um filter sterilized pBIOCAM5 DNA and 50 µL of 1 mg/mL Polyethylenimine 25 kDa (Polysciences Inc.), vortexed and incubated for 10 min at room temperature. Cells were returned to the 250 mL flask and shaken for seven days. The cells were harvested and the supernatant recovered. cOmplete EDTA-free protease inhibitor cocktail (Roche Applied Science) was added and the scFv-Fc antibodies purified in batch with Clontech His-60 Ni Superflow™ resin as described earlier. Eluted in filter sterilized Elution buffer (50 mM sodium phosphate, 300 mM sodium chloride, pH 7.4, 300mM Imidazole) and stored at 4°C.

2.3.9 Generation of peptide-MBP fusion control

Primers were designed to include the DNA sequence of the peptide during the PCR amplification of the maltose binding protein (MBP) in the pAT224 vector (gift from Dr. Andreas Plückthun, University of Zurich, Zurich, Switzerland; GenBank #AY327139). The forward oligonucleotide was synthesized (Integrated DNA Technologies) to contain from 5' → 3': the *NcoI* restriction site, the *E. coli* codon optimized sequence encoding the biomarker peptide, and 20 bases of complementary sequence to allow hybridization to the vector and PCR priming. Forward primers included 8 additional bases on the 5' end to allow for restriction digest of the amplicon. The primers used are from 5'→3'. GBB5fwd: (ATTATATTCCATGGCCAAACTGCATGATGTGGAACTGCATCAGGTGGCGGAACGCGTGGGGAAAACTGAAGAAGGTAAACTGGT); RGS9fwd: (ATTATATTCCATGGCCAAACTGGTGGAAGTGCCGACCAAAATGCGCGTGGGGAAAACTGAAGAAGGTAAACTGGT); CNGA3fwd: (ATTATATTCCATGGCCCGCCTGACCCGCCTGGAAAGCCAGATGAACCGCCGCTGCTGCGGCTTTAGCCCGGATCGCGAAGGGAAAACTGAAGAAGGTAAACTGGT). The reverse primer anneals downstream of the 3' end of the MBP sequence and the amplicon will include the *HindIII* site for sub-cloning purposes (CGTTCTGAACAAATCCAGATGGAGT).

The reaction was performed with 0.3 µM of the forward and reverse primers, 300 ng pAT224-MBP template, 1.25 U of AccuPrime™ Pfx DNA Polymerase (Invitrogen), supplied buffer (includes dNTPs), in 25 µL total volume. Cycling is as follows: denature 2 min at 95°C, denature 15 sec at 95°C, anneal 30 sec at 55°C, elongate 85 sec at 68°C, cycle back to step 2 for 29 more times, final elongation at 68°C for 5 min. The reaction was purified with the PCR clean-up kit (QIAquick, Qiagen) and both the amplicon and pAT224-MBP were digested with *NcoI* and *HindIII* restriction enzymes (NEB). After gel purification (QIAquick, Qiagen) the vector and amplicons were ligated at a 1:9 ratio (vector:insert) using 100 U of T4 DNA Ligase (NEB) in 20 µL total volume and incubated at 16°C overnight. The reactions were spot dialyzed and electroporated into electrocompetent XL-1 Blue cells and plated on LB/Cb overnight at 30°C.

Upon sequence confirmation, the recombinants were grown to OD_{600}=0.7 and induced with 500 µM IPTG for 6 h at 37°C. Cells were pelleted and freeze-thawed at -80°C before sonication. The cleared lysate was batch incubated with Ni-NTA resin (Qiagen) for 5 h at 4°C. Protein was purified using washes of PBS + 10mM immidazole and elution into 500mM immidazole, 20 mM Tris-HCl, 500mM NaCl. Fractions were stored with 30% glycerol at -20°C. Expected size is 46.2 kilodaltons (kDa).

2.3.10 Comparison of scFv with scFv-Fc

The GBB5-MBP control protein was run on a 12% precast Mini-Protean TGX polyacrylamide gel (Bio-Rad) in Tris-Glycine-SDS buffer, at 12 mA for 1.5 h. The protein was then transferred to Polyvinylidene fluoride (PVDF) membrane (Millipore) overnight (12 h) at 25 V in Tris-Glycine-SDS buffer with 20% Methanol. The membrane was blocked with 5% Non-Fat Dried Milk in PBST for 1 h. One PBST and one PBS wash was done for 5 min each. The anti-GBB5-H9 scFv and the anti-GBB5-H9 scFv-Fc version was added at a concentration of 1 µg/mL in 25 mL PBS and incubated with shaking for 2 h. Blot was washed once with PBST and PBS for 5 min each. The secondary antibody 1:5,000 anti-FLAG-HRP M2 (Sigma-Aldrich) in PBS was added to the blot and incubated for 1 h while shaking. The blots were washed once with PBST and PBS for 5 min each. Detection was performed using ECL Prime reagent (GE) and imaged using a Storm 860 Phosphorimager (Molecular Dynamics).

The ELISA was performed as mentioned earlier. Briefly, 50 µL of 15 nM NeutrAvidin™ was coated on 96-well Maxisorp microtiter plates overnight at 4°C. Wells were blocked with 1% casein in PBS. The peptides were immobilized in 50 µL of PBST at 25 nM. The scFv was added in 50 µL volumes of PBST at 30 nM and the Fc was added at 10 nM. Recombinant antibodies were detected with anti-FLAG-HRP, developed with ABTS, and read at 405 nm.

2.3.11 Affinity estimate by photonic crystal biosensor

The SRU Biosystems BIND® Explorer photonic crystal biosensor was used to detect real-time and label-free binding of scFv antibody to the target peptide (28). The provided software program, Experiment Management System (EMS) V2.1, recorded the data and directed the instrument reads. 50 ng/well of peptide in PBS was immobilized onto Streptavidin coated 96-well plate-based photonic biosensors and the binding response allowed to baseline defined by a change of less than 5 pm/minute. The wells were washed with PBST and PBS, and then blocked with filtered 5% BSA in PBS for 1 h. After washing with PBST and PBS, the wells were allowed to come to equilibrium in 50 µL of elution buffer (EB) per well. For each scFv antibody, 50 µL of decreasing concentration was added to 7 wells, and the binding responses recorded after traces had come to a plateau. Overnight end-point values of change in peak wavelength were used to draw the response curve. Data was analyzed using the instrument software or through OriginPro 8.5 graphing software.

2.3.12 Real-time detection chemical biotinylation of anti-GBB5-H9 scFv

The SRU Biosystems BIND® Explorer photonic crystal biosensor reader was used to detect real-time biotinylation of the scFv antibody. The software program Experiment Management System (EMS) V2.1 recorded the data and directed the instrument reads. Peak Wavelength changes were recorded in picometers (pm). After

plate initial equilibration with PBS, 10 µg/mL of the GBB5 peptide in PBS was immobilized onto Streptavidin coated 96-well plate-based biosensors and the binding response allowed to baseline defined by a change of less than 5 pm/minute. The wells were washed with PBST and PBS, and then blocked with filtered 5% BSA in PBS for 1 h. After washing with PBST and PBS, the wells were allowed to come to equilibrium in 50 µL PBS per well. The scFv antibody was added at 0.5 mg/mL (50 µL) to wells containing with the target peptide. After 1 h of binding, the scFv still in solution was removed and the well filled with PBS. Equilibration was observed for 1 h. For chemical biotinylation, 20 M excess EZ-Link® sulfo-NHS-LC-Biotin (ThermoScientific) was added to the scFv well and a control well with only peptide target. Binding was recorded for an additional 2 h. Overnight end-point values of change in peak wavelength were used to draw the response curve.

2.3.13 Electrochemical detection

Two ElectraSense MX300 automated microarray readers were loaned to UIC by the CustomArray Corporation (formerly CombiMatrix, Mukilteo, WA). Training on the device was kindly provided by Mr. John Cooper (Co-founder and Principal Scientist at CustomArray). 12K CustomArray CMOS microchips containing 12,544 individually addressable electrodes were purchased for the assays. Using a computer controlled robotic fluid handling system, 0.1 M pyrrole (Sigma) was deposited on select sets of 5 x

25 electrodes on each quadrant of the 12K chip and 50 µg of antibody in PBS immobilized on the polymerized pyrrole. This process was repeated serially for every different antibody on the chip. To detect TNF-α, the capture antibody (R&D Systems) monoclonal antibody was immobilized and the target protein TNF-α was added in increasing concentrations to each quadrant. The biotinylated detection TNF-α monoclonal antibody was added with a subsequent addition of 1:1000 Poly-80-SA-HRP conjugate (Fitzgerald Industries) in PBST + 1% casein. After washing in the TMB Rinse Solution (BioFx), the electrochemical current was generated by adding the HRP substrate 3,3',5,5'-tetramethylbenzidene (TMB)(BioFx) with hydrogen peroxide. Electrical current signal was recorded by the ElectraSense instrument software hw94_6.3.2 and analyzed by the ElectraSense hw94_5.6.3 software. For the scFv experiments, there was no detection antibody. The scFv was immobilized on the polypyrrole. The biotinylated peptide was added and the peptide detected using the Poly-80-SA-HRP.

2.3.14 Fluorescence microscopy

The anti-GBB5-H9-scFv was cloned into a pKP300ΔIII bacterial expression vector containing a C-terminal Avitag™ with sequence: GLNDIFEAQKIEWHE (Avidity LLC) for site specific mono-biotinylation. The site was biotinylated *in vitro* by the biotin

ligase BirA enzyme (Avidity LLC) for 1 h at 30°C. Excess free biotin was removed by dialysis into 300 mM Imidazole, 300 mM NaCl, and 20 µM Tris-HCl, pH 7.3.

Whole mouse (*Mus musculus*) eye sections were obtained from collaborators Deepak Edwards and Rachida Bouhenni (SUMMA Health Systems, Akron, OH) IRB #10-039. Eyes were fixed in 4% Paraformaldehyde (Sigma-Aldrich) at room temperature for 1 h and then washed four times with PBS. The eyes were incubated in 15% sucrose overnight at 4°C. This was repeated with 30% sucrose. Tissue imbedding was performed in Optimal Cutting Temperature compound (OCT)(Tissue-Tek®) and frozen on dry ice. Sectioning was performed in a Minotome cryostat (International Equipment Company) at -20°C at a thickness setting of 8. The eyes were sectioned along the sagittal plane as to preserve the cell layers of the retina. Sections were stored on glass slides at -20°C until ready for staining.

Slides were warmed to 37°C for 15 min and washed twice with PBS. Slides were kept in a humidity chamber throughout the procedure. The slides were blocked for 1 h at room temperature in 10% Fetal Calf Serum (Gibco®, Life Technologies™), 1 % BSA (Sigma) in PBS then washed two times 5 min in PBS. Primary anti-GBB5-H9-Avi tagged antibody was antibody was diluted at 1 µg/mL into 0.5 mL of 1% Fetal Calf Serum, 0.1 % BSA in PBS and incubated for 1 h at room temp. Anti-Rhodopsin (Abcam), biotinylated by Sulfo-NHS-LC-Biotin (Pierce), was used as a control at 1 µg/mL concentration. The slides were washed once with PBS for 5 min. To allow fluorescent

detection, 1:50 Streptavidin Cy5 (Life Technologies™) with excitation at wavelength 600-650 nm and emission at 670 nm, was incubated with the retinal sections for 1 h at room temperature. Slides were washed twice with PBS for 5 min. Coverslips were mounted with Vectashield mounting medium with DAPI (Vector Laboratories). Slides were visualized on an Olympus Fluorescent microscope with FITC, DAPI, and Cy5 filters. Images were captured using a SPOT™ RT3 2 MP SLIDER digital microscope camera (SPOT™ Imaging Solutions, Diagnostic Instruments, Inc.).

For antigen recovery, the procedure was followed as described above, with this exception: the sections were heated to 96-96°C in DAKO target retrieval Solution (Agilent Technologies) for 10 min before the first blocking step. Slides were allowed to cool to room temperature before proceeding.

2.4 Results and discussion

2.4.1 Phage-display selection on peptide biomarkers

Retinal injury peptides, identified by liquid chromatography tandem mass spectrometry (Edwards and Bouhenni, personal communication), were used as targets for recombinant antibody generation. The protein targets chosen were Calcium Channel Voltage-Dependent, L-type, Alpha 1 subunit (CACNA1F), Cyclic Nucleotide Gated Channel Alpha 3 (CNGA3), Guanine Nucleotide-Binding Protein Beta 5 (GBB5), and

Regulator of G-protein Signaling 9 (RGS9). These were chosen because they were identified to be present and intact in the serum of rabbits with laser induced retinal damage. The state of the remainder of the protein is unknown and may become degraded as it circulates through the rabbit's system. Therefore, an antibody selected to bind to a conformational epitope of the full protein, may not recognize the circulating protein. In addition, we wanted to generate reagents that could work in the sensitive detection method, Stable Isotope Standards and Capture by Anti-Peptide Antibodies (SISCAPA) (29) in a multiple reaction monitoring assay, where digested biomarker proteins are antibody enriched from a sample before quantitative mass spectrometry. The putative biomarkers were also known to be highly expressed in the retina and the commercially available antibodies for the proteins were of poor quality.

After three rounds of phage-display selection on peptide targets, multiple scFv antibodies were isolated for each (**Table I**). Clones with signal intensities of at least two-fold over background were chosen for further characterization. We decided to focus on the GBB5 peptide target since it became apparent that it was the most promising of the putative biomarkers and generated the most scFv binders. From the crystal structure of the GBB5 in complex with the RGS9 (Protein Data Bank entry 2PBI), it appears that the peptide sequence, which we used as the selection target for generating a cognate scFv, is exposed on the surface of the protein. Therefore, it is potentially available for scFv interaction. The phage ELISA of the anti-GBB5 clones demonstrates the displayed scFvs bind specifically to their target (**Fig. 9**).

TABLE I. SUMMARY OF PUTATIVE BIOMARKER PEPTIDES AND ANTIBODIES GENERATED

Biomarker[a]	Peptide Target	Organism Match[b]	# of AAs	# of Ab Clones[c]
CACNA1F Peptide 1: Voltage Dependent Calcium Channel	IRWFSHSTR	Human, Rat, Mouse	9	4
CACNA1F Peptide 3: Voltage Dependent Calcium Channel	TEGNLEQANQELRIVIK	Human	17	4
CNGA3: Cyclic nucleotide gated channel	RLTRLESQMNRRCCGFSPDRE	Mouse	21	8
GBB5: Guanine nucleotide-binding protein	KLHDVELHQVAERV	Human, Rat, Mouse	14	6
RGS9: Regulator of G-protein	KLVEVPTKMRV	Rat	11	3

[a]The biomarker is the full protein matched to the peptide target that was discovered by MS.
[b]The organism match are the animals the peptide is orthologous to in addition to rabbit.
[c]The number of clones is defined by scFvs with unique sequences that bind specifically to their target peptide.

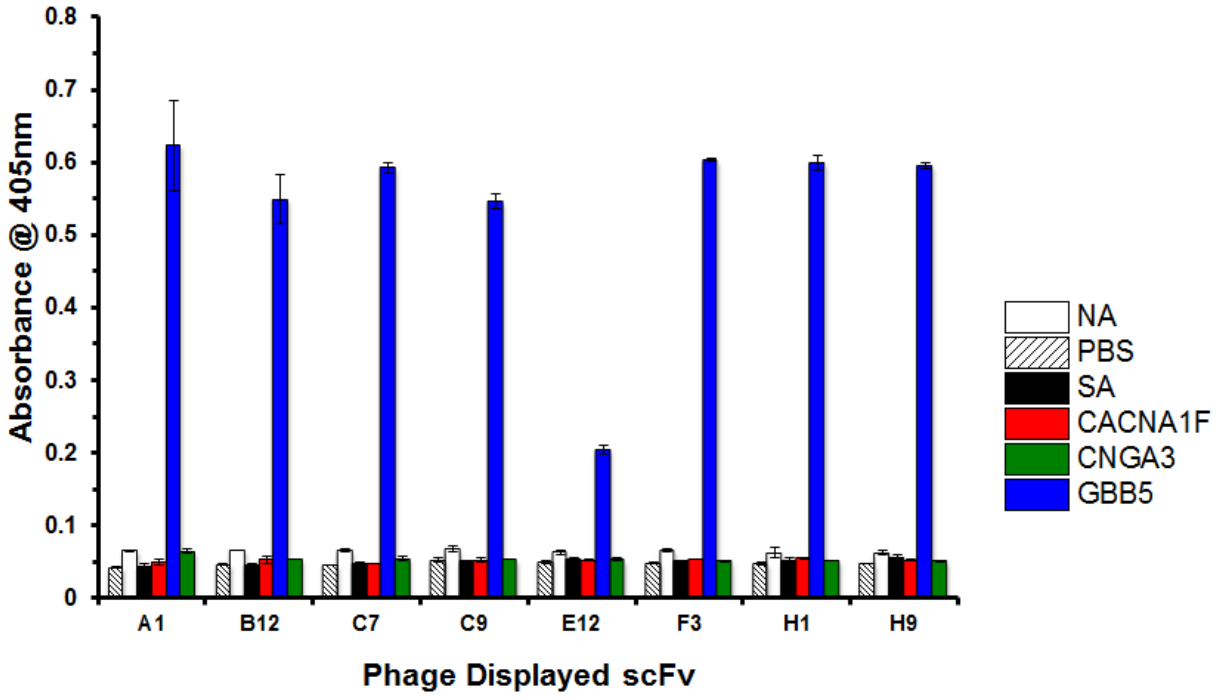

Figure 9. Phage ELISA of selection against GBB5 peptide. ScFv antibodies raised against the GBB5 peptide are displayed on phage and used to probe peptides in an ELISA. The phage-displayed scFvs are named according to the well of the 96-well screen in which they were originally found. Specificity is determined by the intensity of the absorbance signal for the target peptide (GBB5) compared to the background NeutrAvidin™ (NA), Streptavidin (SA), Phosphate Buffered Saline (PBS), and peptides corresponding to retinal proteins CACNA1F and CNGA3.

Upon sub-cloning coding regions into a low-phosphate induced expression vector pKP300DIII and electroporation into TG-1 *E. coli*, the bacterially expressed scFv antibodies retained the specificity they were selected to have for the peptide targets. As seen in the ELISA of five soluble scFvs selected against five different biomarker peptides, the scFvs give a signal 4-10 times over the background (**Fig. 10**).

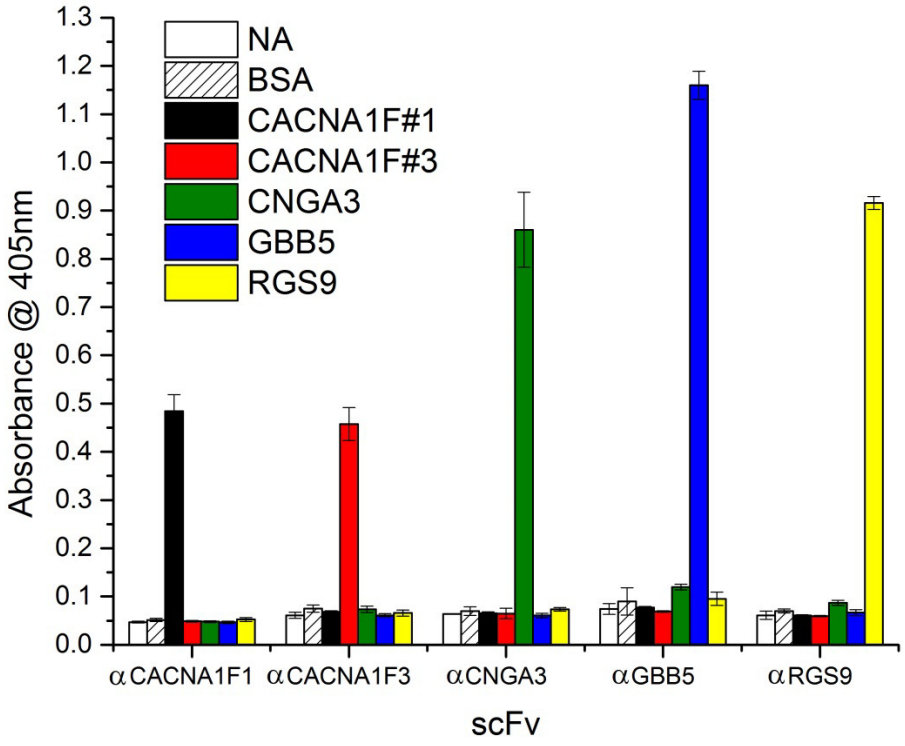

Figure 10. Five scFvs in a soluble ELISA retain their specificity. After sub-cloning of the scFv from the phagemid into the bacterial expression vector, these five scFvs were expressed and purified. An ELISA was performed against all biomarker peptides available to demonstrate the specificity of each antibody.

2.4.2 Affinity estimates using photonic crystal biosensor

The photonic crystal binding assay was utilized here to estimate the binding affinities through end-point readings similar to an ELISA with a chromogenic output. Binding constant (K_D) determinations were estimated by fitting a dose response curve and calculating the Effective Concentration at 50% level (EC_{50}) to be ~300 nM (**Fig. 11**). The K_D estimates for the scFvs against the other biomarkers are shown (**Table II**). The highest affinity scFv was the anti-GBB5-H9, which was about 10-fold greater than the others. Although the difference between the GBB5 binders H9 and A1 is not apparent from the Phage ELISA (**Fig. 9**), the affinity is 10-fold greater in the H9 and recognizes the full length protein in western blot. This result is interesting to note that single-concentration phage ELISAs are not indicative of binding strength to some degree. Titrating antibody, target, or adding in a competitor in solution are better measures of affinity.

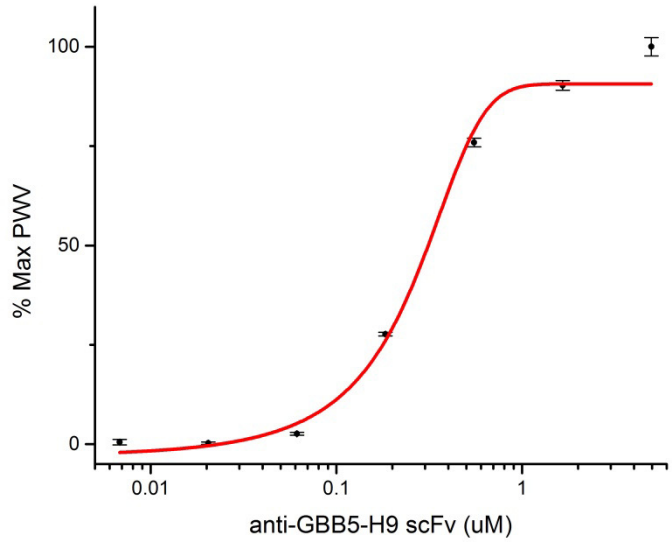

Figure 11. Photonic crystal binding curve. The anti-GBB5-scFv H9 was titrated across wells of a streptavidin coated photonic crystal 96-well microtiter biosensor plate with the GBB5 peptide immobilized on the surface. Using the BIND reader, real-time and label-free binding was recoded until the change in peak wavelength plateaued. Plotting the percentage of the max peak wavelength to the log concentration of the scFv, gives a sigmoidal dose response curve. The EC_{50} of ~ 300 nM was used to estimate binding affinity.

TABLE II. SUMMARY OF EC_{50} VALUES USING THE PHOTONIC CRYSTAL BINDING ASSAY

scFv	Estimated EC_{50} [a]	ELISA	Western
anti-GBB5-H9	306 nM	✓	✓
anti-GBB5-A1	4-6 μM	✓	x
anti-RGS9-A5	2-3 μM	✓	x
anti-RGS9-H1	2-3 μM	✓	x
anti-CNGA3-A6	2-8 μM	✓	n.d.
anti-CNGA3-C9	2-3 μM	✓	n.d.

[a] EC_{50} is the Effective concentration at 50% used here as an estimate of binding affinity.
✓ = successful implementation in assay.
X= failed in assay.
n.d=not determined.

2.4.3 Detection of the cognate protein in western blot

To determine the ability of the anti-GBB5-H9 scFv to recognize the endogenous, cognate protein of the peptide, western blotting was performed on retinal lysates. Retinal lysates from chicken (*Gallus gallus*), rabbit (*Oryctolagus cuniculus*), and mice (*Mus musculus*), were probed with 1 μg/mL of the anti-GBB5-H9-scFv antibody (**Fig. 12**). These three organisms, including humans, contain identical peptide sequences in the orthologous GBB5 photoreceptor protein, which the antibody was selected against.

The expected molecular mass of the GBB5 protein is ~39 kDa. Specific recognition can be seen at the 40 kDa band of the standard protein. Additional bands can be attributed to secondary antibody binding as seen in the adjacent panel. Unfortunately long wash steps reduced the primary antibody to undetectable levels, consistent with observations made with the photonic crystal biosensor. The micromolar affinity antibody, even with very brief rinses, gave no signal by western blot (data not shown) indicating the scFv is washed quickly away because of its fast K_{off}.

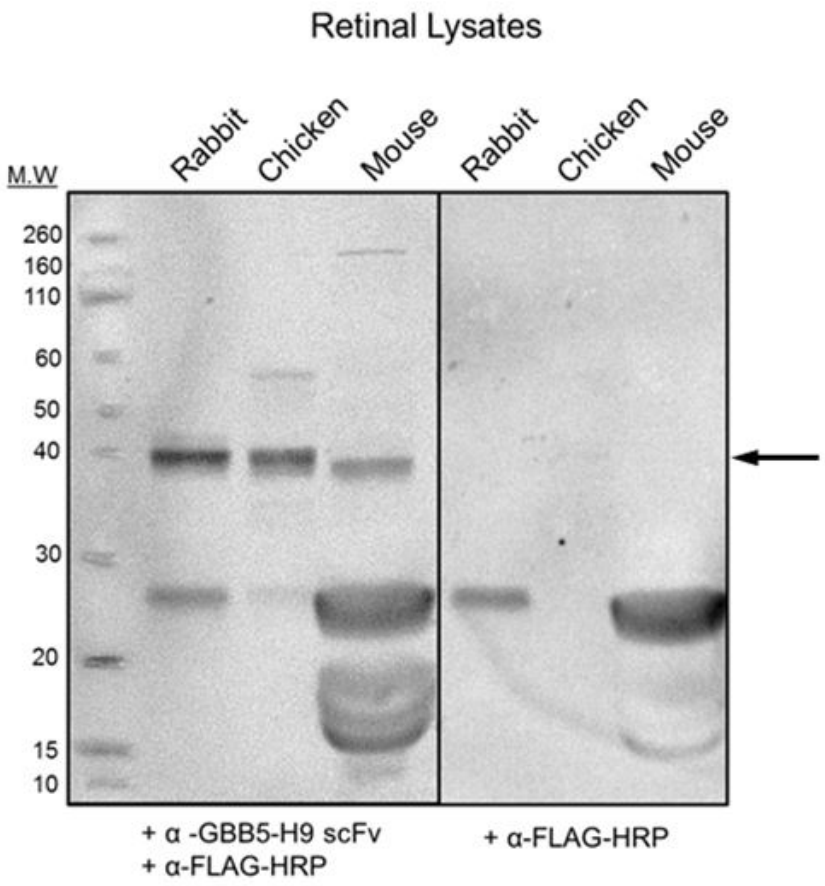

Figure 12. Western blot of retinal lysates. The anti-GBB5-scFv H9 was used to probe retinal lysates from three organisms. GBB5 expected size in rabbit and mouse is 38.7 kDa. Expected size of chicken GBB5 is 38.8 kDa. The left panel is probed with the scFv antibody and the secondary anti-FLAG-HRP antibody. The right panel is the control, probed with the secondary antibody only. Total lysate loaded for rabbit, chicken, and mouse were ~35 µg, ~35 µg, and ~ 50 µg respectively.

2.4.4 Alanine scanning of anti-GBB5 scFvs

To determine which residues of the GBB5 peptide are important for the recognition by two anti-GBB5 scFvs, we synthesized a set of 13 peptides with each subsequent amino acid position mutated to a single alanine per peptide. By immobilizing the peptides and performing an ELISA, we could determine the chromogenic signal generated for each compared to the original. Therefore any decrease in binding could be attributed to the alanine replacing a residue in the peptide that contributes to recognition by the scFv. Important peptide residues for the tight binding H9 clone can be compared to the weaker binding A1 clone (**Fig. 13A**).). Both reagents interact strongly with the negatively charged polar Aspartic Acid, the hydrophobic middle Leucine, and the positively charged polar Histidine (underlined), where mutation of any one of these residues with an Alanine, results in loss of recognition. The main difference between the tight binding, nanomolar affinity clone H9 and the micromolar binding clone A1, is a single residue of the peptide for each (**Fig. 13b**). The tight H9 clone interacts strongly with the positively charged Arginine on the c-terminus of the peptide (red). The A1 instead requires the positively charged Lysine on the n-terminus (red). This difference renders the A1 reagent too weak to be useful in a western blot. Looking at the Complementarity Determining Regions (CDRs) of the two scFvs themselves (**Appendix A**), they are only 40%, similar which is not surprising considering the various families of V_H and V_L present in the germ-line used for library construction (24).

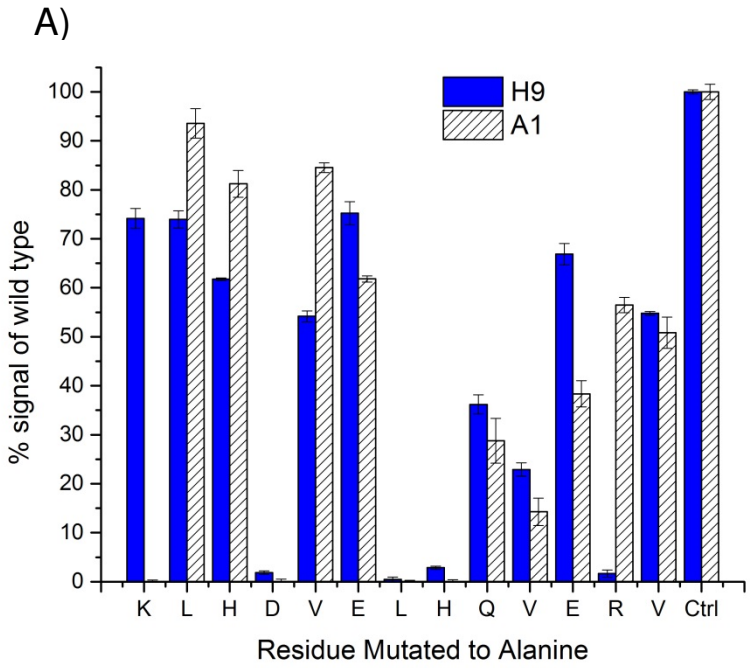

B)

H9: KLHDVELHQVAERV

A1: KLHDVELHQVAERV

Figure 13. Alanine scanning of important residues. A series of GBB5 peptides were synthesized containing one alanine residues inserted at each consecutive position per peptide. The position with an alanine already present was left un-mutated. Two anti-GBB5 scFvs were used in the ELISA. The H9 had a ~300 nM K_D, while the A1 had a 4-6 μM K_D. Complete loss of signal for each mutation, as compared to the wild-type control (Ctrl), was deemed a critical residue (A). The critical residues are summarized in (B) as underlined. The antibodies recognize 4-9 residues with the three overlapping residues being most important (D, L, and H). The red font highlights the different crucial residues for H9 binding as compared to the A1. Gray font indicates a > 50% reduction in signal when mutated, but not completely knocked out.

2.4.5 Comparison of scFv with scFv-Fc

To improve the usefulness of the anti-GBB5-H9 scFv, we decided to dimerize the antibody by sub-cloning the H9 sequence into a vector that would fuse the scFv to a Fc C_{H2}-C_{H3} region from a human IgG (30). Other groups (31) have demonstrated the utility of this approach in enhancing the apparent affinity of scFvs through avidity. Subsequent transient transfection and extracellular expression in the human cell line, HEK-293, allowed for fast and easy purification from the culture media. Free cysteines in the Fc will form disulfide bonds in an intermolecular oxidation to form a dimerized scFv. This would increase the functional affinity through avidity as described in previous investigations (31). The enhancement would only be apparent when probing an immobilized target protein where the antigenic regions are close enough in proximity to allow simultaneous binding by both recognition epitopes of the dimer. When comparing 30 nM of monomer scFv to the 10 nM of dimerized scFv-Fc, the signal strength in ELISA of immobilized GBB5 peptide was about 3.5-fold higher for the scFv-Fc indicating the functional affinity had been improved by the dimerization (**Fig. 14A**). We then compared the two formats in western blot since it would likely be this application that would allow validation of the GBB5 protein as an injury biomarker. However, full length recombinant GBB5 protein was difficult to express and the synthesized peptide of ~2 kDa, was too small to resolve on SDS-PAGE. To circumvent this problem, a GBB5-peptide-MBP fusion protein was employed to determine this. This protein was essentially the 14 amino acids of the GBB5 peptide fused in frame to the N-terminus of

the Maltose Binding Protein and expressed as a single polypeptide. Descending concentrations of target show how the scFv-Fc format detects at a 25-fold lower limit (LOD=10 ng) than the scFv (LOD=250 ng) in western blot (**Fig. 14B**).

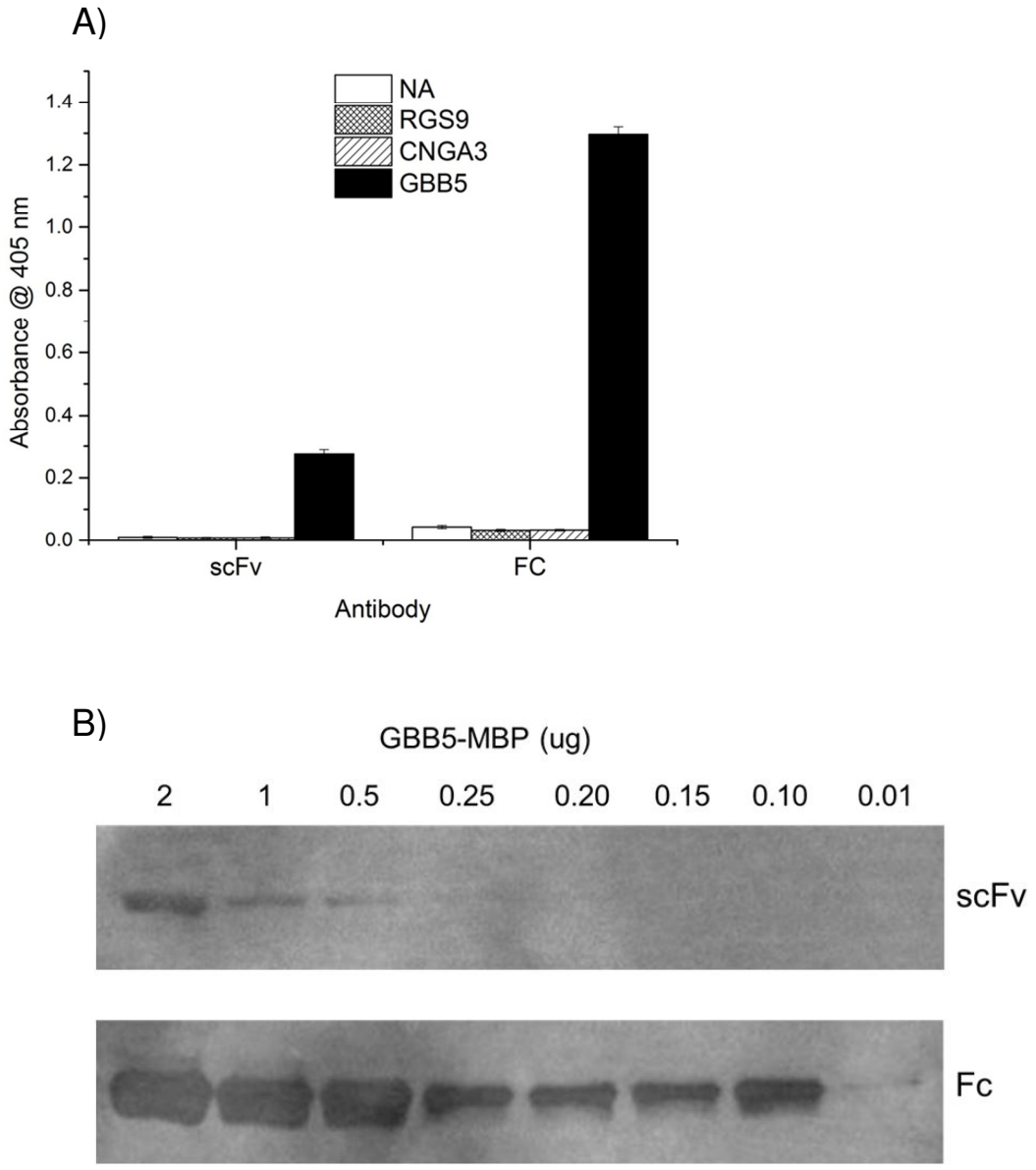

Figure 14. ELISA comparing scFv and the Fc format of the H9. (A) Target peptides are immobilized on a NeutrAvidin™ coated microtiter plate at 25 nM and assayed with 30 nM of monomeric *E. coli* expressed anti-GBB5 H9 scFv or 10 nM of the HEK expressed dimeric Fc format. The secondary antibody anti-FLAG-HRP is added and subsequent chromogenic reagent. Absorbance is recorded at 405 nm. (B) The GBB5-MBP fusion protein (46 kDa) is detected on PVDF membrane using the scFv or Fc format of the H9 clone. Amount loaded is in µg and decreases from left to right.

2.4.6 Real-time detection of chemical biotinylation of anti-GBB5-H9 scFv

For the scFv to be useful for applications like tissue staining and fluorescent microscopy, we needed to add a biotin molecule so we could take advantage of the extremely tight binding of secondary streptavidin conjugates. After performing a chemical biotinylation, we noticed the anti-GBB5-H9-scFv was no longer recognizing its peptide target. In a novel use of the photonic crystal biosensor, we attempted to indirectly observe chemical biotinylation of the anti-GBB5-H9 scFv in real-time. Since the instrument detects surface binding though the peak wavelength shift, it would also detect the loss of binding over time. From sequencing the scFv, it is known that the CDR2 of the Heavy chain (**Appendix A**) contains a Lysine residue. The chemical biotinylation kit reacts with a primary amine group found on the side-chain of Lysine amino acids. Labelling will inhibit any interactions between the side-chain and other proteins. Although the sulfo-NHS-LC-Biotin adds 556.59 Da to the size of a protein for every reaction with a Lysine, we observed a decrease Peak wavelength (PWV) shift during the reaction (**Fig. 15**). This equates to the Lysine at the recognition site of the scFv becoming chemically biotinylated as the antibody is in equilibrium, and subsequently losing its ability to bind to the peptide. In the control reaction, where there is no scFv, there is an increase in PWV when the biotinylation reagent is added. This is a direct measurement of the biotinylation on the immobilized GBB5 peptide. The peptide has a single Lysine residue on the N-terminus. This is not likely contributing to the decrease in the scFv binding since the alanine scanning does not identify the Lysine as

important for anti-GBB5-H9 scFv binding (**Fig. 13**). These results conclude that this particular scFv will become inactive if using chemistry that labels primary amines and experiments requiring a conjugation (biotin, fluorescent tag, or enzyme) has to be done by a different method.

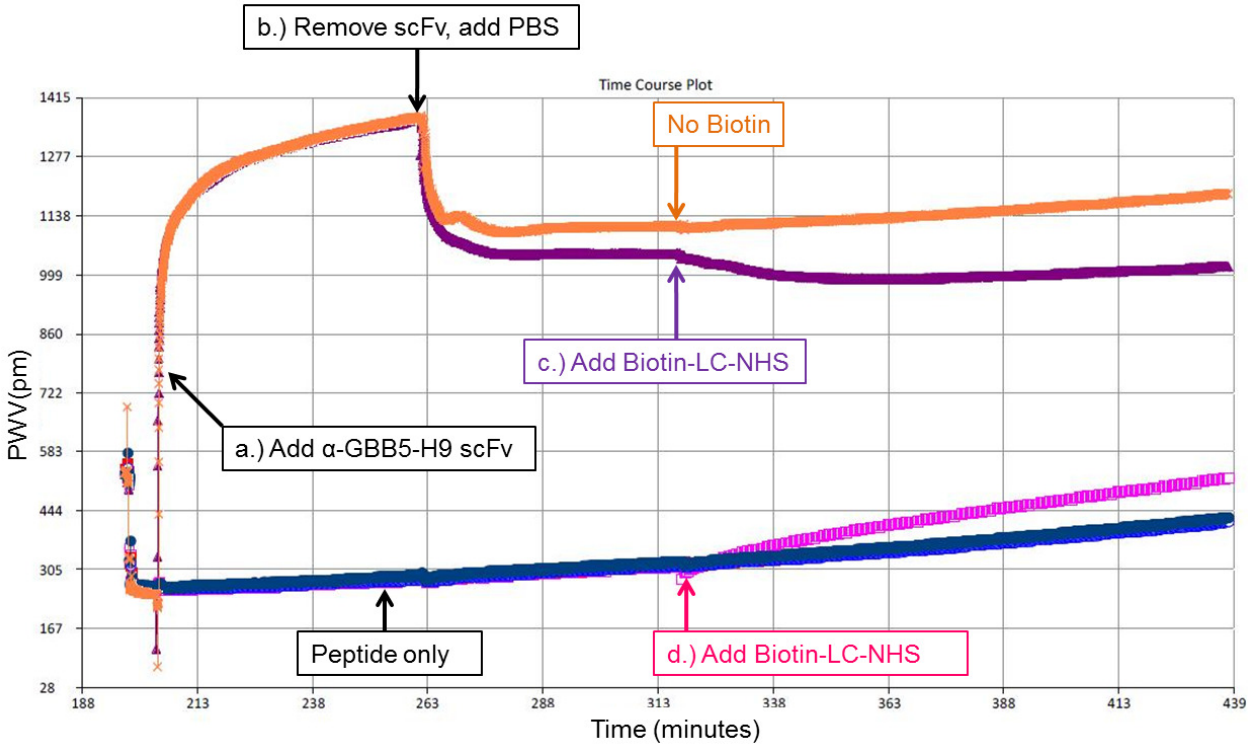

Figure 15. Real-time biotinylation of anti-GBB5-H9 scFv. The photonic crystal binding instrument was used to track the interaction of the anti-GBB5-H9 scFv to the GBB5-peptide. Traces are PWV shift data points taken every 1 second from a single well. All wells have the GBB5 peptide immobilized before data was recorded. To the orange and purple traces (a), the scFv was added and binding can be seen as an increase in PWV measured in picometers along the y-axis. The blue and pink traces are from wells with Peptide in PBS only and show no change. After an hour, the scFv was removed from the orange and purple wells (b) and allowed to baseline. The sulfo-NHS-LC-Biotin was added to the purple (c) and pink wells (d) and data recorded for two additional hours. Increases along the x-axis are equated to an increasing amount of protein binding to the surface.

Electrochemical detection

One aim of building a diagnostic for retinal damage was to also optimize the assay on a platform with the generated antibodies that is amenable to miniaturization and rapid detection. The original concept of the U.S. Air Force funded project was to use a hand-held platform that could quickly perform the assay automatically after sample is collected. To this end we chose to build the assay on an electrochemical detection platform of disposable semiconducting microchips (32). These microarray chips, originally designed for DNA hybridization (33), were tailored for protein detection by the CombiMatrix corporation who designed and engineered the instruments (34). To determine the lower detection limits of this system, we first chose to assay the human protein TNF-α using a commercial kit that provided the target, capture, and detection antibodies. The ElectraSense microarray reader provided by CombiMatrix was employed to detect electrical current generated from an electrochemical oxidation reductionreaction on the surface of polypyrrole deposited on electrodes, indicating the presence of target protein in a classic sandwich type ELISA. Detection limits achieved 100 pg/mL, with little background (**Fig. 16A and 16B**). When comparing this to the results from a traditional ELISA, we saw a ten-fold lower limit of detection with the electrochemical detection platform (**Fig. 16B and 16C**).

Next, the scFvs generated against the retinal biomarkers were implemented in the platform. Here, scFvs were immobilized to the poly-pyrrole, the Biotinylated target peptide captured, and the biotin of the peptide detected by a streptavidin-HRP

conjugate with 80 HRP molecules per streptavidin. Many of the scFvs did not work with direct immobilization. This was likely the result of the orientation at which they adsorbed, blocking the CDRs form binding to the target. The anti-CNGA3 scFv did successfully give a dose-response signal detecting down to 100 ng/mL (**Fig. 17**). This scFv was estimated to have poor affinity in the micromolar range, so it is presumed that a stronger binding antibody would give lower detection limits.

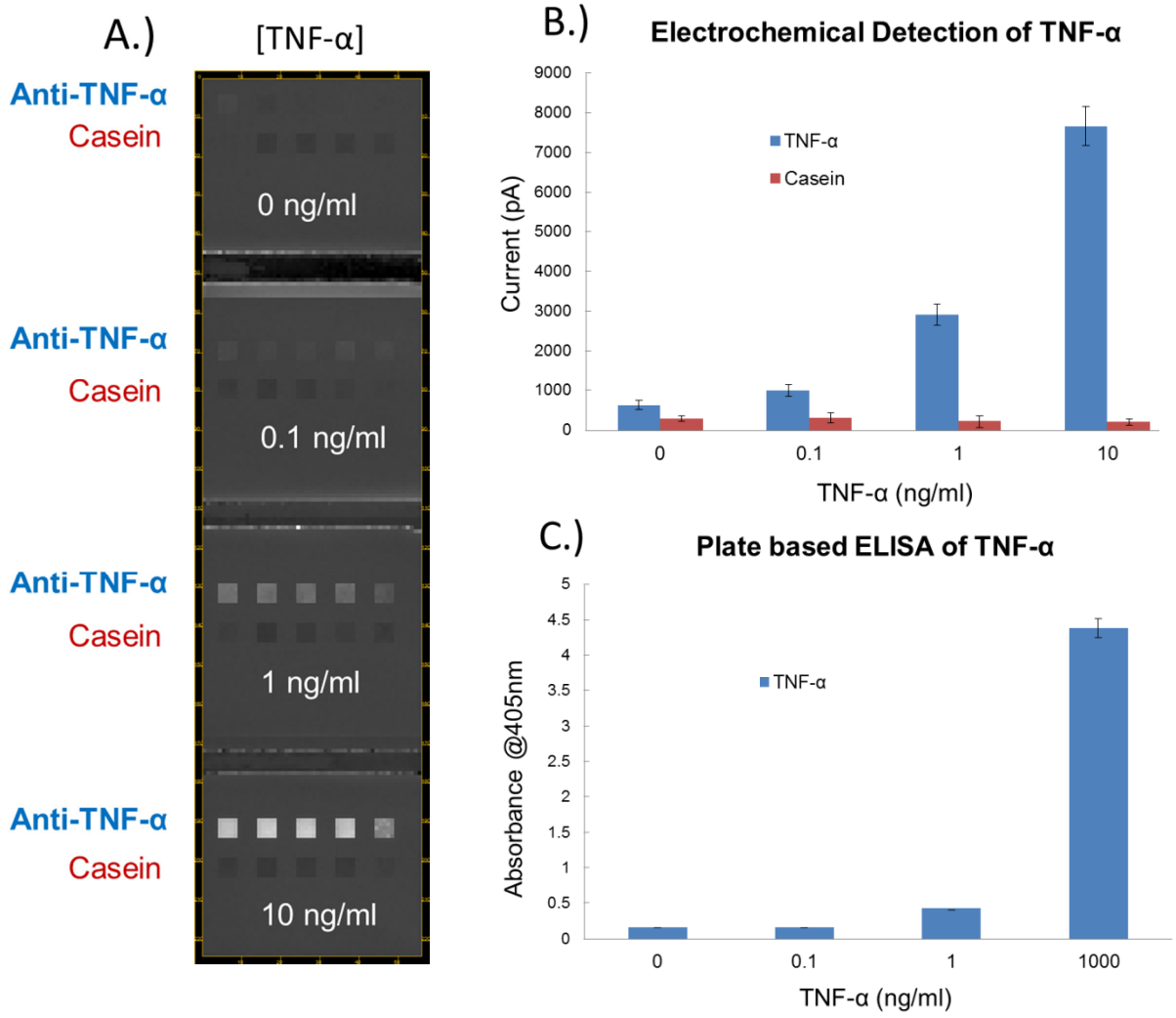

Figure 16. Electrochemical chip detection of TNF-α. A.)The computer generated image of the chip displaying the 12,544 electrodes. White coloring indicates greater current generated. Each square is 25 electrodes. Rows are deposited with a single concentration of antibody in 5 duplicate sets. Increasing concentrations of TNF-α were added to each vertical quadrant (white font). B.) The current generated in pico-amperes for each concentration of target protein versus the casein background. LDL is 0.1 ng/mL. C.) Comparison of the traditional plate based sandwich ELISA detecting the TNF-α down to a LDL of 1 ng/ml.

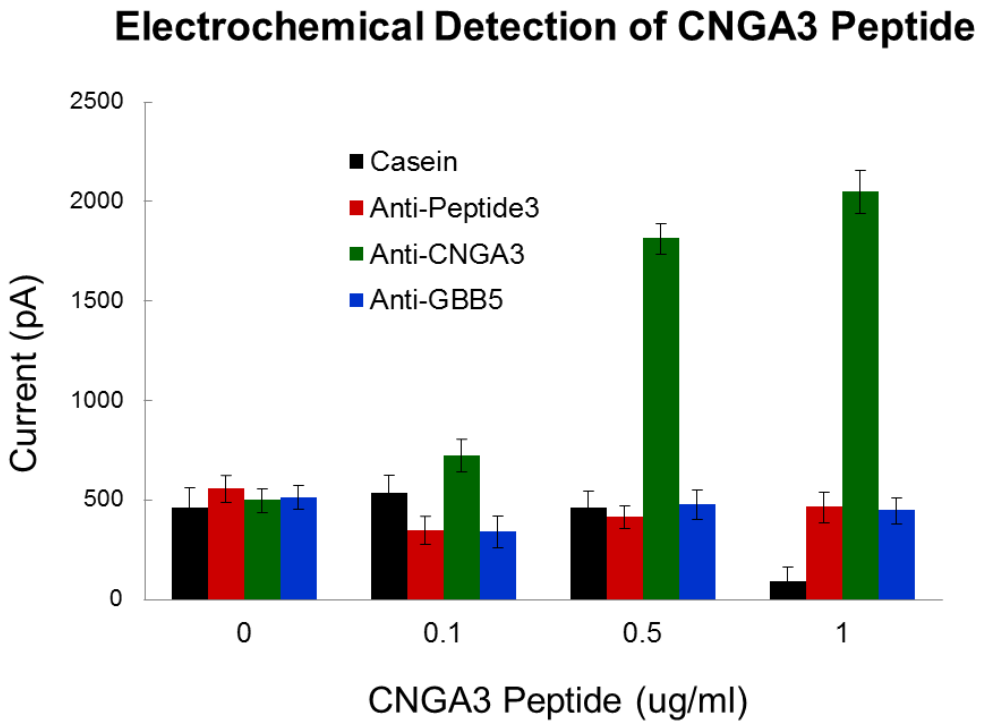

Figure 17. Electrochemical chip detection of CNGA3. Three scFvs (anti-CNGA3, anti-CACNA1F Peptide #3, anti-GBB5) were adsorbed at 50 µg each directly onto the poly-pyrrole, deposited on the electrodes of the microarray chip. The CNGA3 peptide was incubated with each set of antibodies at concentrations 0.1, 0.5, and 1 µg/ml. Current generated from the SA-80-HRP was recorded and plotted along the x-axis in pico-amperes. The LDL for the anti-CNGA3 was 0.1 µg/ml of peptide.

2.4.7 Fluorescence microscopy

To determine if the anti-GBB5-H9 scFv recognized the endogenous native GBB5 protein, we performed fluorescent microscopy of sectioned mouse retinal tissue. X-ray crystallography of the GBB5 in complex with the RGS9 showed the peptide sequence exposed PDB: 2PBI (35)(**Fig. 18**). Most of the residues identified by the alanine

scanning as being crucial for binding appear to be available. However, the Leucine side chain may be buried as is shown in (**Fig. 18D**).

We used the anti-Rhodopsin antibody as a positive control to locate the photoreceptor cell layer and to determine if the target proteins were available for antibody recognition. Originally we planned to use an anti-FLAG-FITC secondary antibody to detect the anti-GBB5-H9, however it was quickly realized that the photoreceptor layer had a high level of auto-fluorescence with the FITC and the Texas Red filters. The Cy5 filter however gave little auto-fluorescence but secondary antibodies with Cy5 fluorophore conjugations were not commercially available. To remedy this limitation, we biotinylated the antibodies either chemically for the anti-Rhodopsin, or enzymatically through the AviTag for the anti-GBB5-H9. This would allow detection by a Streptavidin with a Cy5 conjugation. It was expected for the GBB5 to be present in the photoreceptor cell layer as well as the inner plexiform layer and ganglion cell layer as described by earlier work (36) (**Fig. 19**). As shown in (**Fig. 20**) the anti-rhodopsin recognizes the photoreceptor cell layer (white Arrow), however there is background recognition by the streptavidin-Cy5 of the other layers of the retina. This is confirmed by the negative control of streptavidin-Cy5 only image. There is a clear distinction between the negative and positive controls. The experimental, probing with the anti-GBB5-H9-Avi shows no recognition of the photoreceptor layer. The intense background staining of the remaining layers masks any possible recognition of the inner plexiform or ganglion cell layer.

The failure could be attributed to the unavailability of the epitope while in the tissue. One way to resolve this is to perform antigen recovery by heating the tissue at 96°C in sodium citrate to denature the protein. Since the antibody recognized the GBB5 protein in western blot, it may only to bind to the linear epitope of the denatured protein.

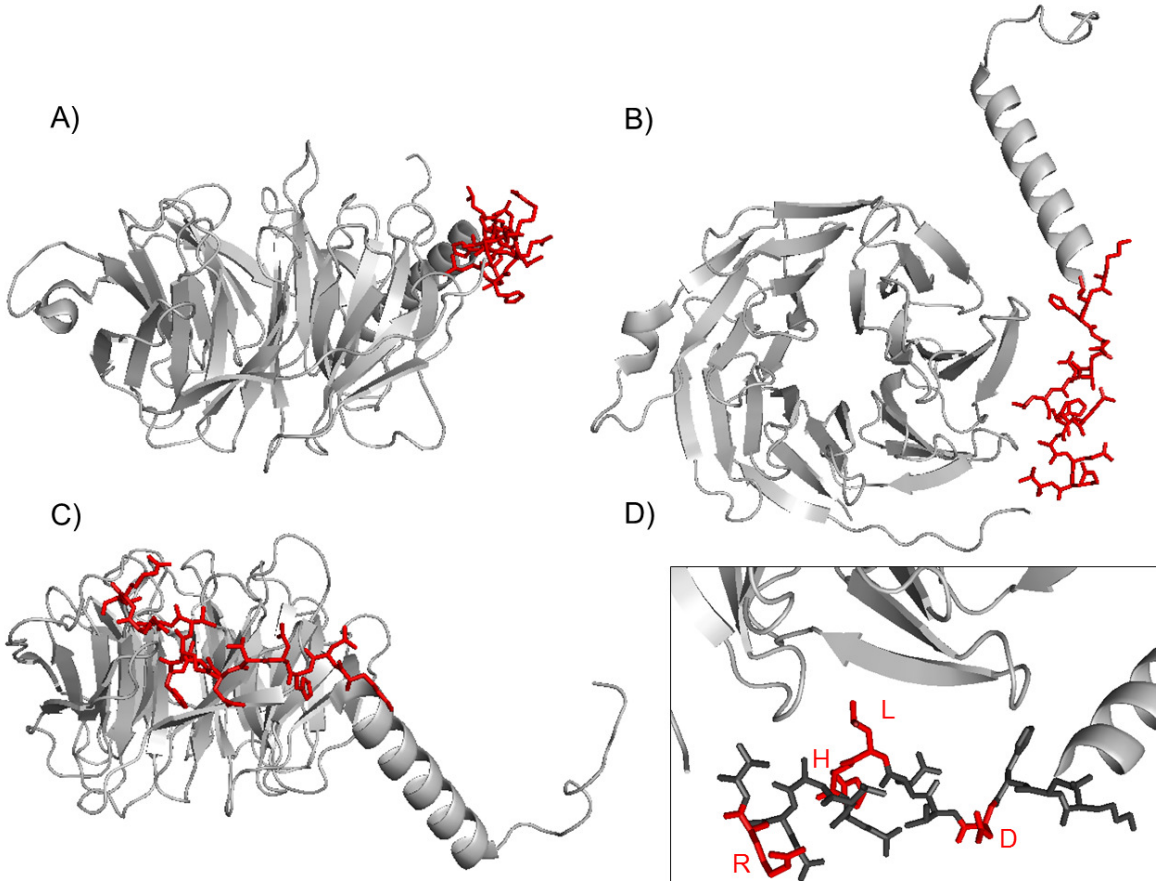

Figure 18. Crystal structure of GBB5 highlighting peptide. PyMol entry 2PBI of GBB5 protein in complex with RGS9 (RGS9 is hidden for clarity). Red amino acids highlight the peptide epitope used in the selection (A, B, C). In relation to the epitope A) Side view, B) top view, C) front view. D) Zoomed in area of the epitope, showing the crucial residues for binding in Red and labeled.

This gave lower background and a higher signal for the anti-rhodopsin antibody. However, the anti-GBB5-scFv still failed to show recognition in the photoreceptor cell layer. After further attempts with increasing amounts of antibody, changes in the Stretptavidin-Cy5 concentration, and slight modifications to the antigen recovery procedure, we can conclude that the antigenic epitope is hidden or in a conformation which the scFv cannot bind (data not shown).

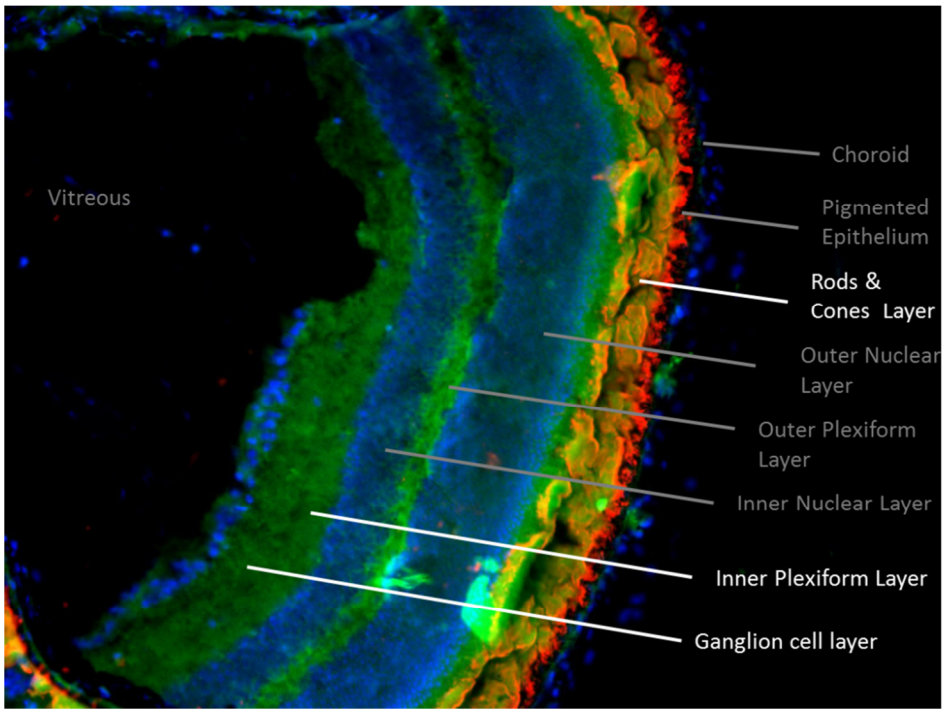

Figure 19. Composite image showing retinal tissue layers. A falsely colored microscopy image of fluorescent staining of the mouse retina. The layers of cells are indicated on the right. Images from three filters are merged. DAPI filter indicates the nuclei (blue). FITC filter shows autofluorescence (green). The Cy5 filter showing the photoreceptor layer as probed for rhodopsin (red).

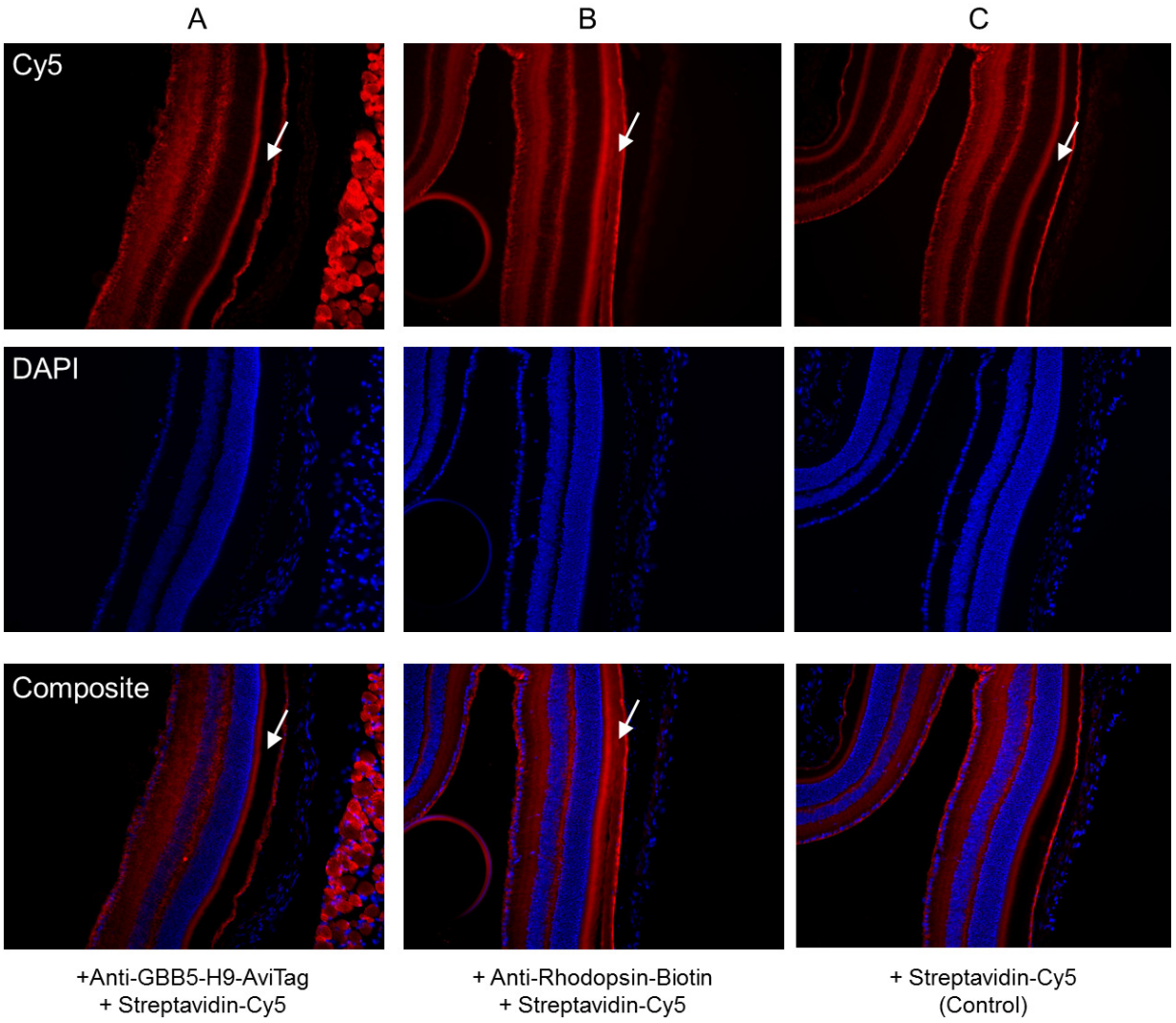

Figure 20. Fluorescence microscopy of retinal tissue. Mouse retinal tissue sections with streptavidin Cy5 as the fluorophore to show location of the primary antibody. Same orientation as Figure 19. White arrows indicate the photoreceptor layer where staining is expected. DAPI was used to identify the nuclei of the cells and for orientation purposes. A) The Biotinylated anti-GBB5-H9-scFv with Streptavidin-Cy5. B) The Biotinylated anti-Rhodopsin antibody with Streptavidin-Cy5. C) Streptavidin-Cy5, only background control.

2.5 Conclusion

In this study, we reported on using a scFv phage-display library to select for antibodies which bind specifically to short peptides. These peptides were implicated as biomarkers in a MS analysis of serum from rabbits that were exposed to laser and incurred retinal damage as a result. One of the recombinant scFv antibodies that were generated against the GBB5 peptide was estimated to have an affinity of 300 nM and subsequently recognized the endogenous protein in western blot of retinal lysate from three organisms.

ScFv antibodies with dissociation constants of 0.5 μM were determined to be the upper limit on western blot detection since the single-digit micromolar scFvs failed in western blot. To increase functional affinities, the scFvs were dimerized through fusion to a human IgG Fc hinge region. This improved lower detection limit, at 25-fold over the monomeric scFv on western blot, will assist in detection of biomarkers which are generally low in concentration. Validation through western blot requires the ability to quantify a range of protein concentrations so healthy, sub-clinical, early stage, and late stage conditions can be monitored. Depending on the biomarker, these abundance ranges can be narrow (fall within 10-fold changes) or wide (span thousand-fold increases) (37). Sensitivity and a large dynamic range are therefore desirable.

We have shown how utilizing mass spectrometry data collected from a laser-induced retinal injury rabbit study can be used to generate recombinant antibodies to

aide in the validation of potential biomarkers. By using MS identified peptides as targets in phage-display library selections of recombinant scFvs, and conversion to the better binding scFv-Fc scaffold, we have increased the chances of recognizing the antigenic epitope existing within the circulating serum. By isolating and enhancing affinity reagents for detecting endogenous proteins by western blot, we have shown this workflow to be a successful strategy towards biomarker validation. We have also shown how dimerization of the scFv improves the functional affinity through avidity and reduces the lower detection limit in western blotting by 25-fold.

As we have generated recombinant antibodies against peptides, our strategy would be amenable to the immuno-multiple reaction monitoring method of Stable Isotope Standards and Capture by Anti-Peptide Antibodies (SISCAPA) (29). This technology uses antibodies against peptides to capture candidate biomarkers in a complex sample that have been subjected to proteolytic digestion. The peptide fragments are subsequently enriched for sensitive detection by mass spectrometry. In parallel, spiked isotopically labeled versions of the peptides are used as standards to quantify the peptide fragments in the sample. Encouraging evidence of this application was recently reported in the development of high-affinity recombinant Fab antibodies against clinically relevant peptides generated through phage-display (38). The Fab antibodies were able to enrich serum spiked peptide fragments and quantify an efficient recovery through comparison to isotopically labeled standards in mass spectrometry.

Although we would require improvement in K_D of our scFvs to be useful in these assays (39), the generation strategy is applicable.

2.6 References

1. Mishra J, Dent C, Tarabishi R, Mitsnefes MM, Ma Q, et al. Neutrophil gelatinase-associated lipocalin (NGAL) as a biomarker for acute renal injury after cardiac surgery. *Lancet* 365: 1231-1238. (2005).

2. Devarajan P. Review: neutrophil gelatinase-associated lipocalin: a troponin-like biomarker for human acute kidney injury. *Nephrology (Carlton)* 15: 419-428. (2010).

3. Thygesen K, Alpert JS, White HD. Universal definition of myocardial infarction. *J Am Coll Cardiol* 50: 2173-2195. (2007).

4. Pineda JA, Lewis SB, Valadka AB, Papa L, Hannay HJ, et al. Clinical significance of alphaII-spectrin breakdown products in cerebrospinal fluid after severe traumatic brain injury. *J Neurotrauma* 24: 354-366. (2007).

5. Smith RA, Manassaram-Baptiste D, Brooks D, Cokkinides V, Doroshenk M, et al. Cancer screening in the United States, 2014: A review of current American Cancer Society guidelines and current issues in cancer screening. *CA: A Cancer Journal for Clinicians* 64: 30-51. (2014).

6. Stamey TA, Yang N, Hay AR, Mcneal JE, Freiha FS, et al. Prostate-Specific Antigen as a Serum Marker for Adenocarcinoma of the Prostate. *New England Journal of Medicine* 317: 909-916. (1987).

7. Prensner JR, Rubin MA, Wei JT, Chinnaiyan AM. Beyond PSA: the next generation of prostate cancer biomarkers. *Sci Transl Med* 4: 127rv123. (2012).

8. Einhorn N, Sjovall K, Knapp RC, Hall P, Scully RE, et al. Prospective evaluation of serum CA 125 levels for early detection of ovarian cancer. *Obstet Gynecol* 80: 14-18. (1992).

9. Gold P, Freedman SO. Demonstration of Tumor-Specific Antigens in Human Colonic Carcinomata by Immunological Tolerance and Absorption Techniques. *J Exp Med* 121: 439-462. (1965).

10. Kohler G, Milstein C. Continuous cultures of fused cells secreting antibody of predefined specificity. *Nature* 256: 495-497. (1975).

11. Bordeaux J, Welsh A, Agarwal S, Killiam E, Baquero M, et al. Antibody validation. *Biotechniques* 48: 197-209. (2010).

12. Schmitz U, Versmold A, Kaufmann P, Frank HG. Phage display: a molecular tool for the generation of antibodies--a review. *Placenta* 21 Suppl A: S106-112. (2000).

13. Smith GP. Filamentous Fusion Phage - Novel Expression Vectors That Display Cloned Antigens on the Virion Surface. *Science* 228: 1315-1317. (1985).

14. McCafferty J, Griffiths AD, Winter G, Chiswell DJ. Phage antibodies: filamentous phage displaying antibody variable domains. *Nature* 348: 552-554. (1990).

15. Kehoe JW, Kay BK. Filamentous phage display in the new millennium. *Chem Rev* 105: 4056-4072. (2005).

16. Van B. Nakagawara RWM, Archie E. Dillard, Leon N. McLin. The Effects of Laser Illumination on Operational and Visual Performance of Pilots During Final Approach. *Department of Transportation/Federal Aviation Administration, Washington, DC (2004) Report No FAA/Report No DOT/FAA/AM-04/9* (2004).

17. Nakagawara VB, Wood KJ, Montgomery RW. Laser exposure incidents: pilot ocular health and aviation safety issues. *Optometry* 79: 518-524. (2008).

18. Marshall J. Thermal and mechanical mechanisms in laser damage to the retina. *Invest Ophthalmol* 9: 97-115. (1970).

19. FAA Fact Sheet 2013.

20. V.B. Nakagawara RWM, A. Dillard et al. The effects of laser illumination on operational and visual performance of pilots conducting terminal operations. *Department of Transportation/Federal Aviation Administration, Washington, DC (2003) Report No FAA/Report No DOT/FAA/AM-03/12*. (2003).

21. Lam TT, Tso MO. Retinal injury by neodymium: YAG laser. *Retina* 16: 42-46. (1996).

22. Mainster MA, Stuck BE, Brown J, Jr. Assessment of alleged retinal laser injuries. *Arch Ophthalmol* 122: 1210-1217. (2004).

23. Scott SE, Bouhenni RA, Chomyk AM, Dunmire JJ, Patil J, et al. Anti-retinal antibodies in serum of laser-treated rabbits. *Invest Ophthalmol Vis Sci* 53: 1764-1772. (2012).

24. Haidaris CG, Malone J, Sherrill LA, Bliss JM, Gaspari AA, et al. Recombinant human antibody single chain variable fragments reactive with Candida albicans surface antigens. *J Immunol Methods* 257: 185-202. (2001).

25. Pershad K, Sullivan MA, Kay BK. Drop-out phagemid vector for switching from phage displayed affinity reagents to expression formats. *Anal Biochem* 412: 210-216. (2011).

26. Simmons LC, Reilly D, Klimowski L, Raju TS, Meng G, et al. Expression of full-length immunoglobulins in Escherichia coli: rapid and efficient production of aglycosylated antibodies. *J Immunol Methods* 263: 133-147. (2002).

27. Falk R, Falk A, Dyson MR, Melidoni AN, Parthiban K, et al. Generation of anti-Notch antibodies and their application in blocking Notch signalling in neural stem cells. *Methods* 58: 69-78. (2012).

28. Cunningham BT, Li P, Schulz S, Lin B, Baird C, et al. Label-free assays on the BIND system. *J Biomol Screen* 9: 481-490. (2004).

29. Anderson NL, Anderson NG, Haines LR, Hardie DB, Olafson RW, et al. Mass spectrometric quantitation of peptides and proteins using Stable Isotope Standards and Capture by Anti-Peptide Antibodies (SISCAPA). *J Proteome Res* 3: 235-244. (2004).

30. Andrade EV, Albuquerque FC, Moraes LM, Brigido MM, Santos-Silva MA. Single-chain Fv with Fc fragment of the human IgG1 tag: construction, Pichia pastoris expression and antigen binding characterization. *J Biochem* 128: 891-895. (2000).

31. Gould LH, Sui J, Foellmer H, Oliphant T, Wang T, et al. Protective and therapeutic capacity of human single-chain Fv-Fc fusion proteins against West Nile virus. *J Virol* 79: 14606-14613. (2005).

32. Oleinikov AV, Gray MD, Zhao J, Montgomery DD, Ghindills AL, et al. Self-assembling protein arrays using electronic semiconductor microchips and in vitro translation. *Journal of Proteome Research* 2: 313-319. (2003).

33. Roth KM, Peyvan K, Schwarzkopf KR, Ghindilis A. Electrochemical Detection of Short DNA Oligomer Hybridization Using the CombiMatrix ElectraSense Microarray Reader. *Electroanalysis* 18: 1982-1988. (2006).

34. Cooper J, Yazvenko N, Peyvan K, Maurer K, Taitt CR, et al. Targeted deposition of antibodies on a multiplex CMOS microarray and optimization of a sensitive immunoassay using electrochemical detection. *PLoS One* 5: e9781. (2010).

35. Cheever ML, Snyder JT, Gershburg S, Siderovski DP, Harden TK, et al. Crystal structure of the multifunctional Gbeta5-RGS9 complex. *Nat Struct Mol Biol* 15: 155-162. (2008).

36. Rao A, Dallman R, Henderson S, Chen C-K. Gβ5 Is Required for Normal Light Responses and Morphology of Retinal ON-Bipolar Cells. *The Journal of Neuroscience* 27: 14199-14204. (2007).

37. Rusling JF, Kumar CV, Gutkind JS, Patel V. Measurement of biomarker proteins for point-of-care early detection and monitoring of cancer. *Analyst* 135: 2496-2511. (2010).

38. Whiteaker JR, Zhao L, Frisch C, Ylera F, Harth S, et al. High-Affinity Recombinant Antibody Fragments (Fabs) Can Be Applied in Peptide Enrichment Immuno-MRM Assays. *Journal of Proteome Research* 13: 2187-2196. (2014).

39. Dyson MR, Zheng Y, Zhang C, Colwill K, Pershad K, et al. Mapping protein interactions by combining antibody affinity maturation and mass spectrometry. *Anal Biochem* 417: 25-35. (2011).

CHAPTER 3

RIBOSOME DISPLAY OF THE FHA DOMAIN

3.1 Abstract

Affinity maturation is an important process in enhancing the functionality of antibodies whether it happens in the immune system of animals to fight infection or through a protein display technology to generate useful reagents for biological investigations. Ribosome-display is a completely *in vitro* technique that can utilize large libraries, incorporate affinity maturation in the selection process, and yield tight binding reagents with picomolar dissociation constants. Like other display technologies it also has the advantage of avoiding the use of research animals and produces renewable reagents that can be tagged, modified, or tailored to a researchers needs.

Here for the first time, we have displayed the phosphothreonine recognizing Forkhead-associated domain in a protein-mRNA-Ribosome complex for the purpose of affinity selection. An FHA isolated by phage-display against a Myc phosphopeptide was converted to the ribosome-display format for affinity maturation using off-rate competitor selections in tandem with error-prone PCR. The ribosome-display procedure was later modified to incorporate a coupled *in vitro* transcription and translation kit to help overcome some of the preparatory hurtles in establishing the technology *de novo* in a laboratory. Although we gained modest improvements in affinities, we have shown that ribosome-display is a robust technology with the versatility to work with various engineered scaffolds and, through the use of kits, is now accessible to more labs.

3.2 Introduction

When using phage-display with small primary libraries to generate affinity reagents for biological applications, a process known as affinity maturation is often required to make them useful (1). This is in effect replicating somatic hypermutation of the immune system. The process involves creation of a secondary library through random mutation of a pool of enriched binders and subsequent transformation into *E. coli* for phage expression. Mutations at sites other than the epitopes involved in antigen recognition, are known to improve binding affinity through slight conformational tweaking that position the interacting residues for better contact (2). A secondary phage-display selection is then performed with increased selection pressure through off-rate competition in order to enrich only the binders with the lowest equilibrium dissociation constants (K_D) which is a measure of the ratio of the dissociation rate constant (k_d) and the association rate constant (k_a). Due to physical limits of molecular diffusion, the association rate constant cannot be increased more than about ten-fold (3,4). Therefore, the K_D can only be improved by decreasing the k_d. Although this maturation process has been shown to improve antibody affinity, the secondary library generation is procedurally laborious and yields a low diversity comparable to the starting library (5).

A second approach is to convert the output of the initial phage-display selection into an alternate display technology like ribosome-display to perform the affinity maturation (6,7). Ribosome-display is a completely *in vitro* procedure that uses an arrested ribosome-mRNA-affinity reagent complex to link the genotype and phenotype,

and allow integrated affinity maturation (4,8). The secondary library generation for ribosome-display is greatly simplified since no transformation of cells is required and therefore library size limits do not apply. Generally in a selection, the larger the diversity of the library, the higher the affinity of the resulting antibodies (9,10). During the conversion from phage- to ribosome-display, error-prone PCR can be controlled by addition of nucleotide analogs to randomly insert 1-6 mutations per clone (11,12). The downstream ribosome-display is conducted *in vitro* with successive rounds of off-rate selection and enrichment through traditional PCR. Cycles of additional diversity through mutation and selection rounds with increasing stringencies can be performed until the desired binding characteristics are achieved. Using this methodology, we attempted to affinity mature the Fork-head associated (FHA) domain reagents by converting the most promising binders into the ribosome-display system, and performing off-rate competition selections.

Of the most interesting binders was one against a dual phosphorylated peptide of the Myc transcription factor. This had been discovered in a phage-display selection of a primary FHA library (13) with a relatively small diversity of 3×10^9 variants (14). This binder was shown to recognize only the peptide version with a single phosphothreonine (pT), however the binding affinity was estimated to be in the low micromolar range. The usefulness with a reagent with a low affinity is limited to very sensitive assays such as ELISA (15). To be used to answer biological questions, the affinity must be improved 100- to 1000-fold. Affinity maturation of this clone through phage-display did not succeed in increasing binding more than 2-fold. Two possible conclusions from this are

reached. One is that there is an intrinsic limit of antibody-antigen binding with the FHA domain. Because the FHA domain was engineered to distinguish between phosphorylated and non-phosphorylated peptides by the phosphothreonine and the residue at the+3 position from the pT (16), there may not be adequate contact for a strong interaction. Although very strong binders have been isolated against short peptides in the past (17), recognition of the single residue modification may be too high a requirement. The second hypothesis is that the primary and secondary libraries were too small in diversity to discover a tight binding reagent.

3.3 Materials and methods

3.3.1 Cloning of FHA into Ribosome-display vector

In order to clone the Myc FHA binder out of the pKP700ΔIII phage-display plasmid and into the pRDV ribosome-display vector (GenBank: AY327136.1), the coding region plus FLAG tag was PCR amplified using AccuPrime™ PFX Taq polymerase (Life Technologies), forward primer: FHA-RD-Fwd (ATTATATTGGATCCGGAATGGAAAATATTACACAACC) containing a *BamHI* restriction site, and reverse primer: FHA-RD-Rev (ATTATATTGAATTCTGCGGTATTTTTAAGATTTGA) containing a *EcoRI* restriction site. PCR program: 2 min at 95°C, 30 cycles of 95°C for 15 sec, 55°C for 30 sec, and 68°C for 45 sec. Final extension for 5 min at 68°C. The column purified PCR product

and the pRDV were digested with *BamHI* (New England BioLabs) and *EcoRI* (New England BioLabs) restriction enzymes. Digests were separated by gel electrophoresis, the appropriate bands excised, and the DNA column purified (Qiagen Gel purification kit). Ligation was performed using T4 DNA ligase (Promega) for 3 h at room temperature. Reaction was dialyzed into water and transformed into the TG-1 strain of *E. coli* by electroporation. Colonies were picked from 2xYT/Cb (50 ug/mL) plates, grown in small overnight cultures, and the plasmid DNA isolated through column purification (Wizard MiniPrep, Promega). Clones were sent for sequence confirmation at the UIC DNA sequencing Facility. The correct clone was named pRDV-FHA-Myc-A4 (**Fig. 21**).

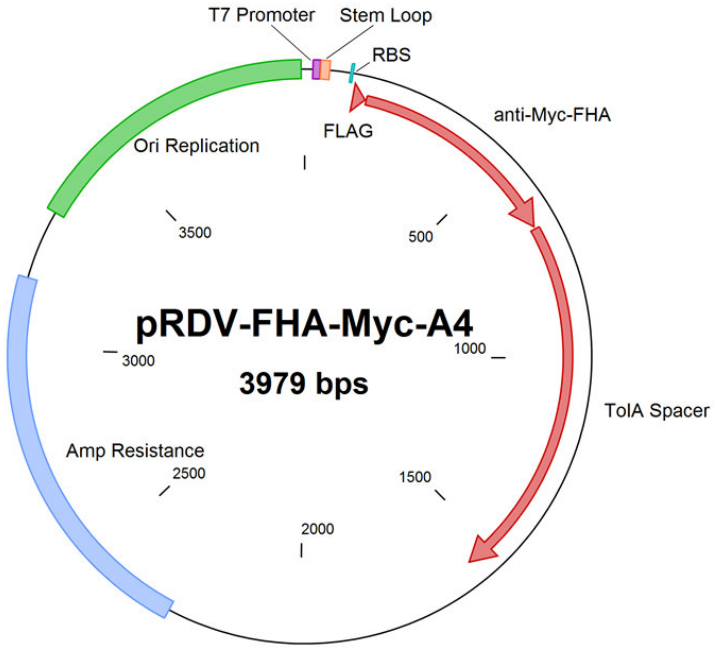

Figure 21. Map of FHA ribosome-display vector. The pRDV vector was modified from the original pRDV (Genbank AY327136.1) to have the FHA scaffold and a n-terminal FLAG tag (Red). The full ribosome-display transcript includes the TolA spacer lacking a stop codon. Other important features are the bacterial origin of replication (green), ampicillin resistance gene (blue), T7 promoter (purple), a 5' stem loop to help decrease nuclease degradation (orange), and a ribosome binding site (RBS, turquoise) to allow translation initiation.

3.3.2 Introduction of additional diversity through mutation

The protocol from Dreier et. al. (12) was followed for the ribosome-display. The procedure will be described in less detail here. All buffers and reagents are made with MilliQ filtered water and passed through a 0.22 um filter after dissolving. Reagent stocks are kept separate from general lab use to avoid RNase contamination. All techniques used are meant to minimize introduction of bacterial or RNase contamination.

To introduce random mutation into the anti-Myc FHA, two reactions of error-prone PCR were performed with 10 ng of the template, 400 µM dNTPs, 1 µM of T7B forward outside primer (ATACGAAATTAATACGACTCACTATAGGGAGACCACAACGG-), 1 µM TolAk reverse outside primer providing the 3' stem loop (CCGCACACCAGTAAGGTGTGCGGTTTCAGTTGCCGCTTTCTTTCT), 1.5 mM $MgCl_2$, 1 U Platinum® Taq DNA Polymerase (Life Technologies), 3 nM or 9 nM 8-oxo-d- dGTP nucleotide analog (Jena Bioscience), and 3 nM or 9 nM dPTP nucleotide analog (Jena Bioscience) in a 50 µL reaction volume. PCR program: 3 min at 95°C, 25 cycles of 95°C for 30 sec, 50°C for 30 sec, and 72°C for 1 min. Final extension for 5 min at 72°C.

3.3.3 Ribosome-display off-rate selection

The ribosome-display selection was performed in two blocks of three selections each. Each block contains a low stringency round where mutation is added with error-prone PCR, a high stringency round with off-rate selection, and a low stringency

recovery round. The first block used 100-fold peptide competitor over the target peptide, while the second block used 1,000-fold peptide competitor.

In-vitro transcription

The transcription of the error-prone PCR product is as follows: 7 mM NTPs, 80 U T7 RNA polymerase (Fermentas), 80 U RiboLock RNase Inhibitor (ThermoScientific), 11.25 µL of each unpurified PCR product (3 nM and 9 nM nucleotide analogs), 0.2 M HEPES, 30 mM magnesium acetate, 2 mM spermidine (Sigma-Aldrich), and 40 mM dithiothreitol (DTT) in a final volume of 100 µL. The reaction was performed at 37°C for 3 h. The RNA was purified using the Illustra MicroSpin G-50 columns (GE Healthcare), frozen in liquid nitrogen, and stored at -80°C.

In-vitro translation

The translation was performed using 50 µL of a home-made *E. coli* S30 extract and 41 µL of premix Z buffer (Birgit Dreier, University of Zurich), 10 ug of the thawed RNA transcript, and 3.6 mM L-Methionine (Sigma-Aldrich), at 30°C for 30 min in a 110 µL total volume. The reaction was stopped with addition of 440 µL of cold 50 mM Tris-acetate, 150 mM NaCl, 50 mM Magnesium acetate, 0.05 % Tween-20, 0.5% BSA, and 12.5 µL Heparin (Sigma-Aldrich).

In-solution selection

The stopped reaction was doubled in volume and split equally between two tubes of 40 µL of MyOne T1 Streptavidin coated magnetic beads (Life Technologies) and

incubated for 1 h with tumbling at 4°C for a de-selection step. The beads were captured on a magnetic separator and the supernatant transferred to freshly blocked tubes. To the positive target tube was added 200 nM Myc Dual phosphorylated peptide (400 ng/µL biotin-KKFELLP**pT**PPL**pS**PSY) and incubated for 1 h at 4°C with tumbling. This supernatant was then added to fresh Streptavidin coated Magnetic beads blocked in TBST +0.5%BSA and incubated for 30 min at 4°C with tumbling. The beads- Ribosome-mRNA-FHA complex was washed once quickly in 500 µL of cold 50 mM Tris-acetate, 150 mM NaCl, 50 mM Magnesium acetate, 0.05 % Tween-20, 0.1% BSA. This was followed by six additional washes of five minutes of tumbling each. The complex was eluted into 100 µL of 50 mM Tris, 150 mM NaCl, 25 mM EDTA, 50 ug/mL of *S. cerivisiae* RNA (Sigma) for 10 min at 4°C. This was added to 400 µL of Lysis Buffer of the High pure RNA isolation kit (Roche) and vortexed. The elution step was repeated. The RNA isolation kit was used to purify the RNA. DNAse was added for 10 min to the column before eluting the RNA into RNase-free water.

Reverse transcription and cDNA amplification

For the reverse transcription, 12.5 µL of the RNA elutions were transferred to two tubes, one for +Reverse Transcription (RT) and the other for –RT control, and denatured at 70°C for 10 min. To the +RT RNA was added 1.25 µM FHA Internal reverse primer (CCAGATCCGAATTCTGCGGTATTTT), 125 µM dNTPs, 20 U Ribolock, 10 mM DTT, 25 U of AffinityScript Multiple temperature reverse transcriptase (Agilent technologies), 1 x AffintyScript buffer. The –RT control had the same reaction components except was lacking the reverse transcriptase. All were incubated at 50°C

for 1 h. To amplify the complementary DNA (cDNA) PCR was performed using 5 µL of the cDNA, 5% DMSO, 1 µM of FHA Internal Forward primer (AGATATATCCATGGCGGACTACAAA),1 µM of FHA Internal Reverse primer, 200 µM dNTPs, 0.5 µL of Herculase II fusion polymerase (Agilent Technologies), 1 x Herculase II reaction buffer, in 50 µL total. PCR program: 3 min at 95℃, 35 cycles of 95℃ for 30 s, 55℃ for 30 sec, and 72℃ for 45 sec. Final extension for 5 min at 72℃. The product was visualized on a 1% agarose gel and analyzed for band intensities signifying selection success.

Digestion and ligation for next round

About 1 ug of the cDNA PCR amplification product was gel purified and digested for 3 h with 2 U of restriction enzymes *EcoRI* (Fermentas) and *NcoI* (New England Biolabs). The reaction was cleaned up with the QIAquick PCR clean-up kit (Qiagen). The digest was ligated into the pre-digested pRDV with 1 U of T4 DNA ligase (New England Biolabs), 100 ng of pRDV, 100 ng of PCR product and 1 x ligation buffer for 1 h at room temperature.

Off-rate selection and low-stringency round

The round was repeated starting from the PCR of the ligation reaction using the outside primers but no nucleotide analogs for mutation. To remove any binders to the non-phosphorylated form of the peptide, ±200 nM of biotin-KKFELLPPTPPLSPSY was added during the de-selection step. The remainder of the selection was performed the same as before, except 20 nM Myc Dual phosphorylated peptide target was added for

binding. After 1 h, non-biotinylated Myc Dual phosphorylated competitor peptide was added at a 2 µM concentration, or 100-fold excess, and tumbled for 2 h at 4°C. The final round of selection was performed as a low stringency round with 200 nM Myc Dual phosphorylated, but no competition step.

The three rounds of selection were repeated in a second block where the off-rate selection now contained 1,000-fold excess competitor peptide with 200 nM Biotinylated peptide and 200 µM non-biotin peptide. In this round, in parallel, ±DTT S30 extract was added to the selection along with the ± non-phosphorylated peptide competitor.

E. coli Expression

To insert the recovered clones into the pET29b bacterial expression vector for binding characterization, PCR was performed using the amplified cDNA, Herculase II fusion polymerase, the internal forward primer, and a pET29b Reverse primer (GCGGCCGC GGTATTTTTAAGATTTGAACGG) which includes a *NotI* site. The PCR product and the pET29b were digested with *NotI* HF (New England Biolabs) and *NcoI* (New England BioLabs) purified by gel electrophoresis, and ligated at room temperature for 1 h. The ligations were transformed by heat shock into 50 µL of chemically competent BL-21 DE3 cells, and grown on 2xYT/Kanamycin (15 ug/mL) plates.

Colonies were picked from the ±DTT selections to inoculate 1 mL of 2xYT with 15 ug/mL Kanamycin in a deep 96-well plate and shaken at 540 rpm overnight at 37°C.

ELISA to identify positive binders

From the overnight culture, transferred 100 µL of each well to fresh 900 µL of 2xYT/Kan and grew for 1 h at 37℃. Induced expression by adding 5.5 mM of IPTG (Isopropyl β-D-1-thiogalactopyranoside) in 100 µL of 2xYT to each of the wells and grew at 30℃, 540 rpm shaking, for 5.5 h. The remainder of the overnight culture was spun down, the supernatant discarded, and the pellets frozen at -20℃. The induced culture was spun down and to each pellet was added 50 µL of B-PERII Lysis reagent (ThermoScientific). This was placed on a shaker for 40 min to resuspend the pellet. The plates were frozen at -20℃ overnight.

Eight Maxisorp 96-well microtiter plates (Nunc) were coated with 100 µL of 66 nM of NeutrAvidin (Life Technologies) in Tris Buffered Saline (TBS) overnight at 4℃. Plates were blocked with 300 µL of TBST, 0.5% BSA for 1 h at room temperature. One hundred microliters of 100 nM biotinyated-Dual Phosphorylated Myc Peptide in TBS, 0.05% Tween, 0.5% BSA were added to the respective +target wells. This was incubated at room temp with rotating for 1 h. The frozen lysis plates were thawed and to all wells was added 1 mL of TBST, 0.5%BSA. This was allowed to resuspend the pellet while shaking for 20 min. The plates were then spun down. Plates were washed 3 times with TBST. For four plates, 100 µL of each lysis was added to both the ±target. To the other four plates, 90 µL of TBST, 0.5% BSA was added on top of 10 µL of the lysis to give a 1:10 dilution. This was incubated with 600 rpm rotation for 1 h. The plates were washed twice with TBST. To all wells, 100 µL of 1:5,000 mouse anti-FLAG-M2 (Sigma) in TBST was added. Plates were incubated at 600 rpm rotation for 1 h. Plates were then

washed twice with TBST. To all wells, was added 100 µL of 1:10,000 Goat anti-Mouse-Alkaline Phosphatase (Sigma-Aldrich) in TBST. This was incubated for 1 h with shaking and the plates washed 3 times with TBST. To detect binders, 50 µL of *para*-Nitrophenylphosphate (Fluka) was added and absorbance determined at 405 nm wavelength after color development.

3.3.4 Purification of matured anti-Myc-FHA and ELISA

To produce the soluble FHA, 25 mL of 2xYT/Kan media was inoculated with the FHA in the pET29b vector from frozen glycerol stock and allowed to grow overnight at 37℃ 250 rpm shaking. The following day, 200 mL 2xYT/Kan culture was inoculated with 2 mL of the overnight culture to get a starting OD of ~0.10. This was grown at 37℃ for ~4 h to get to OD 0.8. IPTG was added at 0.5 mM to induce expression. The induction was allowed to continue at room temp (~30℃) for ~21 h. The culture was spun down at 6,000 rpm for 10 min and then stored at -80℃ overnight.

The culture was spun down and prepared for sonication by resuspending the cell pellet in 25 mL of filter sterilized equilibration buffer (50 mM sodium phosphate, 300 mM sodium chloride, pH 7.4) on ice. To prevent protein degradation, cOmplete EDTA free protease Inhibitor cocktail (Roche Applied Science) was added before performing sonication on ice with 10 s on sonication, 10 s off for a total of 10 min, with 50% amplitude using a SonicDismemberator (Branson inc. Model 500). The lysate was spun at 15,000 rpm for 15 min and the supernatant transferred to a 50 mL centrifuge tube.

The agarose was prepared by washing 200-300 µL of Clontech His60 Ni Superflow™ resin (60mg/mL binding capacity, Clontech Laboratories, inc.) twice with equilibration buffer. Resin was added to the cleared lysate and incubated at 4℃ for 2 h while tumbling. This was spun down for 2 min at 2,000 rpm and the supernatant removed. The pellet was resuspended in 1 mL wash buffer containing 50 mM sodium phosphate, 300 mM sodium chloride, 10 mM Imidazole, pH 7.4. The resuspension was spun and the wash buffer removed. Washes were repeated 5 additional times. The FHA was eluted in 500 µL filter sterilized elution buffer (50 mM sodium phosphate, 300 mM sodium chloride, pH 7.4, 300mM Imidazole) for 10 min. Elution was repeated with additional 500 µL elution buffer. The concentration was determined by NanoDrop A280 (ThermoScientific) and purity determined by SDS-PAGE.

ELISA was performed by coating a 96-well plate with 50 ng per well of NeutrAvidin or with 50 µL of 5% BSA in PBS. Wells were blocked with 1% casein (ThermoScientific) before addition of 50 ng per well of the phosphorylated or non-phosphorylated Myc peptides. To the respective wells, 50 ng of each FHA was added (A4-WT, B11, D12, F1, F3). FHAs were detected through the FLAG tag with anti-FLAG-HRP, and developed with 50 µL of 2,2'-azino-bis(3-ethylbenzothiazoline-6-sulphonic acid (ABTS) (Sigma-Aldrich) in 50 mM Sodium Citrate (pH 4), with 0.03% H_2O_2 .

3.3.5 Size exclusion chromatography of FHA

Size exclusion chromatography was performed on an ÄKTA FPLC (GE Healthcare Life sciences) with a Superdex 200 10/300 GL analytical 24 mL column. Column resolution molecular weight limits are 10-600 kDa. All flow rates were at 0.5 mL/min. The column and samples were equilibrated in PBS before injection. Samples were loaded into a 100 µL sample loop at 1-2 mg/mL concentration. Standards were diluted into PBS from the FPLC standard protein kit (GE). Standards used were: Conalbumin 75 kDa, Ovalbumin 43 kDa, Carbonic Anhydrase 29 kDa, Ribonuclease H 13.7 kDa, and Aprotinin 6.5 kDa. Instrument was controlled by system software UNICORN 5.11 build 407. All standards and FHA samples were run separately and the data aligned in layers for the figures.

3.3.6 Ribosome-display using coupled *in vitro* transcription and translation

The ribosome-display selection for FHA was performed as above but with some major exceptions. The template for ribosome-display was not mutated and therefore a normal PCR was performed. The *in vitro* transcription and translation were coupled in a single step using the EasyXpress Protein synthesis kit (Qiagen). Three reactions were performed, with either 7 mM, 15 mM, or 21.4 mM magnesium acetate to keep the complex together. A combination of cleaned up template (800 ng) and direct from PCR template (200 ng) was used with the 17.5 µL of kit supplied *E. coli* extract and 20 µL of kit supplied buffer in a total reaction volume of 50 µL. This was incubated for 1 h at

30℃. The reaction was stopped as before and the selection proceeded with 100 nM of the biotin-dual phosphorylated Myc peptide. The + and – target were washed 6x before elution, reverse transcription, and cDNA PCR amplification. Results of the three were analyzed by 1% agarose gel electrophoresis.

3.3.7 Pull-down and Western blot of in vitro transcription and translation

The reaction was performed using the cell-free PURExpress coupled *in vitro* transcription and translation kit (New England BioLabs). For the +template reaction, 1 µg of non-purified FHA ribosome display PCR template was added in accordance to the kit instructions. Also included in separate reactions, were a negative no template control and a reaction spiked with 40 ng of purified anti-Myc-FHA without template. The spiked reaction was not subjected to the pull-down conditions. All reactions were incubated at 30℃ for 2 h.

The pull-down was performed by mixing the ±template reactions with 100 µL of PBS and 10 µL of anti-FLAG® M2 Magnetic Beads (Sigma-Aldrich) for 30 min using the KingFisher™ mL robotic bead handler (ThermoScientific). Continuing to use the KingFisher, the beads were washed once in 250 µL of ribosome-display elution buffer (50 mM Tris, 150 mM NaCl, 25 mM EDTA) for 10 min to dissociate the complex. Beads were washed twice in 350 µL elution buffer for 45 s. The beads were resuspended in 30 µL of PBS and 10 µL of NuPage® 4x LDS Loading buffer (Life Technologies) + β-Me

was added and heated to 95℃ for 3 min. The beads were captured by a magnet separator and the supernatant removed for gel electrophoresis.

Gel electrophoresis was run for 1.5 h at 35 mA on a Criterion® TGX Stain-free AnyKd SDS polyacrylamide gel (Bio-Rad). The gel was imaged without staining using the Gel Doc™ EZ (Bio-Rad) which detects fluorescence of trihalo compounds in the gel. Protein was transferred to an activated Immobilon-FL Polyvinylidene fluoride (PVDF) membrane (Millipore) in 25 mM Tris, 192 mM glycine, 0.1% SDS, 20% methanol, pH 8.3, for 12 h at 30 V in 4℃. Blot was washed in PBS for 5 min and blocked for 1 h in 5% non-fat milk. After washing in PBST and PBS for 5 min each, 25 mL of anti-FLAG-HRP (Sigma-Aldrich) in PBST was incubated with the blot. The blot was washed in PBST and PBS for 5 min each. The membrane was placed upside down in 1 mL of WesternSure™ ULTRA Chemiluminescent Substrate (Li-Cor) for 5 min and imaged on the Li-Cor Odyssey® using the chemiluminescence channel for the experimental lanes and the 700 nm channel for the one-color protein molecular weight ladder (Li-Cor).

3.4 Results and discussion

3.4.1 Ribosome-display off-rate selection

The anti-Myc-FHA A4 clone isolated through phage-display was cloned into the ribosome-display vector pRDV in order to perform affinity maturation through successive rounds of off-rate selection, recovery, and enrichment.

The ribosome-display affinity maturation selection was performed in two blocks of three selections each. The first round of every block consisted of adding two sets of nucleotide analogs to the PCR to cause random mutations for additional diversity, followed by a low stringency selection (11). The second round contained off-rate selection, with addition of excess free competitor to recover clones with low dissociation rate constants (k_d). The third round was a recovery round with low stringency to amplify the rare clones that survived the harsh treatment of the previous round. The first block of selections used 100-fold molar excess competitor and the second used 1000-fold excess competitor. In parallel, the last selection block contained de-selection steps with non-phosphorylated Myc peptide to remove any binders that recognize residues excluding the phosphothreonine. To prevent disulfide bond formation between two cysteines and favoring of dimers because of high functional affinity through avidity, S30 extract containing DTT was also used in parallel during the *in vitro* translation steps.

The FHA domain had never been displayed in this system previously, so the first step was to optimize the *in vitro* transcription and translation (IVTT). The first round of

selection with the error-prone PCR was performed with 3 μM and 9 μM of the nucleotide analogs to get a range of mutation frequencies that were expected to be mostly transitions (18). Generally, the more mutations per gene, the more members that are non-functional, but the greater the improvement in affinity after selection (2). The results of the ribosome-display selection are analyzed by agarose gel (**Fig. 22**). The gel compares the IVTT and selection at 37℃ (as is described in the published method (12)), and at 30℃, which was used for the FHA in phage-display (13). The arrows show that there is a more intense band at 30℃ than at 37℃. The size of this band is loosely correlated to the number of binders recovered, but a more intense band is generally considered to be a better result. The minus reverse transcriptase controls help to determine if there is original template DNA contamination carried by the magnetic beads. There appears to be minimal template carryover for both conditions, but there is less at 30℃. This is probably due to slower folding at 30℃ than at 37℃, which will give more functional FHA domains and less that are sticky due to mis-folding. Regardless, these results indicate that the FHA can be used in the ribosome-display system to perform selections.

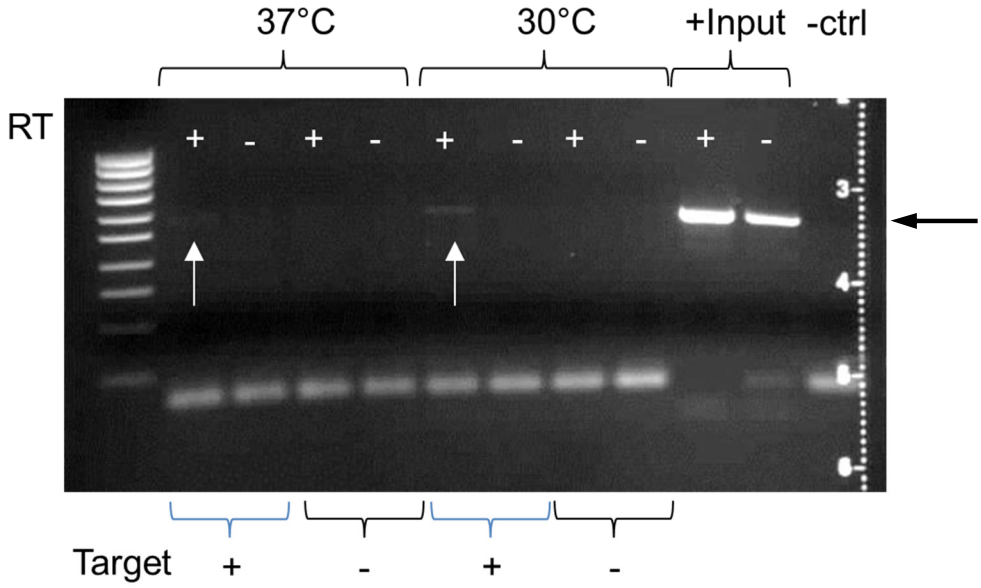

Figure 22. Optimization of ribosome-display conditions with FHA Domain. Two separate ribosome-display selections were performed in parallel using different temperatures (37℃ and 30℃) for the *in vitro* translation. White arrows indicate lanes where PCR product is expected if ribosome-display was successful with translation at 37℃ or 30℃. Black arrow indicates expected size of product. The RT denotes plus and minus reverse transcriptase. "+" Target includes the biotin-phosphopeptide in the selection. "-" Target does not include biotin-phosphopeptide. The "+ input lane" contains ±RT of the *in-vitro* transcription total RNA. The negative control "-ctrl" is the PCR master mix only.

The next round of selection was performed with an off-rate selection using 10-fold molar excess competitor peptide. The final round was the recovery selection of low stringency to enrich the rare clones. After three additional rounds in the second block, the final round results are shown (**Fig. 23**). This gel shows little enrichment of binding clones. The blue arrows indicate the lane with the expected band of highest intensity (+Target, +RT) for each condition. The negative controls show more recovered RNA than the (+) target selections which is unexpected. However, the correlation between

obtaining a tight binding reagent and the intensity of the band is not a strong relationship (19). Therefore, the PCR products were recovered and cloned into a bacterial expression vector and a monoclonal ELISA performed evaluating single clones.

Many of the affinity matured clones had a signal over the original WT anti-Myc-FHA-A4 but few were more than double in intensity (**Fig. 24 A-D**). To eliminate more clones that have weaker binding affinities, the ELISA was repeated but with a 100-fold dilution of the lysate. With concentration of FHA high, the ELISA signal saturates quickly and differences between affinities are masked. The 100-fold dilutions revealed the tightest binding clones. The highest signal clones were chosen to sequence and characterize. The promising clones picked were B11, D12, F1, and F3 (**Fig 24 E**).

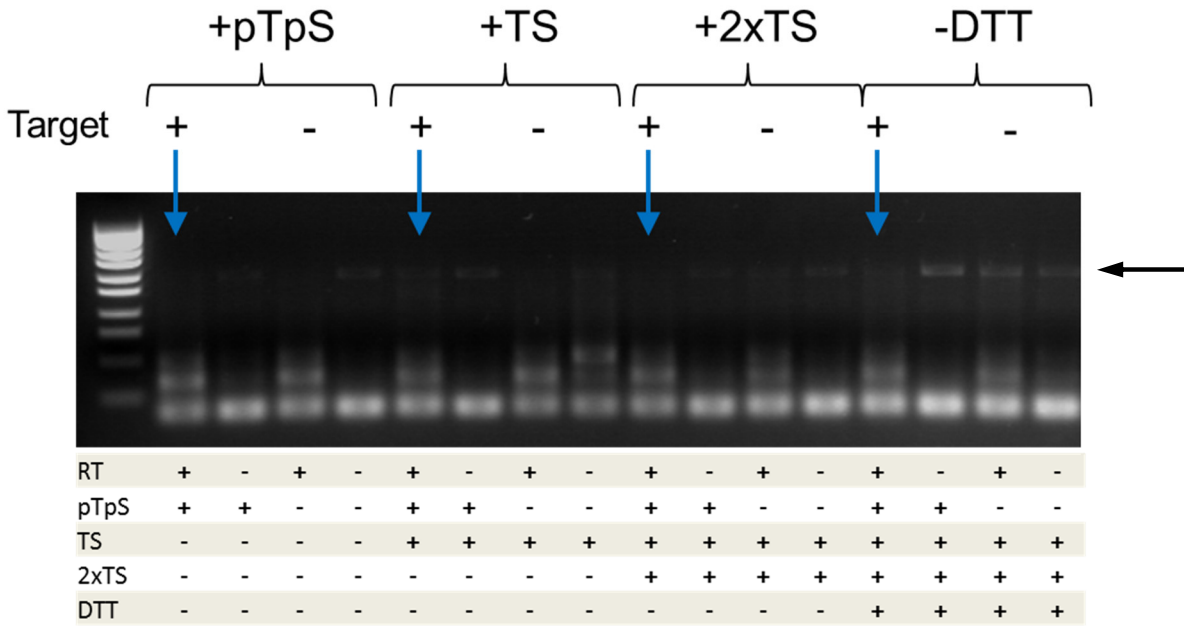

Figure 23. Enrichment of binders after final round. Shows the results after round 3 of block 2. RT=Reverse Transcriptase. Selection conditions: “pTpS” =+Biotin-dual phosphorylated Myc Peptide; “TS”= + De-selection using non-phosphopeptide for 1 round; “2xTS”= + De-selection using non-phosphopeptide for 2 rounds; DTT= Used S30 extract with 1 mM DTT.

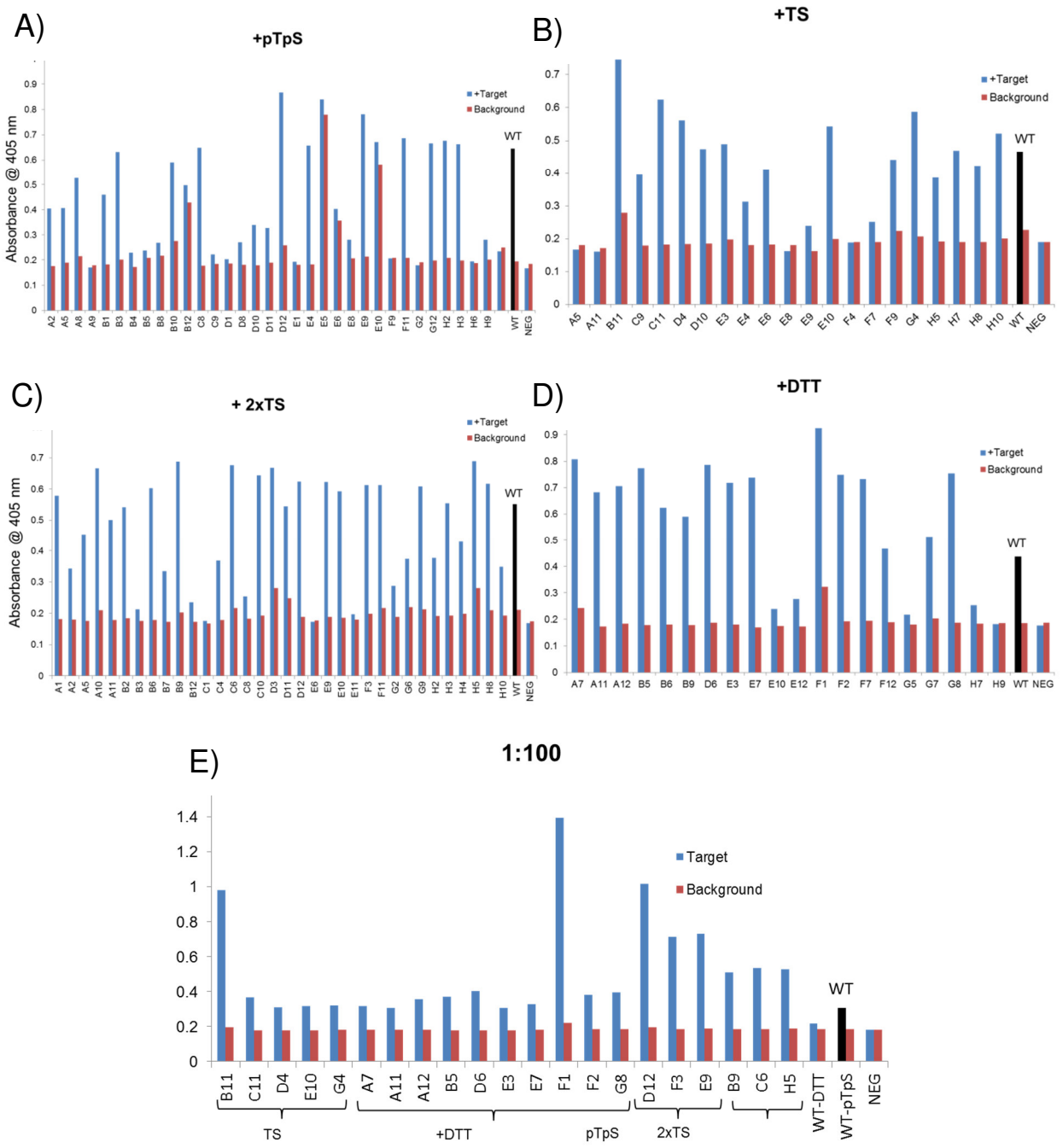
A)
+pTpS
Absorbance @ 405 nm
+Target
Background
WT
A2 A5 A8 A9 B1 B3 B4 B5 B8 B10 B12 C8 C9 D1 D8 D10 D11 D12 E1 E4 E5 E6 E8 E9 E10 F9 F11 G2 G12 H2 H3 H6 H9 WT NEG
B)
+TS
+Target
Background
WT
A5 A11 B11 C9 C11 D4 D10 E3 E4 E6 E8 E9 E10 F4 F7 F9 G4 H5 H7 H8 H10 WT NEG
C)
+ 2xTS
Absorbance @ 405 nm
+Target
Background
WT
A1 A2 A5 A10 A11 B2 B3 B6 B7 B9 B12 C1 C4 C6 C8 C10 D3 D11 D12 E6 E9 E10 E11 F3 F11 G2 G6 G9 H2 H3 H4 H5 H8 H10 WT NEG
D)
+DTT
+Target
Background
WT
A7 A11 A12 B5 B6 B9 D6 E3 E7 E10 E12 F1 F2 F7 F12 G5 G7 G8 H7 H9 WT NEG
E)
1:100
Target
Background
WT
B11 C11 D4 E10 G4 A7 A11 A12 B5 D6 E3 E7 F1 F2 G8 D12 F3 E9 B9 C6 H5 WT-DTT WT-pTpS NEG
TS
+DTT
pTpS
2xTS

Figure 24. Monoclonal ELISA of affinity maturation. Signals from cloned sequences of the ribosome-display affinity maturation are displayed. Blue lines are absorbances of wells with the target peptide. Red lines are of background, no target. WT in black is the original anti-Myc-FHA-A4 from the phage-display selection for comparison. Selection conditions: A) +pTpS = +Biotin pTpS Myc Peptide; B) +TS= +Biotin pTpS Myc Peptide + Deselection using TS Peptide for 1 round; C) 2xTS = +Biotin pTpS Myc Peptide + Deselection using TS Peptide for 2 rounds; D) +DTT= +Biotin pTpS Myc Peptide + Deselection using TS Peptide for 2 rounds but used S30 with DTT. E) The ELISA was repeated using a 1:100 dilution of selected clones.

3.4.2 Sequence Analysis

The sequences of the unique clones are shown compared to the WT anti-Myc and the library scaffold (**Fig. 25**). All of the mutations among the matured clones lay outside the variable loops. The F1 sequence contained an additional cysteine near the c-terminus of the FHA within the disordered region. To determine if intermolecular disulfide bonds were forming, in effect dimerizing the FHA, reducing agent was omitted from the Laemmeli buffer when performing SDS-PAGE. The large shift from 22 kDa to ~45 kDa (black arrow) for the F1, without the reducing agent β-Mercaptoethanol, is evidence that dimerization is occurring (**Fig. 26A**). This is in contrast to the F3 clone which does not have an additional cysteine scaffold mutation and therefore does not dimerize.

The cysteine mutation at amino acid 177 in the F1 clone is interesting in that it arose independently in a phage-display affinity maturation selection of the ERK peptide performed by Dr. Kritika Pershad. It is caused by a single nucleotide mutation of

Cytosine to Thymine. It is unknown whether this region of DNA is susceptible to mutation. The appearance of the same mutation in two separate selection methods, against different targets, and two different researchers, is evidence of the powerful enrichment capabilities of affinity maturation using display selections. Extremely rare occurrences can be amplified in a directed evolution experiment when the mutation provides a selective advantage such as avidity through dimerization.

It is also interesting to note that at amino acid 155 in the G2 sequence, which is the sequence of the thermal-stable FHA scaffold used to construct the phage-display library (13), there is a Serine residue. In the WT anti-Myc clone discovered from this library, there is a scaffold mutation to asparagine. However, in the affinity matured clones B12, F1, and D11 the asparagine has been mutated back to serine.

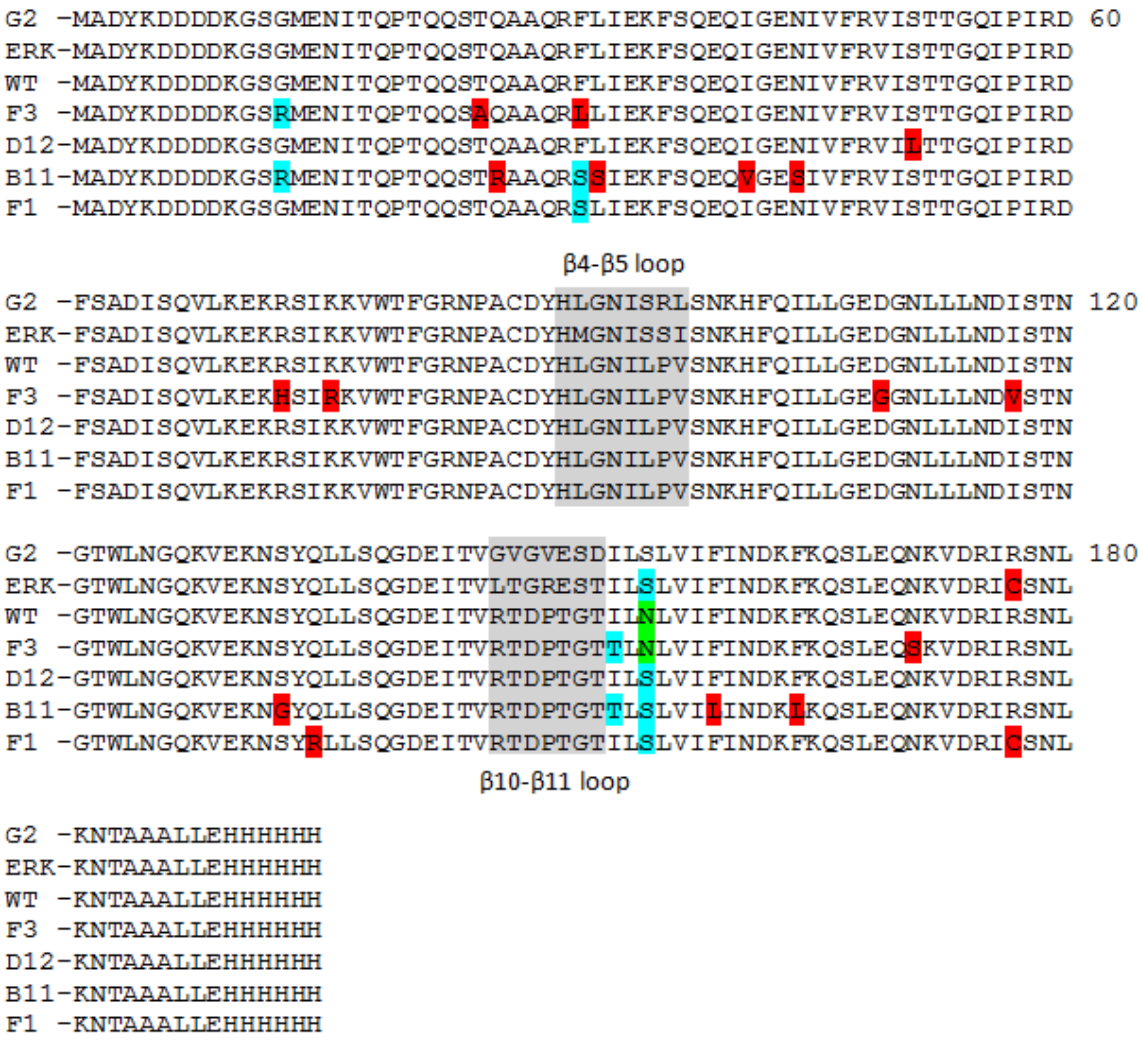

Figure 25. Sequence alignment of affinity matured clones. DNA sequence alignment showing the G2 thermal-stable library scaffold; the anti-ERK FHA with the cysteine at residue 177; the WT original anti-Myc-FHA-A4 clone; and the four anti-Myc affinity matured clones F3,D12, B11, and F1. Bases highlighted in red are unique scaffold mutations. Residue 177 is where mutation results in cysteine. Blue highlights are scaffold mutations shared with at least one other clone. Green are scaffold mutations that reverted back to serine after affinity maturation in most clones. Grey indicates the variable loop regions.

3.4.3 Purification of matured anti-Myc-FHA and ELISA

The anti-Myc-FHA clones with the FLAG tag were expressed through the T7 promoter. Yields were between 20 and 30 mg/L. The preps are of high purity, however, a degradation product can be seen under the expected 22 kDa band (**Fig. 26A**). This degradation is suspected to be the result of the loss of the FLAG tag due to protease cleavage. The degradation product is not seen when the FHA is expressed without the FLAG tag. The original engineering for thermal-stability and bacterial expression did not include this tag in the scaffold, and therefore wasn't considered when the conditions were optimized. Western blot analysis probing against either the N-terminal FLAG tag or the C-terminal poly-His tag confirmed that the degraded protein has lost the FLAG tag and retained the His.

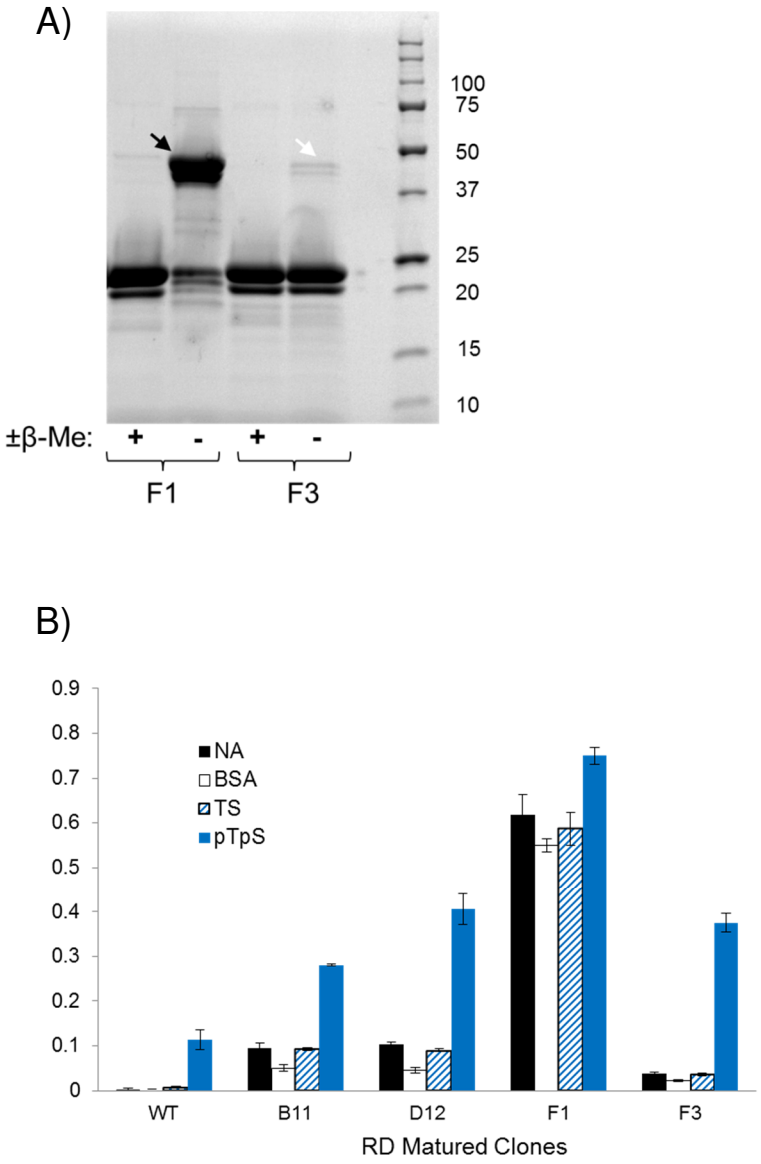

Figure 26. Purification of anti-Myc-FHA and soluble ELISA. A) SDS-PAGE using stain-free system of the F1 clone and the F3 clone. The Laemmeli buffer contained ± β-Mercaptoethanol. Black arrow denotes dimerization due to mutant Cysteine. White arrow shows minor dimerization from internal scaffold Cysteine. B.) ELISA of purified FHA affinity matured clones. Lower-case “p” denotes a phosphorylation. For the NeutrAvidin immobilized targets: TS = Myc peptide without phosphorylations; pTpS = Myc peptide with two phosphorylated residues. BSA= Bovine Serum Albumin. WT is the original anti-Myc-A4 clone. Clones B11, D12, F1, and F3 were affinity matured through ribosome-display.

The soluble ELISA shows the result of the FHA dimerization for the F1 clone (**Fig. 26B**). The overall signal is three times higher than the wild-type, however the background is also three times as high. The best clone with the lowest background and highest signal is F3 with a two-fold increase in binding over the original WT. This shows that the affinity maturation was successful, but the improvement was modest. Affinity maturation using error-prone PCR, off-rate selection with phage-display also yielded a modest increase lending to the notion that an intrinsic limit has been reached for the binding affinity to this particular short phosphopeptide.

3.4.4 Size exclusion chromatography of FHA

To gain more insight into the quality and multimerization states of the anti-Myc-FHA clones, size exclusion chromatography was performed by Fast Protein Liquid Chromatography. The FHA scaffold had never been separated in a non-denaturing method, so the original WT anti-Myc-FHA was analyzed on the FPLC column initially. The expected molecular weight for the FHA is 22 kDa, however when comparing to the standard curve, the peak fraction determined the FHA to be at 33.6 kDa suggesting the three-dimensional shape is causing this discrepancy in size (**Fig. 27A**). There is also evidence of some dimerization seen in a shoulder peak at 68 kDa which is likely a result of the internal cysteine at the scaffold position 87 (**Fig. 27C**). This residue was thought to be inaccessible but shown here to form intermolecular disulfide bonds, although not as readily as the added cysteine in the disordered region. Evidence for this is also in the

faint high molecular weight bands of the SDS-PAGE of clone F3 without β-Mercaptoethanol (**Fig.27A**). Chromatography of the F1 clone with the known exposed cysteine indicates the size of the FHA dimer at about 68 kDa (**Fig. 27B**). An apparent quatramer via the buried cysteine represents a portion (~20%) of the protein population. Additionally, in the D12 affinity matured clone with only the buried cysteine, there is again a population of dimer present at about 10%. This cysteine is the one remaining of the four in the original Rad53 FHA (20) that was left for malemide conjugations after that others were mutated to allow for function when expressing in the reducing environment of bacterial cells (13).

We also wanted to determine if a shift in peak fraction elution could be observed upon FHA binding to the Myc peptide. After adding an excess of peptide to the anti-Myc-FHA WT and allowing 1 hour for binding, the mixture was separated on the column (**Fig. 28**). A shift of about 4.5 kDa is observed which is larger than expected considering the peptide is 1.875 kDa as determined by Mass Spectrometry. This disparity may be due to a small conformational change in the FHA upon binding or is simply at a limit of resolving power of the column. The peptide alone elutes with a calculated size of ~7.5 kDa. Although the size differences can be accounted for here, the peptide molecular weight is out of the range of the column's lower limit of resolution.

A)

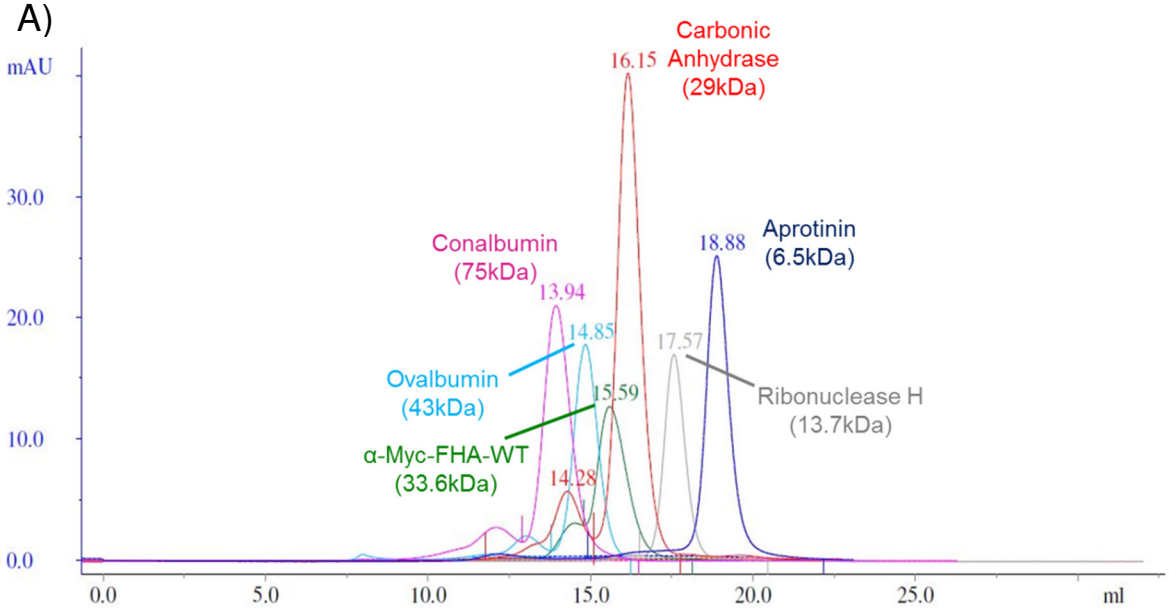
mAU
30.0
20.0
10.0
0.0
0.0
5.0
10.0
15.0
20.0
25.0
ml
Carbonic Anhydrase (29kDa)
16.15
Conalbumin (75kDa)
13.94
14.85
Ovalbumin (43kDa)
15.59
α-Myc-FHA-WT (33.6kDa)
14.28
17.57
18.88
Aprotinin (6.5kDa)
Ribonuclease H (13.7kDa)

B)

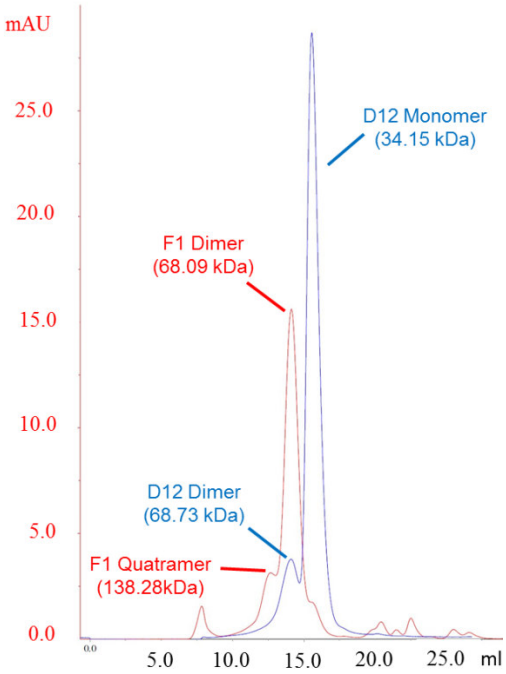
mAU
25.0
20.0
15.0
10.0
5.0
0.0
5.0
10.0
15.0
20.0
25.0
ml
D12 Monomer (34.15 kDa)
F1 Dimer (68.09 kDa)
D12 Dimer (68.73 kDa)
F1 Quatramer (138.28kDa)

C)

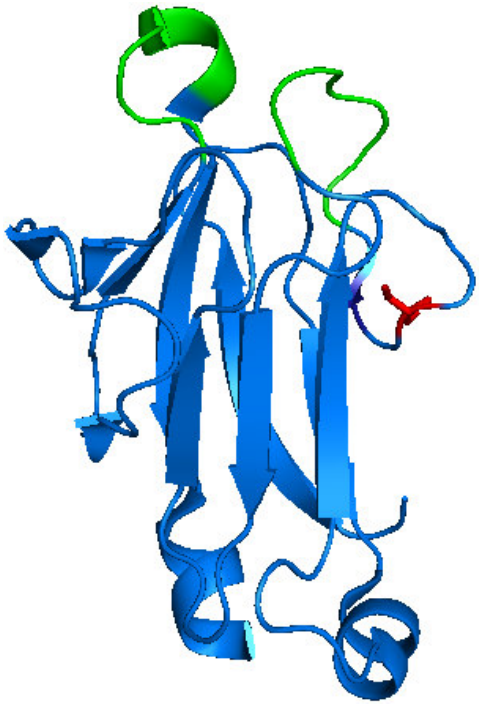

Figure 27. FPLC of anti-Myc-FHA. A) Gel filtration of standar protiens performed in separate runs. The anti-Myc-FHA-WT is in green. Protein is detected by Absorbance at 280 nm and displayed as Absorbance Units. The x-axis denotes the fraction volume eluted from the column after sample injection. B) Gel filtration of the affinity matured dimer F1 (Red) and the monomer D12 (Blue). C) FHA domain (PDB: 1G6G) showing the variable domains (Green) and the internal cysteine (red) with the sulfur directed towards the inside.

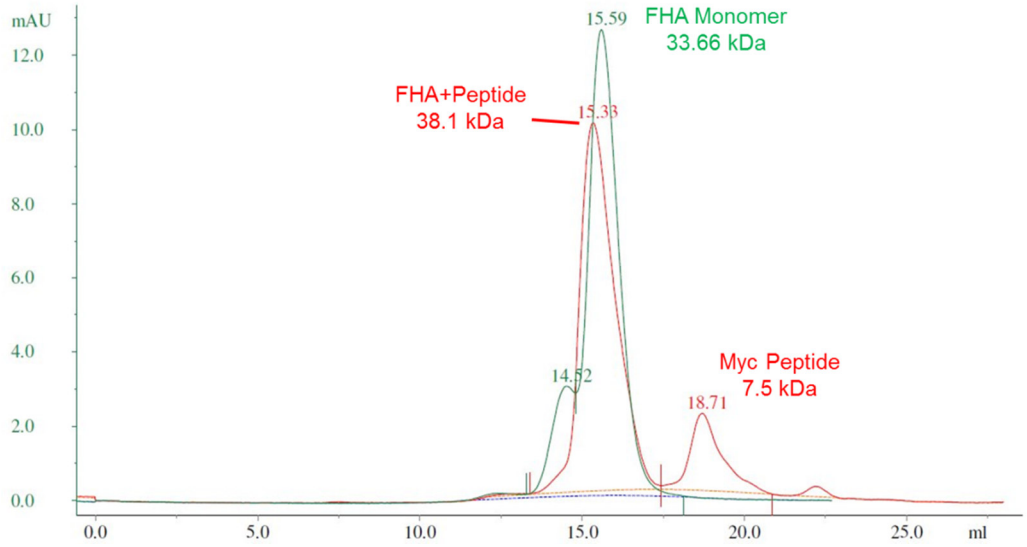

Figure 28. Size shift upon ligand binding. The anti-Myc-FHA-WT is shown before (Green) and after (Red) Myc-peptide binding in a gel filtration separation by FPLC.

3.4.5 Ribosome-display using coupled *in vitro* transcription and translation

One of the hurdles in establishing ribosome-display in a laboratory is the preparation of the S30 ribosomal extract and the optimization of two buffers containing eleven components, three of which the combination of concentrations needs to be optimized. Analysis to monitor the optimization is done by performing ribosome-display.

The success is determined by thickness of band on a gel, but doesn't always correlate to success in an actual selection.

To avoid the preparation of these components, the option of using commercial *in vitro* transcription and translation (IVTT) kits was explored. The EasyXpress coupled IVTT from Qiagen had been used previously for ribosome-display (21). Although more expensive than home-made preparation, the kit is simple, decreases labor and time by about three hours, and reduces chance of RNase contamination. Further, since the laboratory's facilities and equipment could not be partitioned, it was a concern that RNase contamination would destroy the mRNA of the complex before it could be recovered and amplified. Ribosome-display would then be rendered too difficult to establish without a large investment in dedicated equipment and space. Therefore, the kit lowered barriers to attempt the procedure with less investment in resources and allowed the testing of the feasibility of using the technology.

The first attempt with the kit used three different concentrations of Magnesium Acetate to determine the optimal concentration. The kit's buffer components were proprietary so it was uncertain whether the complex would be stabile without added Mg^{2+}. The ribosome-display was performed using the anti-Myc-FHA that had been used successfully in Dr. Andreas Pluckthün's lab at the University of Zurich. Using the method described earlier, a single-round mock selection was conducted where the *in vitro* transcription and translation were performed in the same reaction vessel for 1 hour total. The results were visualized by gel electrophoresis (**Fig. 29**). The gels showed the selections using the 15 mM and 21.4 mM concentrations of Magnesium Acetate gave

the most intense band (white arrows) for the positive target, with reverse transcriptase (+RT) at the expected size of 576 bp. Background binding to the no target control was seen but at a reduced amount when compared to the positive. The minus reverse transcriptase (-RT) indicates there is little DNA template carryover, or at least not enough to account for the +RT positive template result. Further experiments implemented increased washing to remove background binding to the negative control of both the complex and DNA template. These experiments also excluded the addition of Magnesium Acetate during the translation and the ribosome-display was still successful (data not shown).

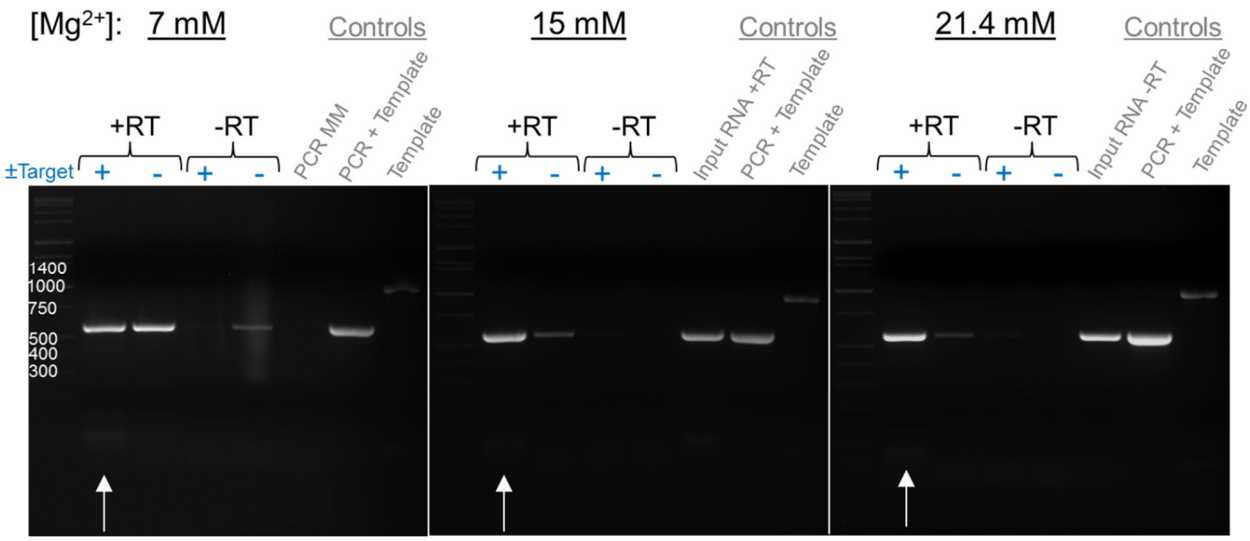

Figure 29. Mock Ribosome-display selection using IVTT Kit. Results of the mock selection of ribosome-displayed anti-Myc-FHA-A4 using the EasyXpress coupled IVTT kit. Three concentrations of Magnesium acetate are used at 7, 15, and 21.4 mM. White arrow points to lane where band is expected at 576 bp. Wells with –RT did not undergo reverse transcription and should not have a product. Wells with minus target should have no band. The wells with "PCR + template" label is a positive control for amplicon size of the final PCR and the original template DNA. The "input RNA+RT" was a positive control for the reverse transcription that used the RNA from the IVTT. The "Template" lanes indicate the size of the original template before amplification. The "PCR MM" well tests for PCR master mix DNA contamination.

3.4.6 Pull-down and Western blot of in vitro transcription and translation

Since the coupled *in vitro* transcription and translation kits have rarely been used in ribosome-display, there is a concern that either or both steps are inefficient when compared to traditional methods (12). If this is the case, then a large DNA library's translated members may be limited in diversity. Limiting the diversity will reduce the chance of yielding high affinity binders from affinity maturation or a primary selection

(10). To utilize large libraries on the order of 1 $x10^{12}$ to $1x10^{13}$, at least equal numbers of RNA transcripts need to be transcribed and at least that many ribosomes need to be present to form the complex. The PURExpress cell-free IVTT kit from NEB was used for these experiments since the number of ribosomes per reaction is 60 pmols or $3.6x10^{13}$ molecules according to the manufacturer, and the translation aspect has been used for successful ribosome-display in the past (22). This kit was also attractive because the purified *E. coli* protein synthesis components omit nucleases, proteases, and release factors (23) and was shown to create highly stable ternary complexes as compared to a S30 cell extract, even at temperatures above 4°C (24). Finally this purified system it is likely to exclude proteins involved in bacterial mechanisms to rescue translation from stalled ribosomes (25,26).

Although the transcription likely produces many-fold more transcripts than required, it is still unknown how well the translation forms complexes. To investigate the yields of FHA protein, an *in vitro* transcription and translation reaction with the kit was performed using the anti-Myc-FHA WT as the ribosome-display template. The nascent FHA-ribosome-RNA complex was isolated from the reaction by pull-down using anti-FLAG antibody conjugated magnetic beads. The complex was eluted with EDTA and the FHA was probed in a western blot (**Fig. 30**). The western blot detected dark bands at 29.35 kDa and at 31.25 kDa. The expected size of the FHA + TolA tether (when released from the complex) is 29.5 kDa, accounting for the more intense of the two bands on the blot. The slightly larger band may be the FHA + TolA as well but at a different translation end-point of the stalled ribosome. It is not known exactly where in

the tether the ribosome stalls. There may be more than one location depending on the extent of RNase degradation from the 3' end or the state of the 3' hairpin intended to stall the ribosome and the nucleases. Alternatively, the larger band could be an artifact in that it is part of a wide band of an overloaded lane, similar to the 1000 ng standard lane. A number of additional faint bands can be seen above and below the two major bands. Some of these can be attributed to terminated protein synthesis and truncated FHA products. The FLAG tag is at the N-terminus of the FHA where it will be translated first in any form of the protein and therefore detected on the western.

Assuming both the most intense bands are the FHA + TolA tether, there is about 1 ug of protein when comparing to the standard concentrations of purified FHA. This is about 2×10^{13} molecules which is close in accordance to the maximum 3.6×10^{13} molecules we would expect if every ribosome was functional and translated one FHA.

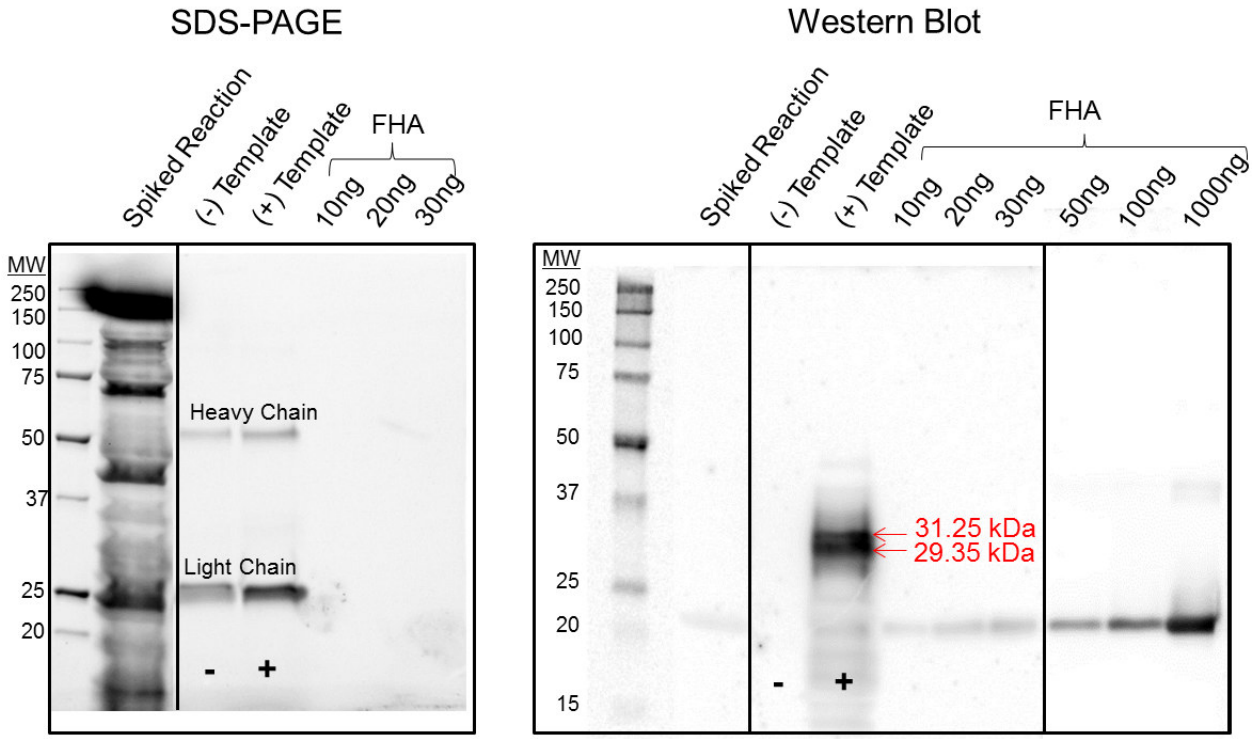

Figure 30. Pull-down and Western blot of IVTT. The left panel is the SDS-PAGE result of the pull-down before transferring to the membrane. The Heavy and Light chains (labelled) originate from the anti-FLAG monoclonal antibody used for the pull-down. The “Spiked” FHA reaction was not purified by the magnetic bead system and therefore contains all components of the IVTT. The anti-Myc-FHA-WT standards were expressed, purified, and diluted before running on the gel. The total amounts are below the detection limits of the gel imaging system. The right panel is the western blot probing the FLAG tag of the FHA. (-) Template is a negative control with the IVTT reaction mix but without the FHA ribosome-display template. (+) Template included 1 ug of FHA DNA template. The FHA expected size is 22 kDa. The expected size of FHA-TolA fusion is 29.5 kDa.

3.5 Conclusion

We showed for the first time that the Fork-head associated domain was amenable to ribosome-display. Using this display technology, we affinity matured a FHA against a Myc phosphopeptide through error-prone PCR and off-rate competition selections. Through these methods, directed evolution was in used to enhance the affinities of the FHA binders. The highest affinity antibodies generated (F1) were found to be dimers formed by intermolecular disulfide bonds of cysteines arising from mutation in the disordered region near the c-terminus. This is an increase in functional affinity due to avidity and only materializes against a high concentration of immobilized target. The reagent displaying this dimerization also lost its specificity for the phosphopeptide when expressed as a soluble protein. It is realized that a reducing agent must be included in all selections where random mutation can give rise to additional cysteines. Of the isolated clones present as monomers, the affinity increased modestly in ELISA about three-fold for the F3 which is what was seen in phage-display. We conclude that the short peptide target was not sufficient in size to generate tighter binding reagents. On top of this, the requirement for specificity against only the phosphothreonine and the +3 residue (16) leaves little room for strong interaction. This may be an intrinsic limit of the FHA domain as equilibrium dissociation constants against phosphothreonine containing epitopes have been at best reported to be ~0.1 μM (27) , 0.36 μM (20) and 1 uM (13).

A second alternative conclusion is that the original FHA library was not of sufficient size to generate tight binding clones. During the affinity maturation, the

random mutagenesis did not mutate the variable loops. In fact, all identified mutations from the selected clones occurred only in the framework. To enhance binding of the FHAs, it may be necessary to target the loops since the few contacts between residues are formed here. This can be done by re-making the primary library in the ribosome-display format where a 100-1000-fold increase in diversity is typical. Affinity maturation may then be rendered unnecessary if resulting affinities are high enough from the initial selection.

Finally we have successfully shown that ribosome-display can be performed with the anti-Myc-FHA using coupled *in vitro* transcription and translation kits. The kit saves setup time, decreases mRNA degradation from nucleases, and reduces significant labor in the procedure. We have also investigated the yields of displayed protein by probing membranes blotted with *in vitro* transcribed and translated FHA lacking a stop codon. Through this analysis, it can be reasonably assumed that large primary or secondary libraries can be constructed and displayed with diversities > $1x10^{13}$. Although we are not directly detecting the concentration of complexes formed, the western blot together with the recovery of RNA from the ribosome-display selection is strong evidence for a degree of efficiency that lends to a successful procedure.

3.6 References

1. Low NM, Holliger P, Winter G. Mimicking Somatic Hypermutation: Affinity Maturation of Antibodies Displayed on Bacteriophage Using a Bacterial Mutator Strain. *Journal of Molecular Biology* 260: 359-368. (1996).

2. Daugherty PS, Chen G, Iverson BL, Georgiou G. Quantitative analysis of the effect of the mutation frequency on the affinity maturation of single chain Fv antibodies. *Proc Natl Acad Sci U S A* 97: 2029-2034. (2000).

3. Northrup SH, Erickson HP. Kinetics of protein-protein association explained by Brownian dynamics computer simulation. *Proc Natl Acad Sci U S A* 89: 3338-3342. (1992).

4. Pluckthun A. Ribosome display: a perspective. *Methods Mol Biol* 805: 3-28. (2012).

5. Huang R, Fang P, Kay BK. Improvements to the Kunkel mutagenesis protocol for constructing primary and secondary phage-display libraries. *Methods* 58: 10-17. (2012).

6. Finlay WJ, Cunningham O, Lambert MA, Darmanin-Sheehan A, Liu X, et al. Affinity maturation of a humanized rat antibody for anti-RAGE therapy: comprehensive mutagenesis reveals a high level of mutational plasticity both inside and outside the complementarity-determining regions. *J Mol Biol* 388: 541-558. (2009).

7. Groves M, Lane S, Douthwaite J, Lowne D, Rees DG, et al. Affinity maturation of phage display antibody populations using ribosome display. *J Immunol Methods* 313: 129-139. (2006).

8. Hanes J, Pluckthun A. In vitro selection and evolution of functional proteins by using ribosome display. *Proc Natl Acad Sci U S A* 94: 4937-4942. (1997).

9. Vaughan TJ, Williams AJ, Pritchard K, Osbourn JK, Pope AR, et al. Human antibodies with sub-nanomolar affinities isolated from a large non-immunized phage display library. *Nat Biotechnol* 14: 309-314. (1996).

10. Ling MM. Large antibody display libraries for isolation of high-affinity antibodies. *Comb Chem High Throughput Screen* 6: 421-432. (2003).

11. Zaccolo M, Williams DM, Brown DM, Gherardi E. An approach to random mutagenesis of DNA using mixtures of triphosphate derivatives of nucleoside analogues. *Journal of Molecular Biology* 255: 589-603. (1996).

12. Dreier B, Plückthun A Rapid Selection of High-Affinity Binders Using Ribosome Display. In: Douthwaite JA, Jackson RH, editors. Ribosome Display and Related Technologies: Springer New York. pp. 261-286.(2012)

13. Pershad K, Wypisniak K, Kay BK. Directed evolution of the forkhead-associated domain to generate anti-phosphospecific reagents by phage display. *J Mol Biol* 424: 88-103. (2012).

14. Kritika Pershad, Unpublished results

15. Dyson MR, Zheng Y, Zhang C, Colwill K, Pershad K, et al. Mapping protein interactions by combining antibody affinity maturation and mass spectrometry. *Anal Biochem* 417: 25-35. (2011).

16. Durocher D, Taylor IA, Sarbassova D, Haire LF, Westcott SL, et al. The molecular basis of FHA domain:phosphopeptide binding specificity and implications for phospho-dependent signaling mechanisms. *Mol Cell* 6: 1169-1182. (2000).

17. Zahnd C, Spinelli S, Luginbuhl B, Amstutz P, Cambillau C, et al. Directed in vitro evolution and crystallographic analysis of a peptide-binding single chain antibody fragment (scFv) with low picomolar affinity. *J Biol Chem* 279: 18870-18877. (2004).

18. Rasila TS, Pajunen MI, Savilahti H. Critical evaluation of random mutagenesis by error-prone polymerase chain reaction protocols, Escherichia coli mutator strain, and hydroxylamine treatment. *Anal Biochem* 388: 71-80. (2009).

19. Personal communication. Birgit Dreier, University of Zurich

20. Liao H, Yuan C, Su MI, Yongkiettrakul S, Qin D, et al. Structure of the FHA1 domain of yeast Rad53 and identification of binding sites for both FHA1 and its target protein Rad9. *J Mol Biol* 304: 941-951. (2000).

21. Kuchař M, Vaňková L, Petroková H, Černý J, Osička R, et al. Human interleukin-23 receptor antagonists derived from an albumin-binding domain scaffold inhibit IL-23-dependent ex vivo expansion of IL-17-producing T-cells. *Proteins: Structure, Function, and Bioinformatics*: n/a-n/a. (2013).

22. Ohashi H, Shimizu Y, Ying BW, Ueda T. Efficient protein selection based on ribosome display system with purified components. *Biochem Biophys Res Commun* 352: 270-276. (2007).

23. Shimizu Y, Inoue A, Tomari Y, Suzuki T, Yokogawa T, et al. Cell-free translation reconstituted with purified components. *Nat Biotechnol* 19: 751-755. (2001).

24. Matsuura T, Yanagida H, Ushioda J, Urabe I, Yomo T. Nascent chain, mRNA, and ribosome complexes generated by a pure translation system. *Biochem Biophys Res Commun* 352: 372-377. (2007).

25. Keiler KC, Waller PR, Sauer RT. Role of a peptide tagging system in degradation of proteins synthesized from damaged messenger RNA. *Science* 271: 990-993. (1996).

26. Karzai AW, Roche ED, Sauer RT. The SsrA-SmpB system for protein tagging, directed degradation and ribosome rescue. *Nat Struct Biol* 7: 449-455. (2000).

27. Pennell S, Westcott S, Ortiz-Lombardia M, Patel D, Li J, et al. Structural and functional analysis of phosphothreonine-dependent FHA domain interactions. *Structure* 18: 1587-1595. (2010).

CHAPTER 4

COMBINING RIBOSOME-DISPLAY WITH PHAGE-DISPLAY TO GENERATE RECOMBINANT AFFINITY REAGENTS

Filed with the USPTO in September 2014. Michael R. Kierny and B. K. Kay. PCT/US2014/057617. Patent Pending.

4.1 Abstract

With patents on phage-display and single-chain fragments of variation (scFv) expiring, many biotechnology companies have begun their own recombinant antibody production pipelines. Ribosome-display is another recent off-patent technology that is seldom implemented in industry even as it has shown great potential to alleviate the growing demand for custom affinity reagents. To aide in producing high quality reagents at a faster pace, we have combined ribosome- and phage-display in a novel fashion which takes advantage of the strengths of each technology. We call the process “Primer Extension for Selection Recovery (PExSR)” and demonstrate the utility by constructing a Fibronectin III monobody library with a $>1x10^{13}$ diversity and performing multiplexed selections against human protein targets to yield single-digit nanomolar affinity binders in ~10 days. The selection method solves intrinsic limits of diversity and quality of phage-display libraries but also reduces the time and labor required to generate a reagent from a full ribosome-display selection.

4.2 Introduction

As the popularity of recombinant affinity reagents continues to grow, methods to rapidly produce greater quantities against more targets will become desirable. Phage-display provides a platform for affinity selection that is easy to perform but requires modification through affinity maturation in order to be useful to the researcher (1). Ribosome-display yields higher affinity reagents but has not been adopted as readily. A

PubMed search query for “phage-display” returns 23 times more hits than a search for “ribosome-display”.

It has been shown that the larger the starting library diversity, the more likely a high affinity reagent will be selected without the need for affinity maturation (2,3). However, due to the limited number of *E. coli* cells that can be feasibly grown, the largest libraries constructed by near heroic efforts for phage-display are on the order of 1×10^{10} members (4,5) which are stored frozen and subjected to freeze-thaw before selection. Ribosome-display, on the other hand typically starts with a freshly translated library with a diversity 100-fold greater (6,7), but requires more steps and effort if not automated.

In the past, ribosome-display has been combined with other display technologies for screening the output from the ribosome-display rounds (8) or for affinity maturation of phage-display selected pools (9,10). Never has it been integrated with phage-display as part of a primary selection scheme.

Table III. Comparison of the two display technologies and the combination of their respective strengths in PExSR.

	Ribosome-display	Phage-display	PExSR
Starting Library size	10^{12}-10^{13}	10^{9}-10^{10}	10^{12}-10^{13}
Hours per round	30	11	15
Steps per round	14	9	10.5
Affinity Kd values	nM to pM	µM to nM	nM to pM
Affinity Maturation	Integrated	Separate selection	Integrated
Library Stability	Freshly made protein	Protein stored frozen	Protein made fresh
Regenerate Library	PCR	Grow Liters of cells	PCR

Here we combine two powerful protein display technologies, ribosome- and phage-display, in a novel way to generate recombinant affinity reagents quicker and more efficiently than each alone (**Table III**). The method reported takes advantage of the large diversity possible with DNA libraries by conducting the first round of selection by ribosome-display. The output from the first round is then converted to a phage-display plasmid using megaprimer annealing and extension to a single-stranded uracilated DNA phagemid where the parental strand is destroyed upon transformation into *E. coli* (11,12,13). The resulting recombinant proteins are then expressed on phage and subjected to additional rounds of off-rate selection (**Fig. 31**). The real advantage however, is shown here in the multiplexing ability of the procedure to increase throughput and efficiency in generating single-digit nanomolar binding

reagents against three antigens on average of 3.5 days per antigen.

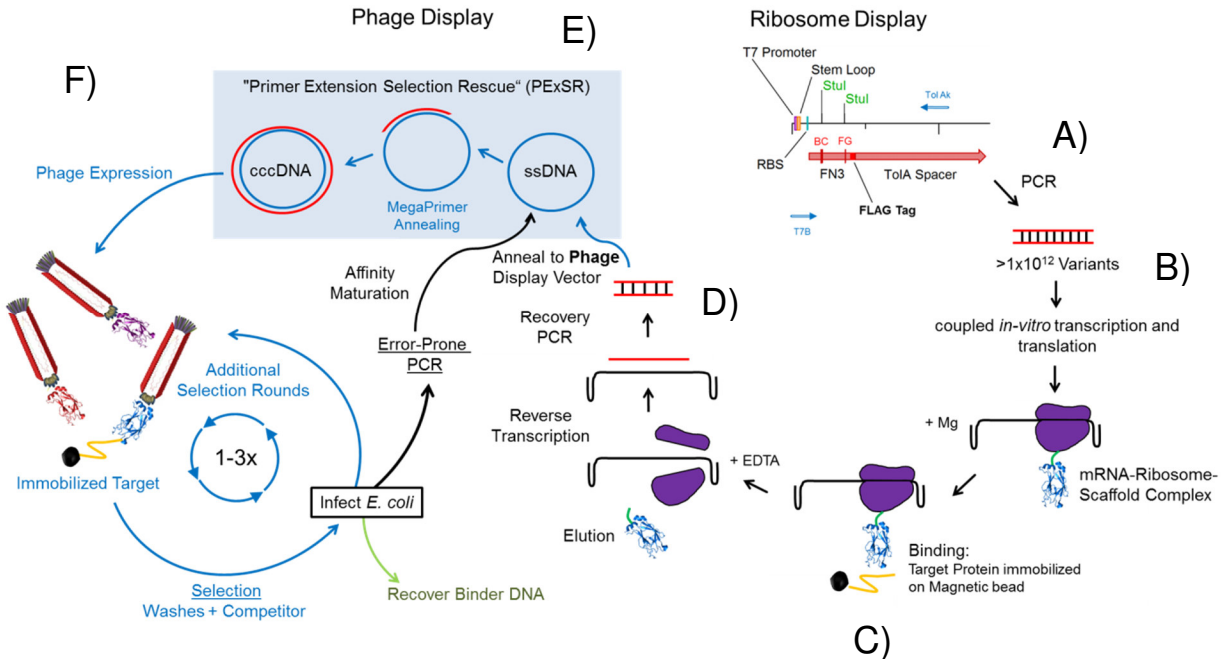

Figure 31. Primer extension for selection rescue. A) The procedure starts with a large dsDNA template made by PCR containing the T7 promoter, RBS, antibody scaffold, Tol A tether and the 5' and 3' hairpins. B) The template is added to the coupled *in vitro* transcription and translation kit to allow the mRNA-ribosome-nascent antibody scaffold complex to form. C) The complex is then subjected to a selection for a given biotinylated target protein. The target protein and complex are captured by streptavidin magnetic beads and washed. The surviving complex is eluted with addition of EDTA to dissociate the complex. The mRNA is reverse transcribed. D) The cDNA is PCR amplified using primers inside of the antibody scaffold. E) PExSR (the crucial step after which the method is named): The PCR product is used as a megaprimer to anneal to a ssDNA phagemid containing a M13 origin of replication and a pIII phage coat protein to allow phage-display. The primer is extended to fill in the remaining plasmid to form a heteroduplex dsDNA. This is transformed into *E. coli* and the phage are expressed. F) Phage-display commences for 1-3 additional rounds of selection where the binders are recovered and screened (green arrow) or affinity matured (black arrow) through error-prone PCR, megaprimer annealing, and increased stringency selections.

4.3 MATERIALS AND METHODS

4.3.1 PExSR Ribosome-display library plasmid

The ribosome display vector pRDV (GenBank accession AY327136) was modified from the original to contain a M13 origin of replication (bps 1539-1748, for ssDNA production) and a Fibronectin III monobody scaffold (bps 117-401) containing a down-stream FLAG tag (bps 402-434, DYKDDDDK) (**Fig. 32**). The FN3 scaffold also contains *StuI* restriction sites and ochre stop codons in the BC and FG variable loops to prevent the parent clone from displaying a full protein. The Tol A tether protein is downstream and in-frame with the FN3 coding region and FLAG epitope. Its purpose is to allow the FN3 to emerge from the ribosomal tunnel so it may freely interact with antigen.

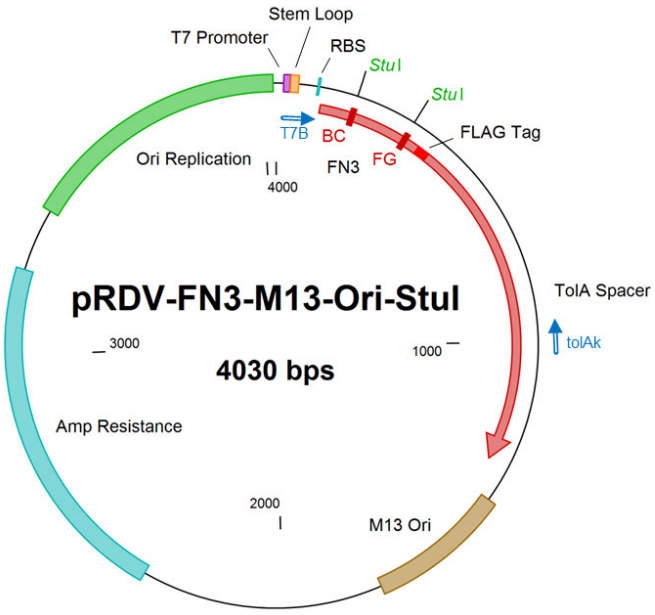

Figure 32. PExSR ribosome-display plasmid. The pRDV plasmid was modified to contain a M13 origin of replication (brown). The FN3 scaffold was cloned downstream of the T7 promoter (purple) the 5' prime stem loop (orange) and the ribosome binding site (orange). The scaffold contains two *StuI* restriction sites within the two variable loop regions BC and FG along with TAA stop codons. The Open Reading Frame is in red. A FLAG tag was introduced between the FN3 and the TolA tether protein. The forward primer T7B and the reverse primer Tol Ak (blue arrows) are to amplify the template for ribosome-display.

Single-stranded DNA production

The pRDV-FN3-StuI plasmid was electroporated into CJ236 electrocompetent cells with genotype: FΔ(*HindIII*)::cat (Tra+ Pil+ CamR)/ *ung-1 relA1 dut-1 thi-1 spoT1 mcrA* (New England BioLabs). Cells were grown to mid-log phase in 2xYT/15 μg/mL Chloramphenicol (Cm)/50 ug/mL Carbenicillin (Cb) and infected with M13K07 helper phage (New England Biolabs) at an MOI of 10 for 1 h at 37 ℃. The phage were

allowed to express overnight (~22 h) in 2xYT/ Cb/50 ug/mL Kanamycin (Kan) at 25 ℃, 230 rpm shaking. After pelleting the cells, the phage were precipitated with 4% PEG_{8000} and 0.5 M NaCl, final concentrations, at room temp for 20 minutes. The resulting phage pellet was resuspended in 4 mL of PBS. The phage were lysed and the ssDNA purified using the QIAprep Spin M13 Kit (Qiagen). The ssDNA was eluted in 50℃ water and the concentration determined by NanoDrop spectrophotometer (ThermoScientific).

4.3.2 Trinucleotide library synthesis

The oligonucleotides for the primer extension are a mixture of triplet phosphoramidite codons (Ella biotech, Munich, Germany), which encode 30% tyrosine, 15% serine, 15 % glycine, and 5% of tryptophan and phenylalanine. The remaining residues are represented at 2.3% each except for cysteine and methionine which are excluded. The lengths of the loops are also varied at 5, 6, 7, and 8 residues for the BC loop and 7, 9, 10, 11, 12, and 13 residues for the FG loop.

4.3.3 Primer Extension

This full procedure can be viewed in detail here (13). Briefly, about 300 pmol of both the BC and FG loop megaprimers were phosphorylated with T4 polynucleotide kinase (New England Biolabs) for 1 h and then allowed to anneal to 100 pmol of the ssDNA pRDV-FN3-StuI by denaturing at 95 ℃ for 2 min and slowly reducing

temperature at 1 ℃ per minute until 24 ℃ was reached. To fill in the remaining portions of the plasmid, the heteroduplex was extended by T7 DNA Polymerase (New England Biolabs) and T4 DNA Ligase (New England Biolabs). The double-stranded hetero-duplex (closed-complementary DNA or cccDNA) results in the recombinant sequence as the coding strand and the parent sequence as the antisense strand.

4.3.4 Phage-TolA Recombinant Confirmation

To determine the recombination rate in order to add sufficient amounts of cccDNA to the PCR to maintain the large diversity, a small amount of the heteroduplex DNA (~10 ng) was sacrificed for transformation into TG-1 *E. coli* cells and plated on 2xYT/Cb to obtain single colonies. From the overnight plates, 96 colonies were grown in 250 µL of 2xYT/Cb in a 96-deep-well plate at 280 rpm, 37 ℃, for 3.5 h. When the cells reached mid-log phase (OD_{600}=0.4), they were infected with M13K07 helper phage at an MOI of 10 for 1 h with 150 rpm shaking at 37 ℃. The cells were spun down and resuspended in 400 µL 2xYT/Cb/Kan and grown overnight for phage expression at 30 ℃. After 16 h, the FN3-FLAG-TolA fusion protein was induced through the T7 promoter with 1 mM IPTG (Isopropyl β-D-1-thiogalactopyranoside) by adding 100 µL 2xYT/Cb/Kan, 5 mM IPTG, to all wells and allowing expression for 5 h.

In parallel, a Maxisorp 96-well microtiter plate (Nunc) was coated overnight at 4 ℃ with 10 ug/mL NeutrAvidin (Life Technologies) in Phosphate Buffered Saline (PBS). The day of the ELISA, the wells were blocked with 200 µL of 1% casein in PBS for 1 h

(ThermoScientific). All washings were done in 300 µL of PBST (0.1% Tween 20), three times each, using a BioTek ELx405 Plate Washer. After washing, 50 µL of 1:5,000 biotin labeled-anti-FLAG antibody (Sigma-Aldrich) in PBST was added to all wells for 1 h.

The overnight culture with the 5 h IPTG induction was spun down at 4,000 rpm for 5 min and 50 µL of the supernatant added to the prepared 96-well Maxisorp plate and incubated with 500 rpm shaking for 1 h. A small amount of fusion protein was assumed to have been secreted into the supernatant, and therefore, lysing of the cells was unnecessary. The plate was washed and 50 µL of 1:5,000 anti-M13-HRP monoclonal antibody (GE Healthcare Life Sciences) added to all wells for 1 h. Washed the plate 5 times with PBST and added the substrate 2,2-Azino-bis (3-Ethylbenozthiazoline-6-Sulfonic Acid)(ABTS)(Sigma-Aldrich) with 0.03% H_2O_2. Plate was read at absorbance 405 nm wavelength after 5, 15, and 30 min using a POLARstar OPTIMA microplate reader (BMGLabtech).

4.3.5 Ribosome-display Template

To generate the ribosome display template, PCR was performed for 185 x 50 µL reactions that amplified both the recombinant and the parent strands of the FN3 monobody. Primers used are described in (14): T7B (ATACGAAATTAATACGACTCACTATAGGGAGACCACAACGG) and Tol Ak

(CCGCACACCAGTAAGGTGTGCGGTTTCAGTTGCCGCTTTCTTTCT). Each reaction contained 1 ug of cccDNA, 0.4 mM dNTPs, 1 µM primers, 3 mM $MgCl_2$, 1 x polymerase buffer and 1 U of Platinum® Taq DNA Polymerase (Life Technologies). Thermalcycling was performed as follows: 3 min at 95 ℃, 30 cycles of 95 ℃ denature for 30 sec, 55 ℃ annealing for 30 sec, and 72 ℃ extension for 45 sec. Final extension for 5 m at 72 ℃. To rid the prep of the parental strand, the reactions were pooled and 192 x 60 µL restriction digests were done with 10 Units/reaction of *StuI* for 3 h at 37 ℃. The digests were pooled and a phenol:chloroform:isoamyl 25:24:1 (Sigma-Aldrich) extraction was performed followed by an ethanol precipitation.

The digest was run on a 0.8% agarose gel and the recombinant, un-digested bands, were extracted to give a yield of 54 pmol or about 3.2×10^{13} molecules. To maintain the diversity but amplify the library for use in many selections, the product was amplified in 50 reactions by PCR using the same primers and conditions as before. After PCR product purification by Qiagen PCR Purification kit, the template DNA was concentrated by eluting in a small volume after ethanol precipitation to around 2 ug/µL. This high concentration is necessary because of reaction volume limits in the *in vitro* transcription and translation kit (New England Biolabs) and the intention to add > 1×10^{13} library members to each selection.

4.3.6 PExSR Selection for MAP2K5

Target proteins were purchased from the Structural Genomics Consortium (SGC). Proteins came in formats lacking and including an N-terminal AviTag for site-specific biotinylation. All proteins had an N-terminal 6x-His tag for IMAC. The target protein is a human protein kinase, Mitogen Activated Protein Kinase Kinase 5 (MAP2K5).

4.3.7 Ribosome-display

Much of the Ribosome-display procedure can be found at (15). Here, the *in vitro* transcription and translation (IVTT) are conducted in parallel using the cell-free PURExpress kit (New England BioLabs) which contains purified *E. coli* translation components and ribosome concentration at 2.4 µM or 60 pmols per reaction which is 3.6×10^{13} molecules. The IVTT was performed for 2 h at 30 °C using 11 ug or 1.4×10^{13} molecules of the template.

The reaction was stopped by the addition of 1 mL of Tris-Buffered Saline with 0.1% Tween 20 (TBST), 0.5% BSA, 50 mM MgAc,12.5 µL 200 mg/mL Heparin (Sigma) and spun down at 4 °C for 5 min.

All steps were done in a 4 °C refrigerator to reduce the amount of RNA degradation by slowing the RNase activity. A mini-centrifuge was used to briefly spin

down the liquid in the tubes for all steps. For all steps, 2 mL Eppendorf LoBind tubes were used to reduce DNA template carry-over.

Preselection: Added 500 µL of the Ribosome-mRNA-FHA complex to two 2 mL tubes with 30 µL of DynaBeads MyOne T1 Streptavidin Coated magnetic beads (Life Technologies) pre-blocked with TBST, 0.5% BSA, and rotated at 4 ℃ for 1 h. The 2 mL tubes were placed into a 50 mL conical for protection from RNase contamination and ease of handling.

The beads were captured by magnetic separation and the supernatant containing the complex added to blocked 2 mL tubes. To the + Target tube was added 100 nM (50 pmols) of biotin-MAP2K5 (16.2 kDa) in TBST. To both tubes was also added 100 mM Dithiothreitol (DTT) to give final concentrations of 0.5 mM to prevent disulfide bond formation and dimerization of binders. This was incubated with rotating for 1 h at 4 ℃.

The complexes with and without target were then added to separate tubes of 30 µL fresh Streptavidin coated magnetic beads blocked in TBST, 0.5% BSA, and incubated for 30 m at 4 ℃ with tumbling.

The beads-ribosome-mRNA-FN3 complex was washed once in 1 mL of cold wash buffer (TBST, 50 mM MgAc, 0.1% BSA) and transferred to a new blocked tube. The beads were then washed 8 additional times with 1 mL wash buffer with five minutes of tumbling each at 4 ℃. During the final wash, the beads were transferred to

a new blocked tube in order to obtain a cleaner elution. This removes any DNA or complexes bound to the tube walls.

The complex was eluted into 100 µL of elution buffer (TBST, 0.5% BSA, 25 mM EDTA, 50 ug/mL of *S. cerevisiae* RNA) for 10 m at 4 ℃. This was added to 400 µL of Lysis Buffer of the High Pure RNA Isolation kit (Roche Applied Science) and shaken to mix. The previous step was repeated with fresh elution buffer using 100 µL for an additional 10 m and then added to the 500 µL of elution and lysis buffer on ice, and mixed.

4.3.8 RNA isolation

The lysis/elution was spun in the High Pure RNA Isolation kit column at 8,000 x g for 1 min. The flow-through was removed by pipetting. 100 µL of diluted DNase I @ 1.8 U/µL in DNase incubation buffer was added to each ± target column and allowed to stand for 15 mi at room temp. 500 µL of Wash buffer 1 was added and centrifuged for 1 min at 8,000 x g. Columns were washed again with 500 µL of Wash buffer 2 and centrifuged 8,000 x g for 1 min. To the columns was added 100 µL of Wash buffer 2 and centrifuged at 13,000 x g for 2 min. Recovered RNA was eluted in 50 µL of Elution buffer (PCR grade water) and incubated for 2 min before centrifugation at 8,000 x g for 1 min into clean tubes. Transferred 4 x 12.5 µL of + target RNA elution to PCR tubes,

and 2 x 12.5µL of the – target to PCR tubes. The RNA was denatured at 70 ℃ for 10 min, then kept on ice until the Reverse Transcription step.

4.3.9 Reverse Transcription

To generate cDNA, the ± target elutions were reverse transcribed using Reverse Transcriptase (+RT). As a control, one reaction from each set were performed without Reverse Transcriptase (-RT). Each of the reactions had a 20.25 µL final volume with final concentrations: 1.23 µM inside Reverse Primer PExSR FN3 (GCCGCTGGTACGGTAGTTAATCGAG), 0.25 mM dNTPs, 1 U/µL of RiboLock RNase inhibitor (ThermoScientific), ± 1.23 U/µL AffinityScript Multiple Temperature Reverse Transcriptase (RT) (Agilent Technologies), 1 x Affinity Transcript Buffer, and 9.9 µM (DTT).

Three +RT reactions were performed with the eluted RNA from the (+) target tube to obtain the most cDNA for the downstream PCR. The controls of the (–) target and –RT were performed once each. All reactions were incubated at 50 ℃ for 1 h.

4.3.10 cDNA Amplification by PCR

To amplify the cDNA, 10 µL of each reverse transcription was used in a 35 cycle PCR with total volume of 50 µL and final concentrations: 0.5 µL Herculase II Polymerase Fusion DNA Polymerase (Agilent Technologies), 1 x Herculase II Reaction buffer, 0.1 mM dNTPS, 5% Dimethyl sulfoxide (DMSO), 1 µM inside Forward Primer

PExSR FN3 (ATGGCCGTTTCTGATGTTCCGCGTA), and 1 µM inside Reverse Primer PExSR FN3. Four reactions were performed for the +target, +RT in order to generate plenty of template for the primer extension. PCR was performed as follows: 3 min at 95 ℃, then 30 cycles of 95 ℃ denature for 30 sec, annealing at 55 ℃ for 30 sec, and extension at 72 ℃ for 45 sec. The final extension was 5 min at 72 ℃. The reactions were purified with the QIAquick PCR Purification kit and eluted in 50 ℃ water.

4.3.11 Primer Extension for Selection Recovery

The primer extension was performed as described in (13). Briefly, 15 pmol of the PCR product was phosphorylated for 1 h at 37 ℃. This was annealed to 5 pmol of Uracilated ssDNA phagemid pKP300-FN3-2xStuI (ssDNA phagemid expressed from M13 phage grown in CJ236 *E. coli* that lacks the Uracil deglycosylase enzyme) by denaturing at 95 ℃ for 2 min and slowly reducing temperature at 1 ℃ per minute until 24 ℃ was reached. To fill in the remaining portions of the plasmid, the heteroduplexes were extended by the action of T7 DNA Polymerase (New England Biolabs) and T4 DNA Ligase (New England Biolabs). The resulting double-stranded DNA was purified on a QIAquick column and transformed by electroporation into 2 x 100 µL of the TG-1 strain of *E. coli* cells, Genotype: [F' *traD36 proAB lacIqZ ΔM15] supE thi-1 Δ(lac-proAB) Δ(mcrB-hsdSM)5(rK - mK -)* (Lucigen Corporation), allowed to recover at 150 rpm in 2 mL of warmed Recovery Media (Lucigen) for 30 min at 37 ℃. Cells were plated on two large 2xYT/Cb agar plates and incubated overnight at 30 ℃.

4.3.12 Phage display

Each plate was scraped into 5 mL of 2xYT media and combined and vortexed. 50 µL was used to inoculate 50 mL of 2xYT /Cb and grown to mid-log phase(OD_{600}= ~0.4). Cells were infected with M13K07 helper phage at an MOI of 10 for 30 min at 37 ℃. Cells were spun down at 4,000 rpm for 7 min and resuspended in 2xYT/CB/Kan media. Culture was shaken at room temp for 18 h. The overnight culture was spun down twice at 12,000 rpm for 10 min. The 50 mL supernatant was precipitated with 10 mL of 24% PEG, 3 M NaCl, final 4% PEG, for 20 min at room temp. The precipitate was spun down at 12,000 rpm for 10 min to pellet the phage. The tubes were rinsed with 1 mL of PBS each, and then the pellet was resuspended in 1 mL of PBS.

Selection: As a de-selection step, 0.5 mL of the phage resuspension was added to 20 µL of prewashed and blocked Streptavidin MagneSphere magnetic beads (Promega) in an Eppendorf LoBind 2 mL tube and tumbled for 1 h at room temp. The beads were captured on a magnetic separator and the phage supernatant transferred to a fresh BSA blocked 2 mL tube. To the phage supernatant was added 10 pmol or (20 nM final) of the target biotin-MAP2K5 and allowed to equilibrate for 1 h with room temperature tumbling. Ten-fold concentration of competitor was added at 200 nM (100 pmol total) of MAP2K5-His-tagged only protein was added and allowed to equilibrate for 2 h with room temp tumbling. The phage, target, and competitor mix were added to 30 µL of pre-blocked SA magnetic beads for 30 min to capture the biotin-MAP2K5. This was washed twice with 1 mL PBST for 5 min each, 2 min on the magnetic separator,

then transferred to fresh a tube and wash 6 additional times with PBST. The final wash was transferred to a fresh tube and eluted into 100 µL of 100 mM Glycine (pH 2) for 10 m. The magnetic beads were captured and the elution neutralized with 12 µL of 2 M Tris pH 10. The eluted phage were added to 1 mL of TG-1 cells grown to OD_{600} 0.4, for 30 m at 37 °C. The cells were plated on large 2xYT/Cb plates and incubated overnight at 30 °C.

For the second round of phage-display, the selection steps were repeated starting with the scrapping of the cells and growing overnight after M13K07 infection. For this round, 100-fold competitor (2 µM final) was added to the phage and biotin target. Washes were performed as described above. However, the final two washes included the 100-fold competitor and 10 minute incubation for each. After two additional washes, the phage were eluted, neutralized, used to infect TG-1 cells, and plated for single colonies on 2xYT/Cb.

4.3.13 MultiPlex Selection

The multiplex selection was performed similar to the selection against MAP2K5 with the following exceptions. The IVTT during the Ribosome-display was increased to three reactions with 33.0 µg (71.61 pmol, 4.3×10^{13} molecules) of template in a single volume to increase the number of FN3 monobody variants exposed to three target proteins. The target proteins added to the single volume were 50 nM (50 pmols) of biotin-USP11, biotin-COPS5, and biotin-CDK2 in TBST (150 pmols target total). After

the PExSR, the selections were separated with a low stringency phage-display round. The following two rounds of phage-display increased competitor concentration from 10-fold over the target to 100-fold over the target. The final round of 100-fold competition was performed overnight (~22 h) at 4 °C, before elution and infection of TG-1 cells. The USP11 target competition steps were done slightly different from the other two targets due to lack of material. There was not enough non-biotinylated USP11 protein available for the in-solution competitions. To solve this, the phage and biotin-USP11 were first bound to the Streptavidin magnetic beads. The empty sites not occupied by the biotinylated USP11, were filled with the addition of 1 µM free biotin. The competition was then performed with the addition of the 10-fold or 100-fold excess of biotin-USP11.

4.3.14 Polyclonal ELISA

Starting from the frozen scraped cells stored in 16% Glycerol at -80 °C, 5 µL was thawed and used to inoculate 5 mL of 2xYT/Cb. Cultures were grown at 37 °C, 250 rpm until mid-log (OD600= ~0.4). The cells were infected with M13K07 Helper phage at a MOI of 10 for 1 h with shaking at 150 rpm, 37 °C. These were spun down at 4,000 rpm for 5 min and resuspended in 50 mL of 2xYT/Cb/Kan and grown overnight ~22 h at 23 °C, 230 rpm.

Maxisorp 96-well microtiter plates were coated overnight with 1 ug/mL NeutrAvidin (ThermoScientific) at 4 ℃. The plates were blocked the next day with 200 µL of 1% Casein blocking buffer in PBS (ThermoScientific) for 1 h. All washings were done in 300 µL of PBST, three times each, using a BioTek ELx405 Plate Washer. Plates were washed before addition of 50 µL of 1-10 nM biotinylated targets in PBST for 1 h with 500 rpm shaking. Plates were washed and the phage culture spun down for 5 min at 4,000 rpm and the supernatant diluted 1:1 with PBST before adding a total of 50 µL/well. This was incubated for 1 h shaking. Plates were washed and 50 µL/well of 1:5,000 anti-M13-HRP bacteriophage monoclonal antibody (GE HealthCare) in PBST was added to all wells for 1 h with shaking. The final wash was performed 5 times and to each well was added 50 µL of the ABTS with 0.03% H_2O_2. Plates were read at absorbance 405 nm after 5, 15, and 30 min using a POLARstar OPTIMA microplate reader (BMGLabtech).

4.3.15 Monoclonal ELISA

The monoclonal ELISA was performed similarly to the polyclonals. For every target 95 colonies were picked from the final selection round and grown in deep-96-well plates with 200 µL of 2xYT media and Cb for 3 h at 37 ℃, 250 rpm shaking. Each culture was infected with M13K07 Helper phage at an MOI of 10, for 30 min, 150 rpm

shaking at 37 °C. These were spun down and resuspended in 400 µL of 2xYT/Cb/Kan, and grown overnight at 23 °C, 230 rpm shaking.

Biotinylated targets were added to appropriate wells in 50 µL volumes at 0.5-1 nM. Background plates with no target protein were also used for each target where only NeutrAvidin was immobilized. Phage were spun down and the supernatant diluted 1:1 (50 µL total) in PBST when adding to each well.

4.3.16 Competition ELISA

The amount of phage supernatant used was optimized depending on the individual binders. Each phage supernatant was mixed with final concentrations of 100, 10, 1, 0.1, 0.01 nM free His-Only-tagged target for 1 h in PBST. This was added to 2 nM biotin-target immobilized on NeutrAvidin coated Nunc Maxisorp plates for 1 h and allowed to equilibrate. Phage were detected with addition of anti-M13-HRP and read at 405 nm after addition of ABTS substrate as described above. The graphing software OriginPro 9.0 (OriginLab) was used to construct the graphs. The curve fitting was performed using the “DoseResponse” function under the sigmoidal fit module.

SLiCE cloning into pET14b

For further characterization of the monobodies, the coding sequences were cloned into a SUMO fusion bacterial expression vector with a T7 promoter (pET14b-SUMO). This was performed by the *in vitro* recombination method known as Seamless Ligation Cloning Extract or SLiCE, see (16) for detailed information. Briefly, the plasmid was linearized by a single restriction enzyme, *StuI*, and purified by agarose gel electrophoresis. This was mixed with a PCR amplicon of the FN3 monobody clone which contained ends that were homologous to the desired insertion location in the linearized plasmid. Addition of extract from *E. coli* strain DH10B and incubation at 37 ℃ for 1 h allowed for electroporation into BL-21 *E. coli* and recovery on 2xYT/Cb plates.

4.3.17 Expression and Purification

A scrapping of bacterial BL-21 frozen stocks of the clones in the pET14b-SUMO plasmid were inoculated into 200 mL of Overnight Express Autoinduction Media (EMD Millipore) and grown at 30 ℃ for 22-24 h. Cells were centrifuged at 4,000 rpm for 10 min, the supernatant removed, and the pellet frozen at -80 ℃. The cells were thawed and resuspended in 25 mL of equilibration buffer (50 mM sodium phosphate, 300 mM sodium chloride, pH 7.4). The cells were cooled on ice with cOmplete EDTA Free protease inhibitor (Roche). Cell lysing was performed with 50% amplitude sonication on ice with 10 sec ON sonication, 10 sec OFF, for five minutes total ON time using a

SonicDismemberator (Branson inc. Model 500). Tubes were spun at 15,000 rpm for 15 min. The supernatant was transferred to a 50 mL protein purification column. The agarose was prepared by washing 300-500 µL of Clontech His60 agarose bead slurry (60 mg/mL binding capacity) twice with equilibration buffer. Resin was added to cleared lysate in columns, the ends sealed, and the columns incubated at 4 ℃ for 2 h while tumbling. The columns were then drained through the matrix and the beads washed with 150 mL of equilibration buffer until the flow though gave an A_{280} NanoDrop 1000 reading of < 0.01 mg/mL. The column was then washed with 100 mL of wash buffer (50 mM sodium phosphate, 300 mM sodium chloride, pH 7.4, 40 mM Imidazole) until again the Abs_{280} < 0.01 mg/mL. The protein was eluted into 1 mL fractions using elution buffer (50 mM sodium phosphate, 300 mM sodium chloride, pH 7.4, 300 mM Imidazole. The concentrations were determined using the NanoDrop 1000. The A_{280} protein module utilized the molecular weight and extinction coefficient parameters to obtain the most accurate determination of concentration. Purity was analyzed by SDS-PAGE.

4.3.18 Isothermal Titration Calorimetry

ITC was performed on a MicroCal iTC200 system (GE Healthcare Life sciences). Both monobody and target were dialyzed overnight at 4 ℃ in 5 L of 200 mM Imidazole, 150 mM NaCl, 25 mM Tris. Protein concentrations were determined by NanoDrop A_{280}. The sample cell contained 200 µL of the target protein at 8 -24 µM and

the 40 µL of titrant monobody in the syringe was 68-237 µM. A total of 21 injections were performed. The first injection volume was 0.5 µL with 200 seconds spacing. The remaining 20 injection volumes were 1.8 µL for 3.6 seconds with 200 seconds spacing and a reference power of 10 ucal/s. Heat change was plotted using the Origin 8.5 software. Measurements were taken during three separate runs and averaged.

4.4 Results and discussion

4.4.1 Library construction

The initial step to demostrate that this approach is better than the two individual technologies was to construct a large library of Fibronectin III monobodies (FN3) by annealing triplet codon oligonucleotides to the BC and FG variable loops of a single-stranded DNA plasmid containing the necessary components for ribosome-display (pRDV-FN3-M13 Ori-StuI, **Fig . 32**). Oligonucleotides with a bias towards insertion of codons for Tyrosine (30%), Glycine (15%), and Serine (15%), were synthesized with varying numbers of triplet codons resulting in 5, 6, 7, and 8 residues for the BC loop and 7, 9, 10, 11, 12, and 13 residues for the FG loop (17,18). These biases were chosen because of evidence of a high percentage of Tyrosine residues at variable regions of various affinity reagents (19,20). It is thought that the prevalence of Tyrosine at interaction sites is attributed to the many types of tight bonds the side-group can form with residues of an antigen. The surrounding Glycine and Serine residues provide

for flexibility of the Tyrosine side chain to position for optimal contact (21). After primer extension, the closed-circular DNA or cccDNA heteroduplex is formed which appears as a double-stranded DNA plasmid when run on an agarose gel (**Fig. 33A**). Comparing the ds pRDV control to the newly formed cccDNA shows similar bands at about 6 kbp and at 2 kbp indicating double-stranded DNA has been formed and the primer extension was a success. The single-stranded pRDV has been completely converted to cccDNA. Additionally, all of the megaprimer has been annealed. The cccDNA (**Fig. 33B**) was used as the template for a large scale PCR.

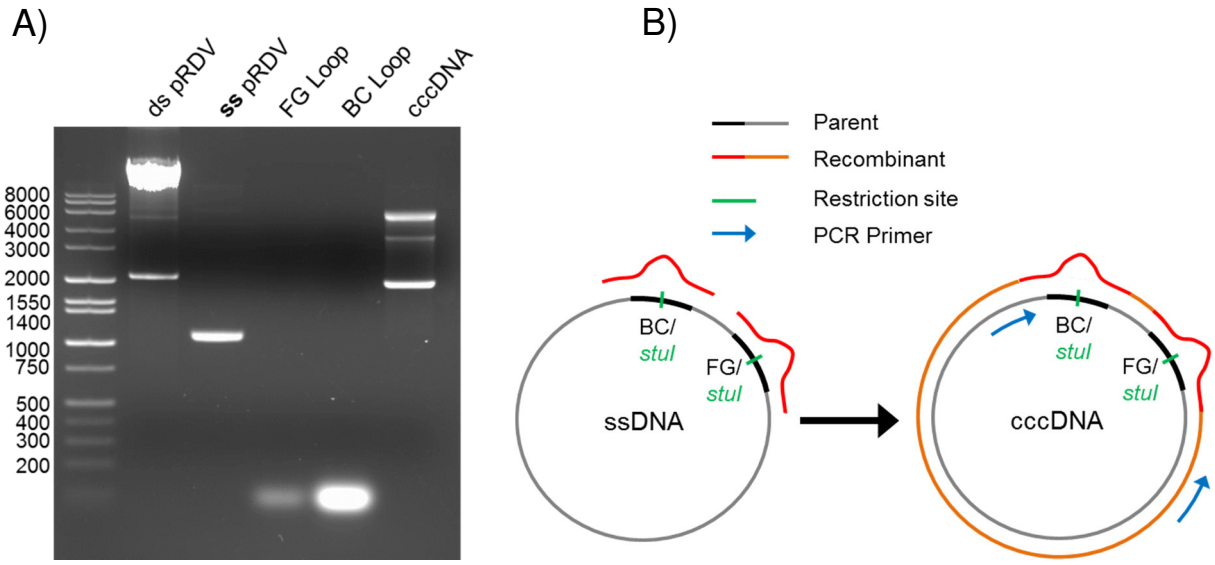

Figure 33. Primer extension to generate plasmid library. A) Primer extension. The "BC Loop" oligonucleotide and the "FG Loop" oligonucleotide are annealed to the "ss pRDV". The primers are extended to complete the heteroduplex "cccDNA". Comparison of the "ds pRDV" to the "cccDNA" shows many similar bands. B) Cartoon of conversion from the ssDNA pRDV to cccDNA. BC and FG loop (red) anneal over the parent strand (black) that contains the *stuI* restriction sites (green) and the stop codons (not shown). The remainder of the DNA is filled in (orange) using polymerase and ligase. The PCR primers (blue) are T7B and tolAk for template generation.

4.4.2 Phage-TolA recombinant confirmation

To confirm the cccDNA library's viability and recombination rate, we came up with a novel assay which takes advantage of the TolA tether region of the ribosome display vector as a tag for phage binding and detection of the monobody. This protein tether is present to allow the nascent monobody to completely emerge from the ribosomal tunnel during translation (6,15). It has been identified as a periplasmic co-receptor for bacteriophage infection of *E. coli* (22). The phage coat protein pIII was shown to bind to the TolA c-terminus of the cell during infection. The C-terminus of the TolA constitutes the tether. We transformed a small amount of the cccDNA and picked 96 colonies to grow. After induction with IPTG and concomitant infection with helper phage, the FN3 monobody-FLAG-TolA fusion was expressed along with the M13 bacteriophage. Immobilization of anti-FLAG-monoclonal antibody captures the FN3 fusion with TolA bound by the phage. The phage coat protein is then detected using an anti-M13 HRP conjugated antibody in an ELISA (**Fig. 34**). The recombination rate was determined to be about 40%. This is likely an underestimation since 70% of the Sanger sequencing chromatograms showed two or more different plasmids per isolate that could not be completely deciphered. Calculations were then be made for the appropriate degree of PCR amplification required to maintain the desired diversity.

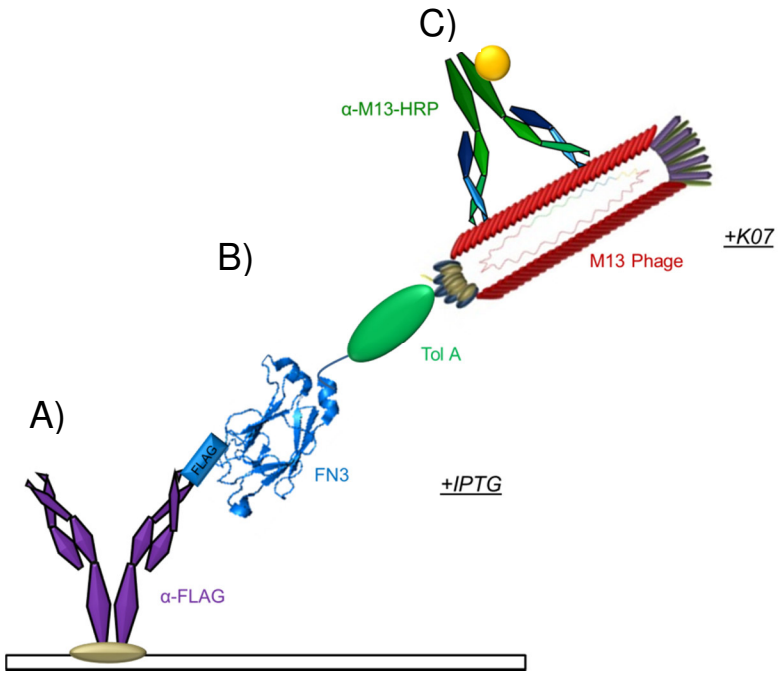

Figure 34. Phage-TolA Recombination ELISA. Simplified diagram of the ELISA to determine recombination rate. A) An anti-FLAG antibody is immobilized on a microtiter well through streptavidin-biotin linkage. B) The cell containing the pRDV plasmids are induced with IPTG to express the FN3-TolA fusion protein that is captured via the FLAG tag. C) Helper-phage infection expresses phage with the pIII coat protein that binds to the TolA. The complex is detected with an anti-M13-HRP antibody that recognizes the pVIII coat protein. Components are not drawn to scale.

4.4.3 Ribosome-display library template

The large scale PCR resulted in two expected species as the coding strand contained the recombinant sequence, while the non-coding strand was the parental strand (**Fig. 35**). Both strands are amplified in the PCR because the primers cannot discriminate between the two when hybridizing at the ends of the constant scaffold. To target the unwanted parental strand for destruction, the *StuI* restriction enzyme

digested at the BC and FG loops that lacked a recombination event. The undigested recombinant strand was separated and extracted by gel electrophoresis. A single product expected at 710 bp results from the PCR which consists of the two species. Fully and partially digested fragments are expected at 514 bp (1 cut at BC), 360 bp (2 cut), 350 bp (1 cut at FG), 197 bp and 153 bp (both 2 cut). The uncut recombinant band at 710 bp band was gel extracted and used for a second round of large scale PCR.

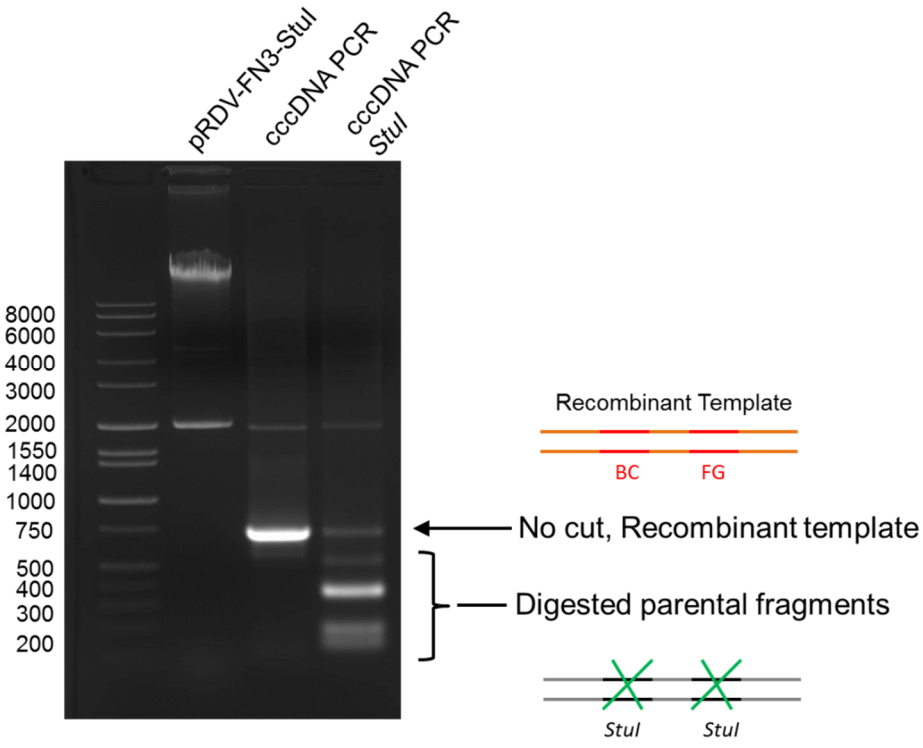

Figure 35. Ribosome display template by cccDNA PCR. Large scale PCR of the cccDNA gives one major band of two species. Digestion with S*tuI* destroys the parental strand (black and gray). Undigested product is recombinant (red and orange).

To obtain a large library size, 24 pmol or ~1.5 x 10^{13} molecules of DNA was purified for ribosome-display template. Additional PCR amplification yielded ~430 pmol or enough for 18 selections with a starting library diversity of 1.5 x 10^{13}. This can theoretically be amplified without loss of diversity assuming no PCR bias. Little bias is plausible because of the constant monobody scaffold. The above effort can be compared to constructing a phage-display library where maintaining a smaller library of 7 x 10^{10} variants requires growing 10 L of cells that then need to be infected, and the phage purified before storage at -80℃ in glycerol.

4.4.4 PExSR selection for MAP2K5

For the first selection attempt using the newly constructed library, we used biotinylated human Mitogen Activated Protein Kinase Kinase 5 (MAP2K5) as a target because of the many antibodies it has elicited in the past. To form the complex, we deviated from the standard procedure (15) and used a coupled *in vitro* transcription and translation (IVTT) kit (23) adding >1.5 x 10^{13} template DNA molecules. The PURExpress IVTT kit from NEB was selected because the PURE system lacks nucleases and release factors (24), has shown to form highly stable ternary complexes (25), contains a known ribosome concentration of 60 pmol or 3.6 x 10^{13} molecules, and has been used in ribosome-display of an scFv in the past (26). The ribosome concentration is the potential bottle-neck of the translated library diversity. The

selection was allowed to proceed in-solution so dimers would not be favorably selected. The complex of RNA-Ribosome-FN3-MAP2K5 was pulled down with streptavidin magnetic beads. After washing and elution of the complex, the recovered RNA was reverse transcribed and PCR amplified.

Success of the selection can be monitored by comparing band intensity to a no-target control on an agarose gel (**Fig. 36**). A greater intensity is seen with (+) target as compared to the control. There is some non-specific binding observed with the (-) target controls but the product recovery is significantly less. The positive control using the starting DNA template in the PCR shows the expected size of the megaprimer at about 285 bp. In this case, the full 710 bp template has been amplified as well. Although the inside primers included in the PCR only amplify a 285 bp region, primers from the library construction PCR (T7B and tolAk) will be carried over even after purification steps, to prime a larger region. Bands resulting from the combinations of the outside and inside primers can be seen in between at expected sizes.

The post-ribosome-display round (RD1) PCR output is the megaprimer for annealing to a single-stranded uracilated phagemid in a step we have named Primer Extension for Selection Rescue (PExSR) to convert to the phage-display format. We also use the term to define the entire method. Transformation into *E. coli* should destroy any non-recombinant uracilated phagemid, however this is not the case. We have observed a large percentage of the transformants to have the unwanted parental plasmid. In this case only 5% were recombinant resulting in a recovery of 2.5×10^7

recombinant clones. The non-recombinants contain the *StuI* site and stop codons in the loops so they will not display and interfere with the selection.

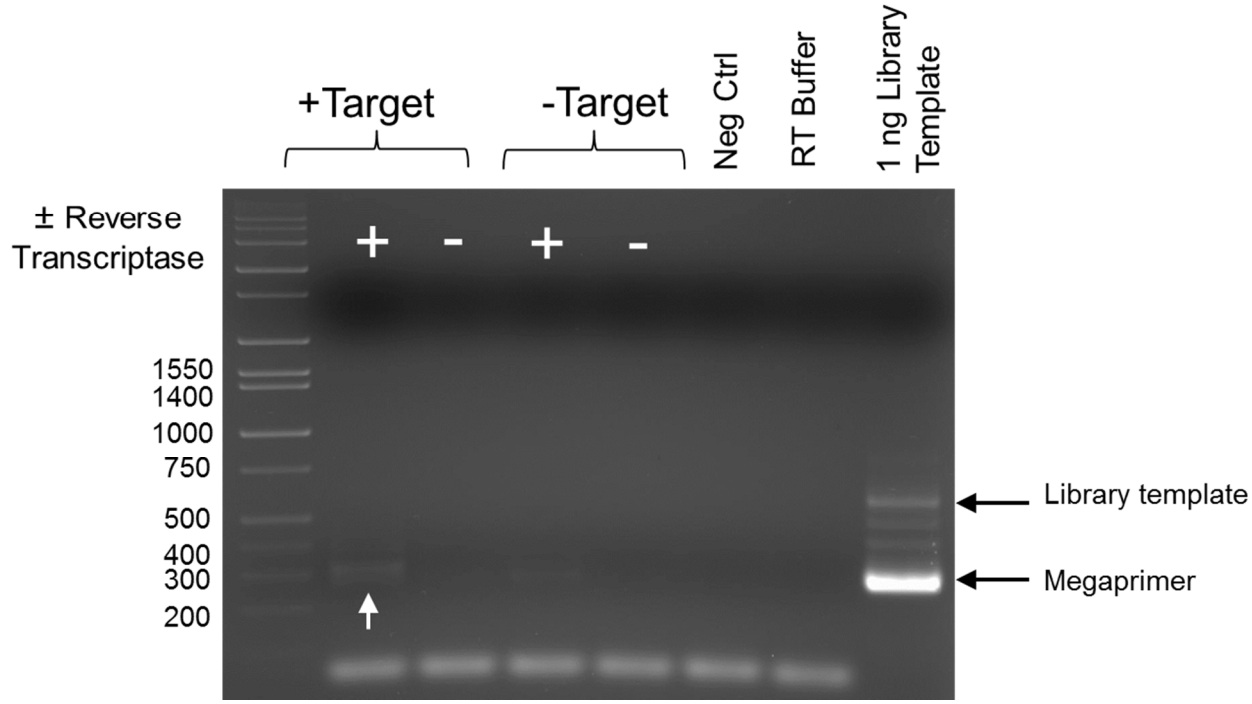

Figure 36. Post-ribosome-display selection. The recovered band can be seen in the (+) target/(+) reverse transcriptase (white arrow) at the expected size of 285+ bp. There is little template DNA carryover as there is only a faint band in the (–) transcriptase. The (-) target shows some non-specific binding but it is significantly less than the (+) target. The PCR of the library template is a positive control to show expected sizes.

The second round of selection (PD1) was completed using phage-displayed clones in a similar manner to the ribosome-display round except that a competitor, in the form of a non-biotinylated target MAP2K5 protein, was added at a 10-fold molar concentration. Any weak binders that have fast off-rates will be bound by the high concentrations of competitor and therefore will not be recovered. The selection progress was monitored by polyclonal and monoclonal ELISAs (**Fig. 37**). The signal increases as the best binding monobodies are enriched. There is binding seen in the polyclonal ELISA after the ribosome-display round. The signal then increases after the first round of phage-display. The monoclonal ELISA identifies 1-2 binders after the ribosome-display round, but it represents only 5% of the 60 colonies picked. After the phage-display selection, the binders are greatly enriched to 85% of the 12 isolated colonies available for analysis. This underscores the necessity of the PD rounds (**Fig 37C**). The final round of selection included 100-fold molar concentration of competitor.

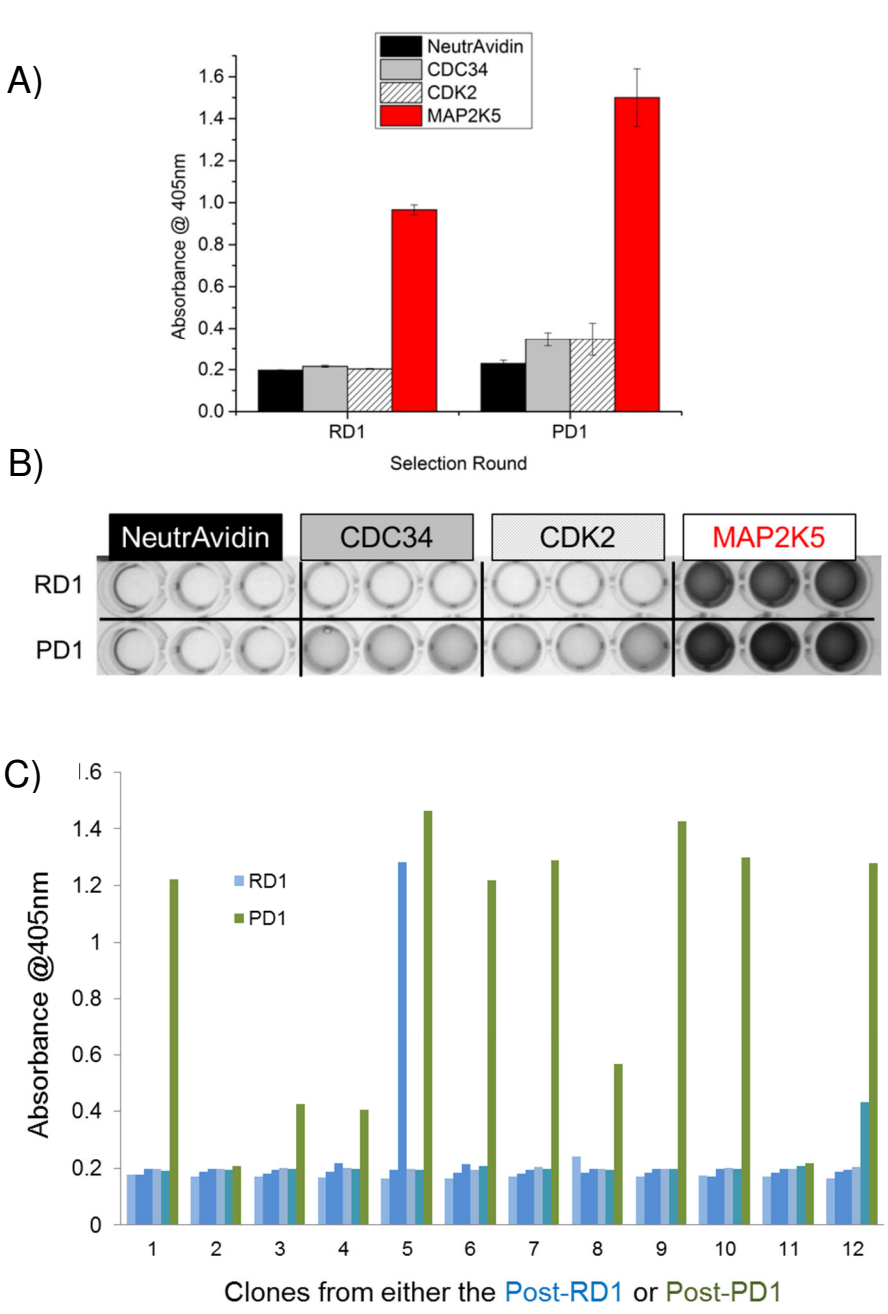

Figure 37. Polyclonal and monoclonal ELISA of first two rounds of PExSR. A) After the ribosome-display selection round (RD1), enrichment is already seen. Following the phage-display round (PD1), the binding monobodies are enriched. B) The image of the microtiter plate of the polyclonal ELISAs. C) Monoclonal ELISA of post-RD1 (blue) and post PD1 (green). 60 colonies were evaluated for the post-RD1. 12 colonies were evaluated for the post-PD1. Low sample size of the PD1 was due to few isolated colonies.

The final monoclonal ELISA identified the best clones where 4 were found to be unique after sequencing (**Appendix A**). A contaminant was discovered in the sequencing that represented about 50% of the recovered clones. This contaminant was identified as a high affinity anti-MAP2K5-FN3, which was developed through phage-display and affinity maturation selection performed by other members of the lab. The clone contains two cysteine residues as well as codons not found in the trinucleotide oligos, and ,therefore, did not arise independently. Antigen stocks were shared among lab members and is assumed to be the point at which contamination of phage occurred. The contaminant turned out to be excellent for comparison to the PExSR generated unique clones. It was also encouraging that the unique PExSR clones were of high enough affinity to survive the competition of the contaminant during the selection.

Cloning of the unique PExSR monobodies into *E. coli* SUMO fusion expression vectors gave protein yields of 5-10 mg/L. To determine a rough estimate of binding constant, competition ELISAs were employed where many monobodies can be assayed in parallel at a low cost. Using the Inhibitory Concentration at 50% level (IC_{50}) as the measure of binding affinity, we compared one monobody obtained through our novel PExSR method with the best monobody from the traditional method of phage display followed by error-prone PCR and affinity maturation (**Fig. 38**). Using PExSR that took 8 days to complete, the binding constant of the best clone was around 0.5 nM, while the phage-display method which took 21 days to complete gave a binding constant of 3 nM.

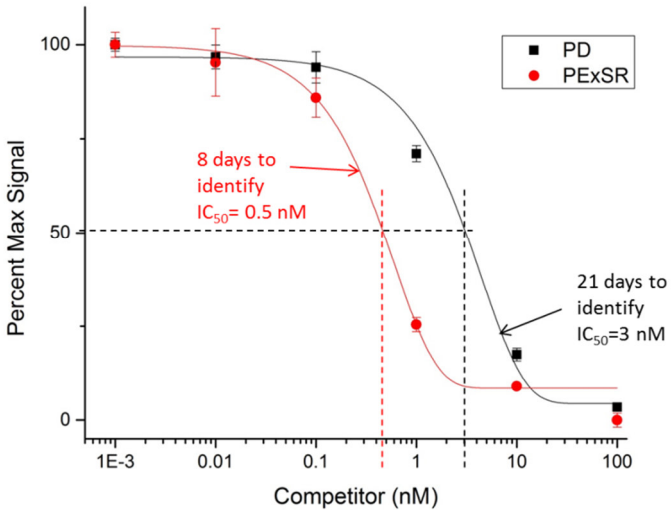

Figure 38. Soluble competition ELISA of the anti-MAP2K5 FN3 monobodies. Comparison of the IC_{50} values of monobodies obtained by PExSR (red) and traditional phage-display (PD) selection followed by affinity maturation (black). The greater the shift of the sigmoidal curve to the left, the lower the dissociation rate. Competitor was non-biotinylated MAP2K5 mixed in solution with the purified FN3 monobody. Signal was produced by FN3 that dissociated from the competitor and associated with the immobilized Biotinylated-MAP2K5. It should be noted that the PD monobody was also the "contaminant" clone mentioned in the text.

4.4.5 Multiplexed selection

We next investigated whether we could multiplex the selection by adding multiple target proteins to the initial ribosome-display selection round (27), and then separating the specific binders in the subsequent phage-display rounds (**Fig. 39**). Three human target proteins for the selection were chosen based on a range of difficulty to generate antibodies: COP9 Signalosome Subunit 5 (COPS5), Ubiquitin

Specific Peptidase 11 (USP11), and Cyclin-Dependent Kinase 2. To expose the targets to a large library, we used three times the number of library members in three combined *in vitro* transcription and translation reactions. The theoretical diversity of the ribosome displayed monobodies was >4 x 10^{13}.

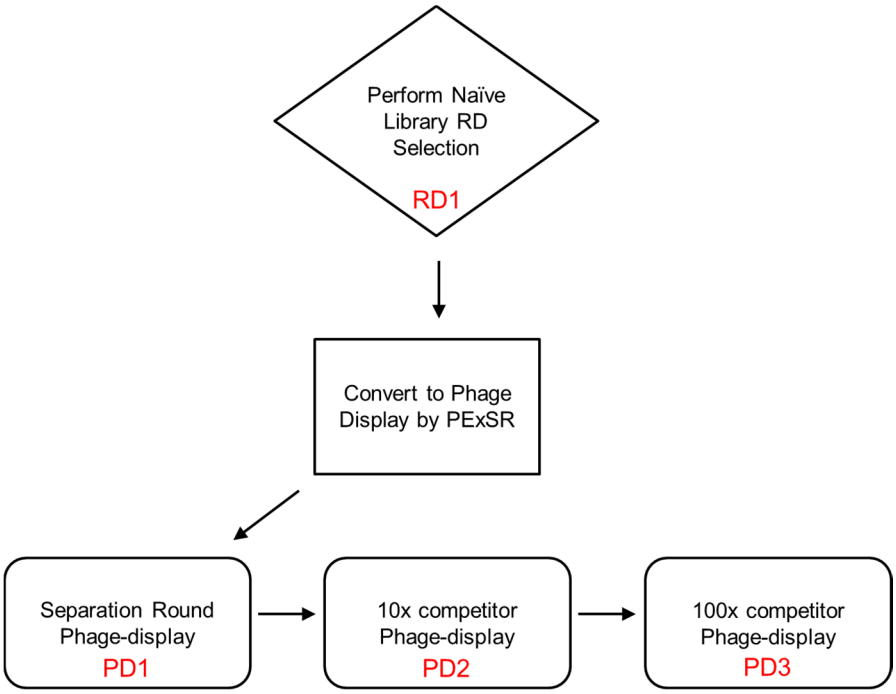

Figure 39. Multiplexed PExSR Flow Chart. During RD1, multiple targets proteins are pooled and exposed to a large naïve ribosome display library and a selection round is performed. The recovered cDNA is used to convert to phage display using PExSR. The PD1 step separates the targets into different vessels and a fraction of the phage pool is added to each. A low-stringency round proceeds which retains the antibodies against the specific separated target in the vessel but removes antibodies against the other targets. The targets remain separated in subsequent rounds (PD2 and PD3) where competitor (free protein that cannot be captured) is added at increasing concentrations.

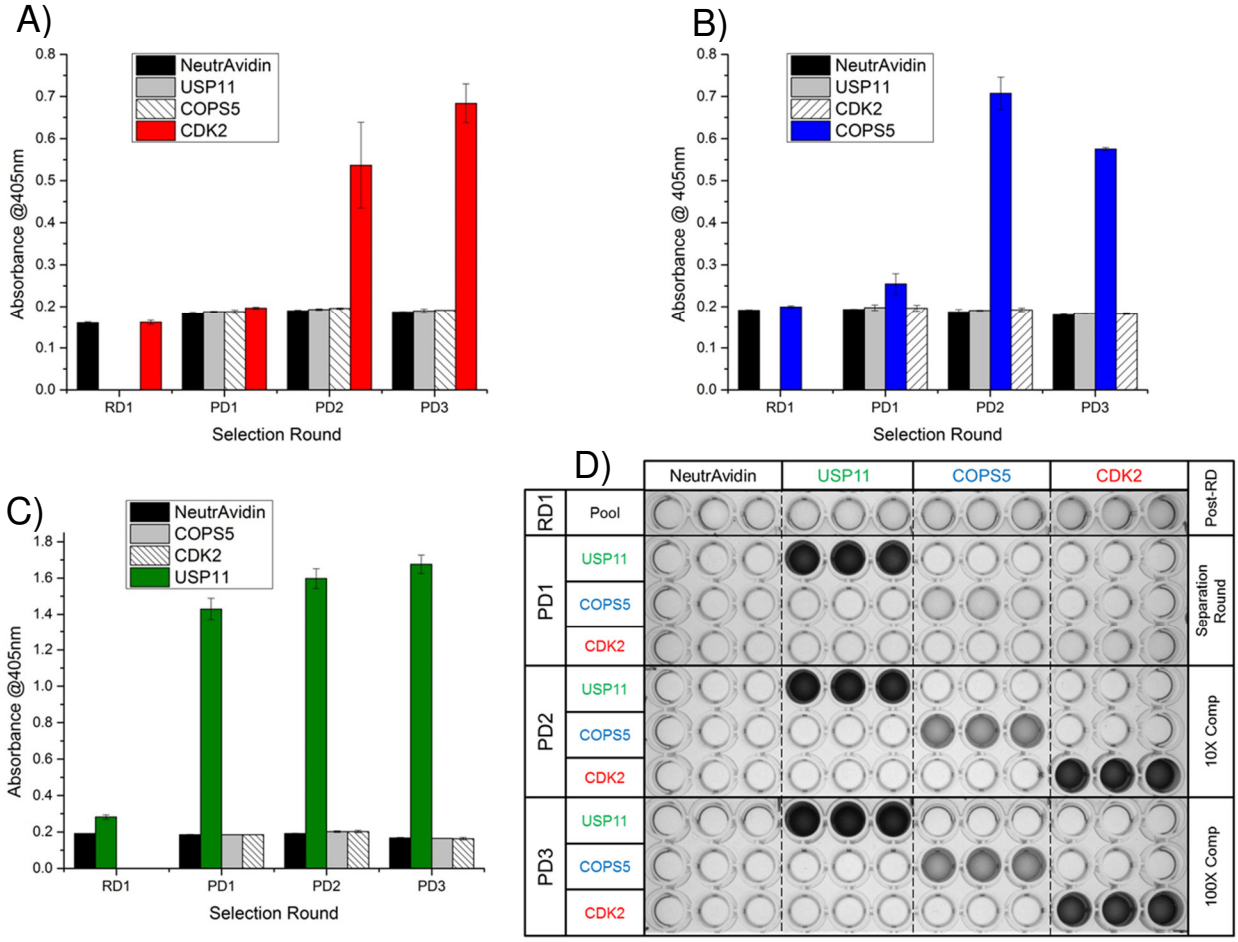

Figure 40. Multiplexed selection of three target proteins. Four rounds of selection were performed. RD1 contained a mix of the three antigens. PD1 was used as a separation round with low stringency selection pressure. PD2 and PD3 included off-rate competition.

The ribosome-display round (RD1) and PExSR were performed as described earlier. The conversion library was estimated to be >4 x 10^8 clones. The first phage-display round (PD1) was of low stringency with the targets now separated. The second (PD2) and third round (PD3) included off-rate selections with 10-fold and 100-fold excess competitor. The enrichment of monobodies of each target through the rounds can be seen in polyclonal ELISAs (**Fig. 40**). As expected, the tightest binding monobodies are selected and enriched as the selection progresses which translates to greater signal intensity. After the second round of phage display (PD2), further selection rounds gained modest improvements in binding affinity as can be detected by ELISA signal intensity. Competition ELISAs showed a rough estimate of binding constants (**Fig. 41**). Two monobodies with unique sequences were found that bound IC_{50} ~3 nM to the COPS5 target. Also for the USP11, two different monobodies resulted with IC_{50} at ~10 nM. The CDK2 selection resulted in only one unique sequence with IC_{50} at ~7 nM.

To get a better determination of the binding kinetics, we performed Isothermal Titration Calorimetry on select FN3 monobodies. The USP11 monobody gave excellent exothermic heat change. The ITC resulted in a K_D of 6 ±2.27 nM for the B7 clone (**Fig. 42 A**) and a K_D of 3.76 ±1.66 nM for the C9 clone (**Fig. 42 B**). The binding constants are within 2-fold of the estimated K_Ds as determined by the IC_{50} of the competition ELISA. This agreement gives us confidence that the IC_{50} estimations of the remaining clones are also in close accordance with the actual binding constant (**Table IV**).

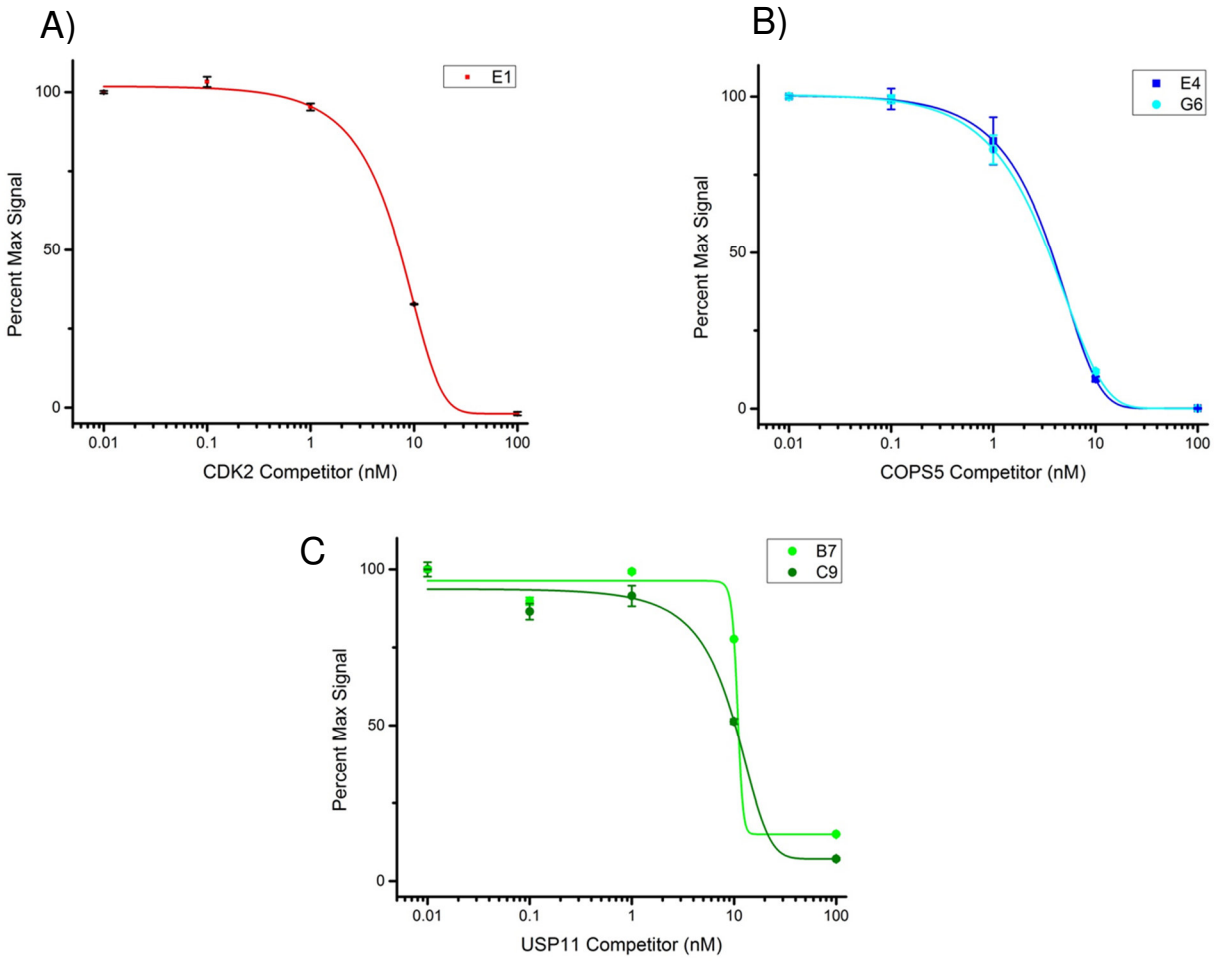

Figure 41. Competition ELISAs of FN3 monobodies against three targets. Competition phage ELISAs were performed for the FN3 monobodies isolated after the multiplexed PExSR. Dissociation constants were determined by the IC_{50} of the curves. anti-CDK monobodies (Red); anti-COPS5 monobodies (Blue); anti-USP11 monobodies (green).

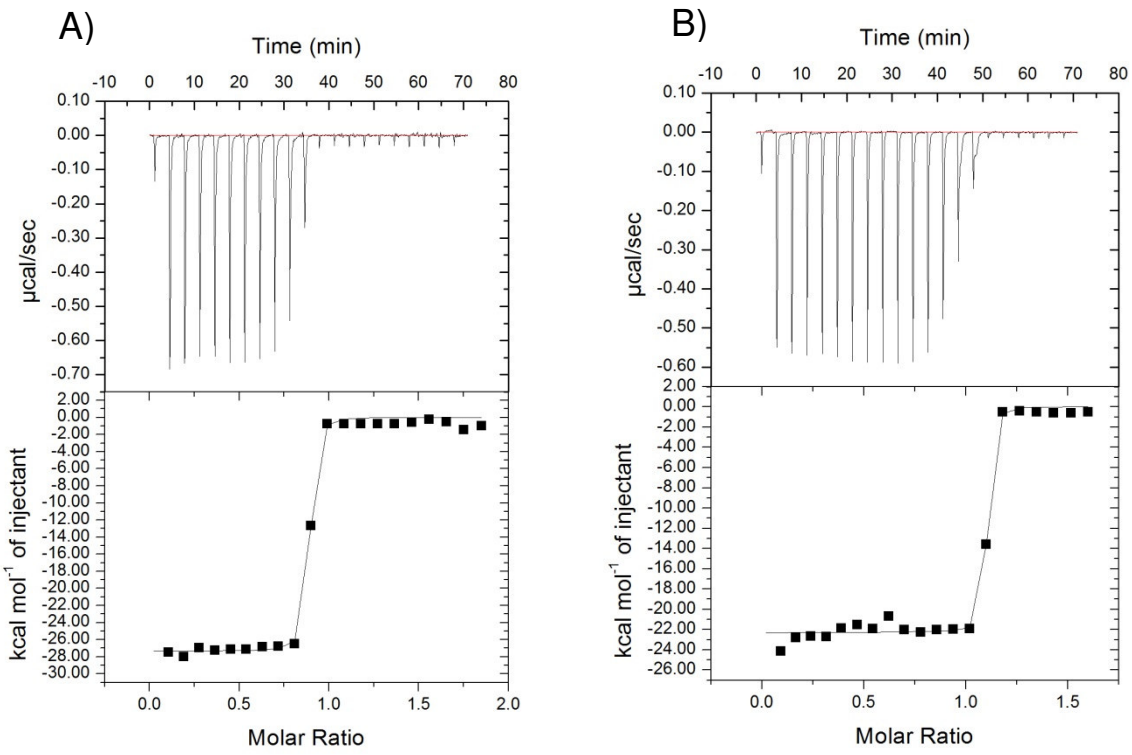

Figure 42. Isothermal Titration Calorimetry of USP11 monobodies. ITC was performed 3 times for each monobody and averaged. Monobody was titrated into the antigen in 1.8 µL injections. A) B7 clone, K_D= 6 ±2.27 nM, N=0.85. B) C9 clone K_D= 3.76 ±1.66 nM, N=1

TABLE IV. SUMMARY OF BINDING CHARACTERISTICS FOR PEXSR GENERATED MONOBODIES

FN3	**Clone**	**Estimated IC_{50} [a] (nM)**	**ITC K_D [b] (nM)**
anti-MAP2K5	H1	0.5	n.d.
anti-CDK2	E1	7	n.d.
anti-COPS5	E4	3	n.d.
anti-COPS5	G6	3	n.d.
anti-USP11	B7	10	6 ± 2.27
anti-USP11	C9	10	3.76 ± 1.66

[a] IC_{50} is the Inhibitory concentration at 50% used here as an estimate of binding affinity.
[b] Isothermal Titration Calorimetry was performed for the USP11 monobodies KD is the Equilibrium Binding constant.
n.d=not determined.

4.5 Conclusion

In conclusion, we have combined ribosome-display with phage-display in a novel, integrated fashion to rapidly select for FN3 monobodies in less than a week and a half and have named the process PExSR. We have constructed a library of ~ $1x10^{13}$ monobody variants using primer extension and verified its functionality with a novel Phage-TolA assay. We have also multiplexed the PExSR procedure to affinity select for multiple targets at once to yield single-digit nanomolar dissociation constants with an average production time of 3.5 days per antigen. Through robotics implementation, we can reasonably increase throughput further to tackle 15 antigens at once. If binding characterizations can be automated, we even foresee selecting for almost 100 antigens at a time.

The monobodies generated here by PExSR are, to the best of our knowledge, the tightest binding reagents of the FN3 scaffold ever generated without an extensive and laborious 10 rounds of mRNA selection (28) or through affinity maturation (29,30). We also generated identifiable binders after a single round of ribosome-display, which is a first for our lab. Our technology brings together the strengths of the two display technologies to produce affinity reagents faster, in a simpler procedure, with higher quality, than either alone. This procedure may be attractive to industrial and academic labs as it lowers hurdles of using ribosome-display by removing some of the more labor intensive steps, but still yielding useful reagents.

4.6 References

1. Huang R, Fang P, Kay BK. Isolation of monobodies that bind specifically to the SH3 domain of the Fyn tyrosine protein kinase. *N Biotechnol* 29: 526-533. (2012).

2. Vaughan TJ, Williams AJ, Pritchard K, Osbourn JK, Pope AR, et al. Human antibodies with sub-nanomolar affinities isolated from a large non-immunized phage display library. *Nat Biotechnol* 14: 309-314. (1996).

3. Ling MM. Large antibody display libraries for isolation of high-affinity antibodies. *Comb Chem High Throughput Screen* 6: 421-432. (2003).

4. Dower WJ, Miller JF, Ragsdale CW. High efficiency transformation of E. coli by high voltage electroporation. *Nucleic Acids Res* 16: 6127-6145. (1988).

5. Sheets MD, Amersdorfer P, Finnern R, Sargent P, Lindquist E, et al. Efficient construction of a large nonimmune phage antibody library: the production of high-affinity human single-chain antibodies to protein antigens. *Proc Natl Acad Sci U S A* 95: 6157-6162. (1998).

6. Pluckthun A. Ribosome display: a perspective. *Methods Mol Biol* 805: 3-28. (2012).

7. Hanes J, Pluckthun A. In vitro selection and evolution of functional proteins by using ribosome display. *Proc Natl Acad Sci U S A* 94: 4937-4942. (1997).

8. Pelletier JN, Arndt KM, Pluckthun A, Michnick SW. An in vivo library-versus-library selection of optimized protein-protein interactions. *Nat Biotechnol* 17: 683-690. (1999).

9. Groves M, Lane S, Douthwaite J, Lowne D, Rees DG, et al. Affinity maturation of phage display antibody populations using ribosome display. *J Immunol Methods* 313: 129-139. (2006).

10. Finlay WJ, Cunningham O, Lambert MA, Darmanin-Sheehan A, Liu X, et al. Affinity maturation of a humanized rat antibody for anti-RAGE therapy: comprehensive mutagenesis reveals a high level of mutational plasticity both inside and outside the complementarity-determining regions. *J Mol Biol* 388: 541-558. (2009).

11. Kunkel TA. Rapid and efficient site-specific mutagenesis without phenotypic selection. *Proc Natl Acad Sci U S A* 82: 488-492. (1985).

12. Sidhu SS, Lowman HB, Cunningham BC, Wells JA. Phage display for selection of novel binding peptides. *Methods Enzymol* 328: 333-363. (2000).

13. Huang R, Fang P, Kay BK. Improvements to the Kunkel mutagenesis protocol for constructing primary and secondary phage-display libraries. *Methods* 58: 10-17. (2012).

14. Dreier B, Plückthun A Rapid Selection of High-Affinity Binders Using Ribosome Display. In: Douthwaite JA, Jackson RH, editors. Ribosome Display and Related Technologies: Springer New York. pp. 261-286.(2012)

15. Dreier B, Pluckthun A. Ribosome display: a technology for selecting and evolving proteins from large libraries. *Methods Mol Biol* 687: 283-306. (2011).

16. Zhang Y, Werling U, Edelmann W. SLiCE: a novel bacterial cell extract-based DNA cloning method. *Nucleic Acids Res* 40: e55. (2012).

17. Fellouse FA, Wiesmann C, Sidhu SS. Synthetic antibodies from a four-amino-acid code: a dominant role for tyrosine in antigen recognition. *Proc Natl Acad Sci U S A* 101: 12467-12472. (2004).

18. Gilbreth RN, Koide S. Structural insights for engineering binding proteins based on non-antibody scaffolds. *Curr Opin Struct Biol* 22: 413-420. (2012).

19. Mian IS, Bradwell AR, Olson AJ. Structure, function and properties of antibody binding sites. *J Mol Biol* 217: 133-151. (1991).

20. Zemlin M, Klinger M, Link J, Zemlin C, Bauer K, et al. Expressed Murine and Human CDR-H3 Intervals of Equal Length Exhibit Distinct Repertoires that Differ in their Amino Acid Composition and Predicted Range of Structures. *Journal of Molecular Biology* 334: 733-749. (2003).

21. Koide S, Sidhu SS. The importance of being tyrosine: lessons in molecular recognition from minimalist synthetic binding proteins. *ACS Chem Biol* 4: 325-334. (2009).

22. Riechmann L, Holliger P. The C-terminal domain of TolA is the coreceptor for filamentous phage infection of E. coli. *Cell* 90: 351-360. (1997).

23. Kuchař M, Vaňková L, Petroková H, Černý J, Osička R, et al. Human interleukin-23 receptor antagonists derived from an albumin-binding domain

scaffold inhibit IL-23-dependent ex vivo expansion of IL-17-producing T-cells. *Proteins: Structure, Function, and Bioinformatics*: n/a-n/a. (2013).

24. Shimizu Y, Inoue A, Tomari Y, Suzuki T, Yokogawa T, et al. Cell-free translation reconstituted with purified components. *Nat Biotechnol* 19: 751-755. (2001).

25. Matsuura T, Yanagida H, Ushioda J, Urabe I, Yomo T. Nascent chain, mRNA, and ribosome complexes generated by a pure translation system. *Biochem Biophys Res Commun* 352: 372-377. (2007).

26. Ohashi H, Shimizu Y, Ying BW, Ueda T. Efficient protein selection based on ribosome display system with purified components. *Biochem Biophys Res Commun* 352: 270-276. (2007).

27. Suggestion credited to Shohei Koide, University of Chicago

28. Xu L, Aha P, Gu K, Kuimelis RG, Kurz M, et al. Directed Evolution of High-Affinity Antibody Mimics Using mRNA Display. *Chemistry & Biology* 9: 933-942. (2002).

29. Gilbreth RN, Esaki K, Koide A, Sidhu SS, Koide S. A dominant conformational role for amino acid diversity in minimalist protein-protein interfaces. *J Mol Biol* 381: 407-418. (2008).

30. Koide A, Wojcik J, Gilbreth RN, Hoey RJ, Koide S. Teaching an old scaffold new tricks: monobodies constructed using alternative surfaces of the FN3 scaffold. *J Mol Biol* 415: 393-405. (2012).

CHAPTER 5

CONCLUSIONS

5.1 Recombinant affinity reagents are our future

In the coming years, recombinant affinity reagents will take on a larger role, replacing traditional antibodies in the catalogs of commercial antibody suppliers and in the portfolios of pharmaceutical companies. Laboratories will find it necessary to implement technologies like phage- and ribosome-display to stay competitive in the affinity reagent research arena. Animal immunizations to produce antibodies will become an antiquated method while investigators demand highly customized tools to satisfy their ever-increasingly complex scientific endeavors.

5.2 Affinity reagents for retinal injury biomarkers

In this thesis, I have provided a pathway to the generation of antibodies against retinal injury related proteins as a result of laser exposure. Although we were unable to reach the point of validation of the proteins as biomarkers, we showed how mass spectrometry data can be used to develop antibodies against peptide fragments in phage-display selections of single-chain Fragments of variation. One of these scFv antibodies recognized its cognate endogenous protein in western blot of retinal lysates.

From discovery work done by our collaborators, we had a set of 5 peptide fragments from four proteins that we had chemically synthesized. These were the antigens in phage-display selections using a 1x10^9 scFv library. The outcome of these selections appeared to be positive by ELISA. However in retrospect, we should have gone through more extensive selections and affinity maturations to develop the tightest

binders possible for each target, before attempting the downstream biological assays (1). It was only until later that we realized that devoting more time to perfecting the selections should be paramount in a project that depends on the detection of miniscule concentrations of protein. It was also discovered that the libraries used in the selection were amplified incorrectly by inexperienced members of the lab that likely reduced the actual diversity to well below the theoretical. A library of 1x10^7-1x10^8 would help explain why the majority of the scFv antibodies obtained had dissociation constants in the high nanomolar to low micromolar range (2).

Most of the antibodies were only useful in ELISA but little else. The clone that was of sufficient quality to work in western blot of the endogenous protein was discovered through laborious screening. This caused us to realize that there was little correlation between signal intensity and binding strength in a post-selection phage ELISA where only one data point is collected and the concentration of expressed phage is uncontrollable. Signal strength was the measure we had originally used to gauge the quality of a binding reagent. To gain a better estimate for binding strength, we now frequently employ competition ELISA to differentiate binders at roughly 10-fold intervals of binding constant before taking them on to characterization or biological investigations (3).

In parallel, we were developing a platform on which to implement our recombinant antibodies. It had been one of the aims of the U.S. Air Force funded project to construct a miniaturized, rapid biomarker detection device that could be easily transported to an airplane sitting on a tarmac or deck of an aircraft carrier, in order to

assay pilots for retinal damage. The assessment would determine if the pilot was allowed to fly after a laser illumination event. Here we turned to a technology invented by the semiconductor industry that would allow detection by electrical current generated upon antibody recognition (4). We showed that this could work on the electrodes of a microchip platform using our scFv antibodies, however the detection limits were not low enough to be useful as a sensitive diagnostic of injury. Again, the poor affinities of the scFvs limited us in this assay format.

To improve the antibodies, we tried two avenues. One was affinity maturation through error-prone PCR and off-rate selection. This method had many hurtles. The initial problem was generating secondary libraries of sufficient size by cloning or Kunkel mutagenesis. Once this was overcome, the stringent selections would result in the isolation of clones with added cysteines that would promote homodimerization and through functional affinity would become enriched, even under reducing conditions. In addition, any clones that were more efficient at display or phage expression/cell growth would become greatly amplified, drowning out others that may have been tighter binders but slower growers.

The second route we took was to direct stable dimerization through the Fragment crystallizable format. This we conceded would only be useful in assays where the target antigen was immobilized. Since IgGs are standard for biomarker detection and western blots are of the most common assays for biomarker validation, we thought that this may yield some better results. The dimerization did enhance lower detection limits on western blot by 25-fold to 10 ng of target. The problem here was the expression of the

Fc through tissue culture. Long set-up times and modest yields provided only enough material for small scale experiments, which was not amenable to binding kinetic characterizations that require large quantities of antibody.

Although we did not get as far as we'd have liked in the biological investigations using our antibodies, we learned how to properly construct and perform selections on libraries of recombinant affinity reagents. Using a constant scaffold that is engineered to express highly in bacteria is crucial to a successful implementation of the reagent as others have done (5,6). Struggling with low yields of the human scFvs because of various light and heavy chain families of the framework cost immense effort and time. Maturing or engineering the reagents to robustly express and bind specifically at a high affinity is of the most difficult and time consuming aspects. However, when this is carefully performed, the down-stream applications will be infinitely easier and pay dividends in interesting biological investigations.

5.3 Ribosome-display of the Forkhead-associated domain

In this project, we wanted to test if the Forkhead- associated domain was amenable to ribosome-display, and then if the application of affinity maturation could enhance its dissociation binding constant for a phosphopeptide. Past efforts had failed to increase affinities of an anti-Myc FHA through the use of mutated secondary library and phage-display selection. Other investigators have used ribosome-display to affinity mature reagents initially discovered through phage-display (7). The selection procedure

of ribosome-display is attractive because it closely replicates Darwinian evolution through successive rounds of mutation and increasing selection pressures (8). The rounds can be performed as many times as desired since the error-prone PCR is integrated into the selection procedure (9). Ribosome-display has been used in this fashion to improve dissociation constants against peptides 500-fold, down to a K_D of 1 pM (10).

To replicate this kind of improvement, the anti-Myc-FHA was successfully used in ribosome-display for the first time while working in collaboration in the lab of the method's inventor, Dr. Andreas Plueckthun's at the University of Zurich. Here we performed six rounds of selection on the FHA. This included two rounds of mutation, two rounds of off-rate competitor selection, and two rounds of low-stringency recovery. The off-rate competition selections are crucial to gaining affinity. Harsh and frequent washing with long incubation times has limitations when trying to discriminate between low-nanomolar and picomolar binders (11).

The procedure can be monitored by the quantity of PCR product recovered, then visualized on agarose gel. The final selection round output did not show a large enrichment in the recovered nucleic acid but most were found to bind better than the original FHA. Again, there were dimers formed by cysteine mutants, but the clones did not predominate. We observed this identical cysteine mutation arise independently in other selections using the same scaffold but different target, different display system, and different researcher. It would be advisable for future engineering of this scaffold to target this region for modification to reduce the chance of cysteine mutations. All of the

other mutations were found in the scaffold framework and thus were assumed to contribute to better positioning of the antigen interacting domains. The most promising clones were a modest 3-fold better in binding measured by ELISA. Even though the tightest binding FHA ever found has a K_D of 100 nM (12), we conclude that the properties of this particular phosphothreonine peptide may impose some physical limitations on binding by the FHA domain. Therefore, a high affinity and specific binder may not be possible with this scaffold.

5.4 Ribosome-display using coupled IVTT

After learning ribosome-display, the benefits of establishing it at UIC were clear. However, there were some pitfalls. The major caveat reported in the method literature is the potential for RNase contamination to degrade the essential mRNA that needs to be recovered after selection (13). To reproduce the RNase-free separate facilities and equipment seen in Zurich, would require a large financial investment. Further, the S30 ribosomal extract preparation and optimization is a daunting task. To circumvent the extract preparation, keep the costs minimal, and test the feasibility of performing ribosome-display in less than ideal conditions, we decided to try a commercially available coupled *in vitro* transcription and translation kit. Although kits have been used in the past (14), and in some cases shown to be better (15), it was not recommended by the experts in Zurich. The ribosome-display with the coupled IVTT turned out to work

well with the shared facilities at UIC. It also saved time and labor by performing the two steps simultaneously.

Using ribosome-display for affinity maturation was attractive, but we figured that it would better suited for naïve selections. In this case, we would want large libraries to obtain the best reagents (16). Since the library is composed of DNA, we knew we could easily generate large amounts of sequences, however we needed to ensure that a large amount of mRNA-protein-complex was forming as well. The bottle neck seemed to be at the concentration of ribosomes. To test this we used a kit with a known concentration of purified ribosomes and components (17). After the IVTT, we performed a pull-down and western blot of the translated FHA. Although we cannot determine the amount of intact complex at the end of the IVTT, we could determine that at least the number of FHA-TolA fusion proteins was about equal to the number of DNA molecules added to the reaction. This provided enough evidence to build our own library.

5.5 Primer Extension for Selection Recovery

From literature searches (18,19) and personal correspondences, it was obvious that ribosome-display was a far more powerful technology than phage-display. However, barely any labs are currently employing it because of its large input of human energy required. One of the most noteworthy advantages of ribosome-display is the large and freshly translated library, exploited in the first selection round. The downstream rounds do not necessarily need to have a large library. Phage-display

could easily handle the diversity of the recovered first round clones. Phage-display in our hands was simpler, faster, and cheaper than ribosome-display so why not switch to a more procedurally efficient technology. We could make this switch by taking advantage of the constant framework of engineered affinity reagents to allow for PCR amplification and annealing to ssDNA in a procedure identical to Kunkel mutagenesis, but without the mutagenesis (20,21). The conversion of ribosome- to phage-display step we have dubbed Primer Extension for Selection Recovery (PExSR). After the ribosome-display Selection, the DNA is Recovered and used as a Primer to anneal to a single-stranded plasmid. The primer is then Extended to fill in the complementary base pairs to complete the heteroduplex. We also applied the name to the entire process of beginning a selection in ribosome-display and finishing in phage-display as an integrated procedure.

The process was first explored on the small scale as a proof-of-concept using the Fibronectin III scaffold of phage-displayed generated clones (not discussed in the PExSR chapter). The technical aspects of the procedure worked well but affinity maturation was not the intent of developing PExSR. Although phage- to ribosome- to phage-display could be useful, the advantage of PExSR could only truly be realized by starting from a primary library. The library was constructed on the FN3 scaffold using oligonucleotides with triplet codons of varying length but with a bias towards tyrosine, glycine, and serine amino acids. This bias was chosen after reports in the literature implicating tyrosine residues as overabundant contributors in antibody contacts with antigen (22) and reports of other researchers using a more focused set of residues

when building libraries (23). Here we varied two loops, the BC and FG. The third loop, DE, was considered as well, however we wanted to be able to compare the PExSR process to phage-display libraries that also have only the two loops varied. It would be interesting to vary the third loop in another library to see if even tighter binding monobodies can be found.

The ribosome-display FN3 library was first used against the MAP2K5 protein. After PExSR using off-rate competition selection, it was estimated that one of the recovered clones had a binding constant of ~0.5 nM, which is the lowest we have seen in the literature from a three round FN3 selection. Although we have yet to get more precise binding kinetic data, the correlation of our estimates by competition ELISA to Isothermal Titration Calorimetry data of other binders, gives us confidence that the MAP2K5 FN3 has a picomolar dissociation constant. It took 8 days to generate the 0.5 nM FN3 against MAP2K5 using PExSR. On the other hand, using phage-display selection, it took 21 days, generation of a secondary library, and affinity maturation to obtain a 3 nM MAP2K5 FN3.

We then multiplexed the selection where we added three different protein targets into the same ribosome-display reaction and then separated the binders in the following phage-display rounds with off-rate competition. This resulted in low nanomolar binders as estimated by competition ELISA. With multiplexing, production time has dropped to 3.5 days per antigen. A few of the binders gave no heat change upon binding and therefore an alternate method to obtain binding characteristics will have to be used. We were however able to obtain ITC binding kinetic data for two monobodies to confirm the

correspondence to the competition ELISA. The two anti-USP11 monobodies that were estimated by IC_{50} to be10 nM were determined by ITC to have K_Ds of 3.72 nM and 6 nM. With these reagents in hand, biologically relevant assays can be performed without further manipulation. At these affinities, western blotting and immunoprecipitation is likely to succeed.

By increasing the number of targets in the multiplex selection and automating parts of the procedure, we can make PExSR more high-throughput and in effect more valuable. We believe that the PExSR process could lead to more efficiently produced affinity reagents and help decrease the usage gap between traditional immunoglobulin antibodies and recombinant reagents, in scientific investigations.

5.6 References

1. Dyson MR, Zheng Y, Zhang C, Colwill K, Pershad K, et al. Mapping protein interactions by combining antibody affinity maturation and mass spectrometry. *Anal Biochem* 417: 25-35. (2011).

2. Ling MM. Large antibody display libraries for isolation of high-affinity antibodies. *Comb Chem High Throughput Screen* 6: 421-432. (2003).

3. Friguet B, Chaffotte AF, Djavadi-Ohaniance L, Goldberg ME. Measurements of the true affinity constant in solution of antigen-antibody complexes by enzyme-linked immunosorbent assay. *J Immunol Methods* 77: 305-319. (1985).

4. Cooper J, Yazvenko N, Peyvan K, Maurer K, Taitt CR, et al. Targeted deposition of antibodies on a multiplex CMOS microarray and optimization of a sensitive immunoassay using electrochemical detection. *PLoS One* 5: e9781. (2010).

5. Kohl A, Binz HK, Forrer P, Stumpp MT, Pluckthun A, et al. Designed to be stable: crystal structure of a consensus ankyrin repeat protein. *Proc Natl Acad Sci U S A* 100: 1700-1705. (2003).

6. Pershad K, Wypisniak K, Kay BK. Directed evolution of the forkhead-associated domain to generate anti-phosphospecific reagents by phage display. *J Mol Biol* 424: 88-103. (2012).

7. Groves M, Lane S, Douthwaite J, Lowne D, Rees DG, et al. Affinity maturation of phage display antibody populations using ribosome display. *J Immunol Methods* 313: 129-139. (2006).

8. Pluckthun A. Ribosome display: a perspective. *Methods Mol Biol* 805: 3-28. (2012).

9. Hanes J, Pluckthun A. In vitro selection and evolution of functional proteins by using ribosome display. *Proc Natl Acad Sci U S A* 94: 4937-4942. (1997).

10. Luginbuhl B, Kanyo Z, Jones RM, Fletterick RJ, Prusiner SB, et al. Directed evolution of an anti-prion protein scFv fragment to an affinity of 1 pM and its structural interpretation. *J Mol Biol* 363: 75-97. (2006).

11. Zahnd C, Sarkar CA, Pluckthun A. Computational analysis of off-rate selection experiments to optimize affinity maturation by directed evolution. *Protein Eng Des Sel* 23: 175-184. (2010).

12. Pennell S, Westcott S, Ortiz-Lombardia M, Patel D, Li J, et al. Structural and functional analysis of phosphothreonine-dependent FHA domain interactions. *Structure* 18: 1587-1595. (2010).

13. Dreier B, Plückthun A Rapid Selection of High-Affinity Binders Using Ribosome Display. In: Douthwaite JA, Jackson RH, editors. Ribosome Display and Related Technologies: Springer New York. pp. 261-286.(2012)

14. Kuchař M, Vaňková L, Petroková H, Černý J, Osička R, et al. Human interleukin-23 receptor antagonists derived from an albumin-binding domain scaffold inhibit IL-23-dependent ex vivo expansion of IL-17-producing T-cells. *Proteins: Structure, Function, and Bioinformatics*: n/a-n/a. (2013).

15. Matsuura T, Yanagida H, Ushioda J, Urabe I, Yomo T. Nascent chain, mRNA, and ribosome complexes generated by a pure translation system. *Biochem Biophys Res Commun* 352: 372-377. (2007).

16. Vaughan TJ, Williams AJ, Pritchard K, Osbourn JK, Pope AR, et al. Human antibodies with sub-nanomolar affinities isolated from a large non-immunized phage display library. *Nat Biotechnol* 14: 309-314. (1996).

17. Ohashi H, Shimizu Y, Ying BW, Ueda T. Efficient protein selection based on ribosome display system with purified components. *Biochem Biophys Res Commun* 352: 270-276. (2007).

18. Zahnd C, Wyler E, Schwenk JM, Steiner D, Lawrence MC, et al. A designed ankyrin repeat protein evolved to picomolar affinity to Her2. *J Mol Biol* 369: 1015-1028. (2007).

19. Schilling J, Schoppe J, Pluckthun A. From DARPins to LoopDARPins: novel LoopDARPin design allows the selection of low picomolar binders in a single round of ribosome display. *J Mol Biol* 426: 691-721. (2014).

20. Kunkel TA. Rapid and efficient site-specific mutagenesis without phenotypic selection. *Proc Natl Acad Sci U S A* 82: 488-492. (1985).

21. Huang R, Fang P, Kay BK. Improvements to the Kunkel mutagenesis protocol for constructing primary and secondary phage-display libraries. *Methods* 58: 10-17. (2012).

22. Mian IS, Bradwell AR, Olson AJ. Structure, function and properties of antibody binding sites. *J Mol Biol* 217: 133-151. (1991).

23. Gilbreth RN, Koide S. Structural insights for engineering binding proteins based on non-antibody scaffolds. *Curr Opin Struct Biol* 22: 413-420. (2012).

APPENDICES

APPENDIX A

Amino acid sequences of retinal biomarker scFvs

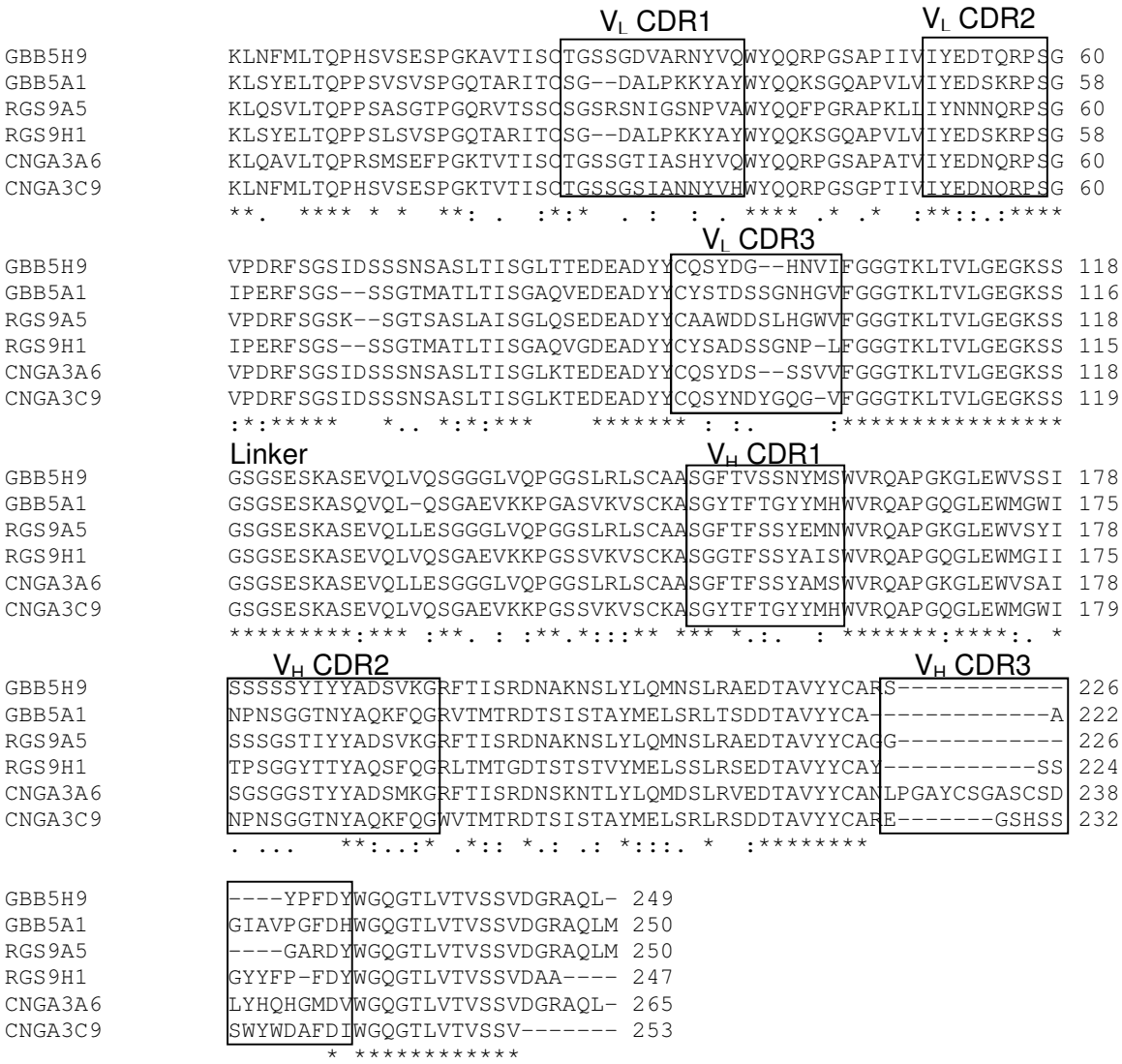

CLUSTAL 2.1 multiple sequence alignment

Sequence alignment of full length GBB5

```
H.sapien         ----------------------------------------MATEGLHENETLASLKSE 18
O.cuniculus      ----------------------------------------MATDGLHENETLASLKIE 18
G.gallus         ----------------------------------------MATEGLHENETLASLKNE 18
M.musculus       MCDQTFLVNVFGSCDKCFKQRALRPVFKKSQQLNYCSTCAEIMATDGLHENETLASLKSE 60
                                                         ***:************ *

H.sapien         AESLKGKLEEERAKLHDVELHQVAERVEALGQFVMKTRRTLKGHGNKVLCMDWCKDKRRI 78
O.cuniculus      AESLKGKLEEERAKLHDVELHQVAERVEALGQFVMKTRRTLKGHGNKVLCMDWCKDKRRI 78
G.gallus         AESLKGKLEEERAKLHDVELHQVAERVEALGQFVMKTRRTLKGHGNKVLCMDWCKDKRRI 78
M.musculus       AESLKGKLEEERAKLHDVELHQVAERVEALGQFVMKTRRTLKGHGNKVLCMDWCKDKRRI 120
                 ************************************************************

H.sapien         VSSSQDGKVIVWDSFTTN------------------------------------------ 96
O.cuniculus      VSSSQDGKVIVWDSFTTNKEHAVTMPCTWVMACAYAPSGCAIACGGLDNKCSVYPLTFDK 138
G.gallus         VSSSQDGKVIVWDSFTTNKEHAVTMPCTWVMACAYAPSGCAIACGGLDNKCSVYPLTFDK 138
M.musculus       VSSSQDGKVIVWDSFTTN------------------------------------------ 138
                 ******************

H.sapien         ----------------------------KILTASGDGTCALWDVESGQLLQSFHGHGADV 128
O.cuniculus      NENMAAKKKSVAMHTNYLSACSFTNSDMQILTASGDGTCALWDVESGQLLQSFHGHGADV 198
G.gallus         NENMAAKKKSVAMHTNYLSACSFTNSDMQILTASGDGTCALWDVESGQLLQSFHGHGADV 198
M.musculus       ----------------------------------------KEHAVTMPCTW-----V 150
                                                          * .  : .       *

H.sapien         LCLDLAPSETGNTFVSGGCDKKAMVWDMRSGQCVQAFETHESDINSVRYYPSGDAFASGS 188
O.cuniculus      LCLDLAPSETGNTFVSGGCDKKAMVWDMRSGQCVQAFETHESDINSVRYYPSGDAFASGS 258
G.gallus         LCLDLAPSETGNTFVSGGCDKKAMVWDMRSGQCIQSFETHDSDINSVRYYPSGDAFASGS 258
M.musculus       MACAYAP--SGCAIACGGLDNKCSVYPLTFDKNENMAAKKKS-VAMHTNYLSACSFTN-- 205
                 :.   **  :* ::..** *:*. *: :  .:  :   .:.* :     * *. :*:.

H.sapien         DDATCRLYDLRADREVAIYSKESIIFGASSVDFSLSGRLLFAGYNDYTINVWDVLKGSRV 248
O.cuniculus      DDATCRLYDLRADREVAIYSKESIIFGASSVDFSLSGRLLFAGYNDYTINVWDVLKGARV 318
G.gallus         DDATCRLYDLRADREVAIYSKESIIFGASSVDFSLSGRLLFAGYNDYTINVWDVLKGSRV 318
M.musculus       --SDMQILTASGDGTCALWDVE-------SGQFSLSGRLLFAGYNDYTINVWDVLKGSRV 256
                   :  ::    .*   *::. *       * :************************:**

H.sapien         SILFGHENRVSTLRVSPDGTAFCSGSWDHTLRVWA 283
O.cuniculus      SILFGHENRVSTLRVSPDGTAFCSGSWDHTLRVWA 353
G.gallus         SILFGHENRVSTLRVSPDGTAFCSGSWDHTLRIWA 353
M.musculus       SILFGHENRVSTLRVSPDGTAFCSGSWDHTLRVWA 291
                 ********************************:**
CLUSTAL 2.1 multiple sequence alignment
```

Homo sapien- GenBank: CAB55946.1

Oryctolagus cuniculus- NCBI Reference Sequence: NP_001075639.1

Gallus gallus- NCBI Reference Sequence: XP_004943849.1

Mus musculus- GenBank: EDL26314.1

Sequence of pRDV-FN3-M13-Ori-StuI

ACCCGACACCATCGAAATTAATACGACTCACTATAGGGAGACCACAACGGTTTCCCGAAT

TGTGAGCGGATAACAATAGAAATAATTTTGTTTAACTTTAAGAAGGAGATATATCCATGG

CCGTTTCTGATGTTCCGCGTAAGCTGGAAGTTGTTGCTGCGACCCCGACTAGCCTGCTGA

TCAGCTGGGATGCTCCTTAATGAAGGCCTCTTTATTACCGTATCACGTACGGTGAAACCG

GTGGTAACTCCCCGGTTCAGGAGTTCACTGTACCTGGTTCCAAGTCTACTGCTACCATCA

GCGGCCTGAAACCGGGTGTTGACTATACCATCACTGTATACGCTGTTACTTAATGAAGGC

CTTATAGCAAGCCAATCTCGATTAACTACCGTACCAGCGGCGACTACAAAGATGACGATG

ACAAAGAATTCGGATCTGGTGGCCAGAAGCAAGCTGAAGAGGCGGCAGCGAAAGCGGCGG

CAGATGCTAAAGCGAAGGCCGAAGCAGATGCTAAAGCTGCGGAAGAAGCAGCGAAGAAAG

CGGCTGCAGACGCAAAGAAAAAAGCAGAAGCAGAAGCCGCCAAAGCCGCAGCCGAAGCGC

AGAAAAAAGCCGAGGCAGCCGCTGCGGCACTGAAGAAGAAAGCGGAAGCGGCAGAAGCAG

CTGCAGCTGAAGCAAGAAAGAAAGCGGCAACTGAAGCTGCTGAAAAAGCCAAAGCAGAAG

CTGAGAAGAAAGCGGCTGCTGAAAAGGCTGCAGCTGATAAGAAAGCGGCAGCAGAGAAAG

CTGCAGCCGACAAAAAAGCAGCAGAAAAAGCGGCTGCTGAAAAGGCAGCAGCTGATAAGA

AAGCAGCGGCAGAAAAAGCCGCCGCAGACAAAAAAGCGGCAGCGGCAAAAGCTGCAGCTG

AAAAAGCCGCTGCAGCAAAAGCGGCCGCAGAGGCAGATGATATTTTCGGTGAGCTAAGCT

CTGGTAAGAATGCACCGAAAACGGGGGGAGGGGCGAAAGGGAACAATGCTTCGCCTGCCG

GGAGTGGTAATACTAAAAACAATGGCGCATCAGGGGCCGATATCAATAACTATGCCGGGC

AGATTAAATCTGCTATCGAAAGTAAGTTCTATGACGCATCGTCCTATGCAGGCAAAACCT

GTACGCTGCGCATAAAACTGGCACCCGATGGTATGTTACTGGATATCAAACCTGAAGGTG

GCGATCCCGCACTTTGTCAGGCTGCGTTGGCAGCAGCTAAACTTGCGAAGATCCCGAAAC

CACCAAGCCAGGCAGTATATGAAGTGTTCAAAAACGCGCCATTGGACTTCAAACCGTAGT

AGAGATCCGGCTGCTAACAAAGCCCGAAAGGAAGCTGAGTTGGCTGCTGCCACCGCTGAG

CAATAACTAGCATAACCCCTTGGGGCCTCTCCGAGATAGGGTTGAGTGTTGTTCCAGTTTGG

AACAAGAGTCCACTATTAAAGAACGTGGACTCCAACGTCAAAGGGCGAAAAACCGTCTAT

CAGGGCGATGGCCCACTACGTGAACCATCACCCTAATCAAGTTTTTTGGGGTCGAGGTGC

CGTAAAGCACTAAATCGGAACCCTAAAGGGAGCCCCCGATTTAGAGCTTGACGGGGAAAG

CCGGCGAACGTGGCGAGAAAGGAAGGGAAGAAAGCGAAAGGAGCGGGCGCTAGGGCGCTG

GCAAGTGTAGCGGTCACGCTGCGCGTAACCACCACACCCGCCGCGCTTAATGCGCCGCTA

CAGGGCGCGTGATCTAGATCCCCACGCGCCCTGTAGCGGCGCATTAAGCGCGGCGGGTGT

GGTGGTTACGCGCAGCGTGACCGCTACACTTGCCAGCGCCCTAGCGCCCGCTCCTTTCGC

TTTCTTCCCTTCCTTTCTCGCCACGTTCGCCGGCTTTCCCCGTCAAGCTCTAAATCGGGG

CATCCCTTTAGGGTTCCGATTTAGTGCTTTACGGCACCTCGACCCCAAAAAACTTGATTA

GGGTGATGGTTCACGTAGTGGGCCATCGCCCTGATAGACGGTTTTTCGCCCTTTGACGTT

GGAGTCCACGTTCTTTAATAGTGGACTCTTGTTCCAAACTGGAACAACACTCAACCCTAT

CTCGGTCTATTCTTTTGATTTATAAGGGATTTTGCCGATTTCGGCCTATTGGTTAAAAAA

TGAGCTGATTTAACAAAAATTTAACGCGAATTTTAACAAAATATTAACGTTTACAATTTC

AGGTGGCACTTTTCGGGGAAATGTGCGCGGAACCCCTATTTGTTTATTTTTCTAAATACA

TTCAAATATGTATCCGCTCATGAGACAATAACCCTGATAAATGCTTCAATAATATTGAAA

AAGGAAGAGTATGAGTATTCAACATTTCCGTGTCGCCCTTATTCCCTTTTTTGCGGCATT

TTGCCTTCCTGTTTTTGCTCACCCAGAAACGCTGGTGAAAGTAAAAGATGCTGAAGATCA

GTTGGGTGCACGAGTGGGTTACATCGAACTGGATCTCAACAGCGGTAAGATCCTTGAGAG

TTTTCGCCCCGAAGAACGTTTTCCAATGATGAGCACTTTTAAAGTTCTGCTATGTGGCGC

GGTATTATCCCGTATTGACGCCGGGCAAGAGCAACTCGGTCGCCGCATACACTATTCTCA

GAATGACTTGGTTGAGTACTCACCAGTCACAGAAAAGCATCTTACGGATGGCATGACAGT

AAGAGAATTATGCAGTGCTGCCATAACCATGAGTGATAACACTGCGGCCAACTTACTTCT

GACAACGATCGGAGGACCGAAGGAGCTAACCGCTTTTTTGCACAACATGGGGGATCATGT

AACTCGCCTTGATCGTTGGGAACCGGAGCTGAATGAAGCCATACCAAACGACGAGCGTGA

CACCACGATGCCTGTAGCAATGGCAACAACGTTGCGCAAACTATTAACTGGCGAACTACT

TACTCTAGCTTCCCGGCAACAATTAATAGACTGGATGGAGGCGGATAAAGTTGCAGGACC

ACTTCTGCGCTCGGCCCTTCCGGCTGGCTGGTTTATTGCTGATAAATCTGGAGCCGGTGA

GCGTGGGTCTCGCGGTATCATTGCAGCACTGGGGCCAGATGGTAAGCCCTCCCGTATCGT

AGTTATCTACACGACGGGGAGTCAGGCAACTATGGATGAACGAAATAGACAGATCGCTGA

GATAGGTGCCTCACTGATTAAGCATTGGTAACTGTCAGACCAAGTTTACTCATATATACT

TTAGATTGATTTAAAACTTCATTTTTAATTTAAAAGGATCTAGGTGAAGATCCTTTTTGA

TAATCTCATGACCAAAATCCCTTAACGTGAGTTTTCGTTCCACTGAGCGTCAGACCCCGT

AGAAAAGATCAAAGGATCTTCTTGAGATCCTTTTTTTCTGCGCGTAATCTGCTGCTTGCA

AACAAAAAAACCACCGCTACCAGCGGTGGTTTGTTTGCCGGATCAAGAGCTACCAACTCT

TTTTCCGAAGGTAACTGGCTTCAGCAGAGCGCAGATACCAAATACTGTCCTTCTAGTGTA

GCCGTAGTTAGGCCACCACTTCAAGAACTCTGTAGCACCGCCTACATACCTCGCTCTGCT

AATCCTGTTACCAGTGGCTGCTGCCAGTGGCGATAAGTCGTGTCTTACCGGGTTGGACTC

AAGACGATAGTTACCGGATAAGGCGCAGCGGTCGGGCTGAACGGGGGGTTCGTGCACACA

GCCCAGCTTGGAGCGAACGACCTACACCGAACTGAGATACCTACAGCGTGAGCTATGAGA

AAGCGCCACGCTTCCCGAAGGGAGAAAGGCGGACAGGTATCCGGTAAGCGGCAGGGTCGG

AACAGGAGAGCGCACGAGGGAGCTTCCAGGGGGAAACGCCTGGTATCTTTATAGTCCTGT

CGGGTTTCGCCACCTCTGACTTGAGCGTCGATTTTTGTGATGCTCGTCAGGGGGGCGGAG

CCTATGGAAAAACGCCAGCAACGCGGCCTTTTTACGGTTCCTGGCCTTTTGCTGGCCTTT

TGCTCACATG

Amino acid sequences of PExSR generated FN3 monobodies

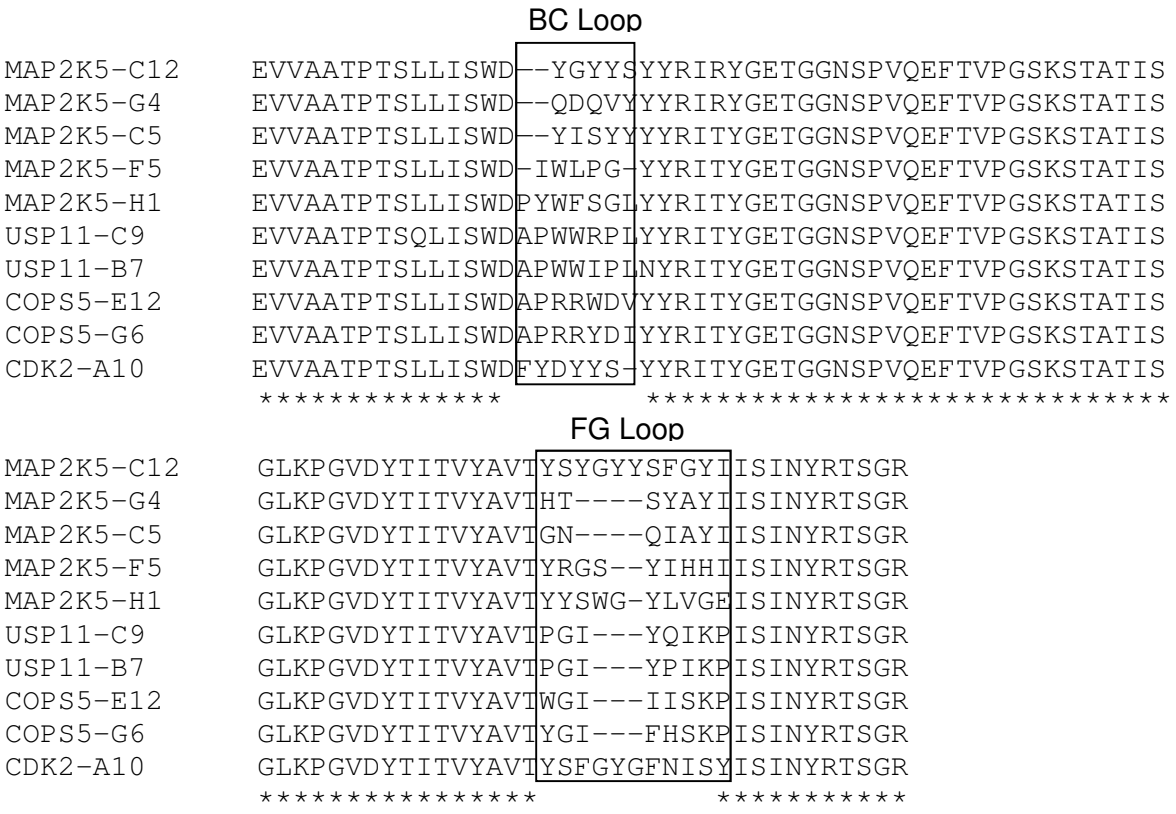

CLUSTAL 2.1 multiple sequence alignment

Amino acid sequences of peptide-MBP fusions

GBB5-MBP

MAGLNDIFEAQKIEWHEGSMAKLHDVELHQVAERVGKTEEGKLVIWINGDKGYNGLAE
VGKKFEKDTGIKVTVEHPDKLEEKFPQVAATGDGPDIIFWAHDRFGGYAQSGLLAEITP
DKAFQDKLYPFTWDAVRYNGKLIAYPIAVEALSLIYNKDLLPNPPKTWEEIPALDKELKA
KGKSALMFNLQEPYFTWPLIAADGGYAFKYENGKYDIKDVGVDNAGAKAGLTFLVDLIK
NKHMNADTDYSIAEAAFNKGETAMTINGPWAWSNIDTSKVNYGVTVLPTFKGQPSKPF
VGVLSAGINAASPNKELAKEFLENYLLTDEGLEAVNKDKPLGAVALKSYEEELAKDPRI
AATMENAQKGEIMPNIPQMSAFWYAVRTAVINAASGRQTVDEALKDAQTGSGGTPGR
PAAQASHHHHHH

RGS9-MBP

MAGLNDIFEAQKIEWHEGSMAKLVEVPTKMRVGKTEEGKLVIWINGDKGYNGLAEVGK
KFEKDTGIKVTVEHPDKLEEKFPQVAATGDGPDIIFWAHDRFGGYAQSGLLAEITPDKA
FQDKLYPFTWDAVRYNGKLIAYPIAVEALSLIYNKDLLPNPPKTWEEIPALDKELKAKGK
SALMFNLQEPYFTWPLIAADGGYAFKYENGKYDIKDVGVDNAGAKAGLTFLVDLIKNKH
MNADTDYSIAEAAFNKGETAMTINGPWAWSNIDTSKVNYGVTVLPTFKGQPSKPFVGV
LSAGINAASPNKELAKEFLENYLLTDEGLEAVNKDKPLGAVALKSYEEELAKDPRIAAT
MENAQKGEIMPNIPQMSAFWYAVRTAVINAASGRQTVDEALKDAQTGSGGTPGRPAA
QASHHHHHH

CNGA3-MBP

MAGLNDIFEAQKIEWHEGSMARLTRLESQMNRRCCGFSPDREGKTEEGKLVIWINGD
KGYNGLAEVGKKFEKDTGIKVTVEHPDKLEEKFPQVAATGDGPDIIFWAHDRFGGYAQ
SGLLAEITPDKAFQDKLYPFTWDAVRYNGKLIAYPIAVEALSLIYNKDLLPNPPKTWEEIP
ALDKELKAKGKSALMFNLQEPYFTWPLIAADGGYAFKYENGKYDIKDVGVDNAGAKAG
LTFLVDLIKNKHMNADTDYSIAEAAFNKGETAMTINGPWAWSNIDTSKVNYGVTVLPTF
KGQPSKPFVGVLSAGINAASPNKELAKEFLENYLLTDEGLEAVNKDKPLGAVALKSYEE
ELAKDPRIAATMENAQKGEIMPNIPQMSAFWYAVRTAVINAASGRQTVDEALKDAQTG
SGGTPGRPAAQASHHHHHH

Anti-GBB5-H9- scFv-Fc H9 (pBIOCAM5)

MGDNDIHFAFLSTGAMLTQPHSVSESPGKAVTISCTGSSGDVARNYVQWYQQRPGSA
PIIVIYEDTQRPSGVPDRFSGSIDSSSNSASLTISGLTTEDEADYYCQSYDGHNVIFGGG
TKLTVLGEGKSSGSGSESKASEVQLVQSGGGLVQPGGSLRLSCAASGFTVSSNYMS
WVRQAPGKGLEWVSSISSSSSYIYYADSVKGRFTISRDNAKNSLYLQMNSLRAEDTAV
YYCARSYPFDYWGQGTLVTVSSAAAHKTHTCPPCPAPELLGGPSVFLFPPKPKDTLMI
SRTPEVTCVVVDVSHEDPEVKFNWYVDGVEVHNAKTKPREEQYNSTYRVVSVLTVLH
QDWLNGKEYKCKVSNKALPAPIEKTISKAKGQPREPQVYTLPPSRDELTKNQVSLTCL
VKGFYPSDIAVEWESNGQPENNYKTTPPVLDSDGSFFLYSKLTVDKSRWQQGNVFSC
SVMHEALHNHYTQKSLSLSPGKGSHHHHHHKLDYKDHDGDYKDHDIDYKDDDDK

COPYRIGHT EXCLUSION STATEMENTS

Article from Chapter 1:

Michael R. Kierny, T. Cunningham, and B. K. Kay. Detection of biomarkers using recombinant antibodies coupled to nanostructured platforms. *Nano Reviews* (2012), doi:10.3402/nano.v3i0.17240.

Notices:

You do not have to comply with the license for elements of the material in the public domain or where your use is permitted by an applicable exception or limitation.

No warranties are given. The license may not give you all of the permissions necessary for your intended use. For example, other rights such as publicity, privacy, or moral rights may limit how you use the material.

The applicable mediation rules will be designated in the copyright notice published with the work, or if none then in the request for mediation. Unless otherwise designated in a copyright notice attached to the work, the UNCITRAL Arbitration Rules apply to any arbitration.

More info.

You may also use a license listed as compatible at https://creativecommons.org/compatiblelicenses

More info.

Merely changing the format never creates a derivative.

More info.

Article from Chapter 2:

Michael R. Kierny, Thomas D. Cunningham, Rachida A. Bouhenni, Deepak Edward, and Brian K. Kay. Generating recombinant antibodies for detection of biomarkers of retinal injury from laser exposure. Submitted for review to *PLOS One* (October 2014).

the UNCITRAL Arbitration Rules apply to any arbitration.

More info.

You may also use a license listed as compatible at https://creativecommons.org/compatiblelicenses

More info.

A commercial use is one primarily intended for commercial advantage or monetary compensation.

More info.

Merely changing the format never creates a derivative.

More info.

VITA

Michael Kierny
University of Illinois at Chicago | 900 South Ashland Avenue, MBRB Room 4314
Chicago, IL, 60607
Phone: (312) 996-0392 | E-mail: mkiern2@uic.edu

EDUCATION:

University of Illinois at Chicago 2007-Present
Ph. D. Candidate in Molecular, Cellular, and Developmental Biology
Expected graduation date: December 2014

Iowa State University B.S. Biology
Graduated 2006

RESEARCH EXPERIENCE:

Roche Innovation Site in Penzberg, Germany 2014-Present
Lab of Dr. Manuel Simon
Intern in pharmaceutical research and early development (pRED)

- Developed general methods for drug load conjugation
- Generated various antibody drug conjugates (ADCs)
- Performed ADC analytics and cytotoxicity assays

University of Illinois at Chicago 2007-Present
Ph. D. Thesis Advisor: Dr. Brian Kay
Research Assistant

- Performed phage display selections of antibody libraries to generate reagents for biomarker validation and detection
- Conducted protein engineering to improve antibodies
- Learned ribosome display methods as visiting researcher at University of Zurich; Lab of Andreas Plückthun

Iowa State University Biochemistry Dept. 2004-2007
Lab of Dr. Marit Nilsen-Hamilton
Lab Assistant

- Cloned, expressed, and characterized a bovine lipocalin protein orthologous to the human protein NGAL

Molecular Express Inc. & Ames Laboratory US Dept. of Energy 2005
Lab of Dr. Marit Nilsen-Hamilton
Lab Assistant

- Worked on development of a repetitious RNA aptamer with multiple binding sites

Iowa State University Biology Dept. 2003-2006
Undergraduate Teaching Lab of Linda Westgate
Lab Assistant

- Set up teaching labs for general biology, prepare solutions, poured media, collected specimens and repair lab equipment

SKILLS:

Phage-display, Ribosome-display, Western Blotting, ELISA, Size exclusion chromatography by ÄKTA FPLC Purifier/Avant, aSEC HPLC, DNA Subcloning, Surface Plasmon Resonance, Isothermal Titration Calorimetry, Real-Time PCR, Fluorescence microscopy, tissue sectioning and immuno-staining, *E. coli* protein expression and purification, *Pichia pastoris* protein expression, HEK- 293 expression

PUBLICATIONS:

- Kierny MR, Cunningham TD, Kay BK. Detection of biomarkers using recombinant antibodies coupled to nanostructured platforms. Nano Reviews 3:17240 (24 pages, 174 references), 2012.
- Kierny MR, Cunningham TD, Bouhenni RA, Edward D, Kay BK. Generating recombinant antibodies for detection of biomarkers of retinal injury from laser exposure. Submitted to PLOS One.
- Kierny MR, Huang R, Kay BK. Combining Ribosome Display with Phage Display to Generate Recombinant Affinity Reagents. In preparation.

PATENT:

- Kierny MR, Kay BK. 2014. Method and Kit for Generating High Affinity Antibodies. PCT/US2014/057617, filed September, 2014. Patent Pending.

POSTER PRESENTATIONS: 2008-2013

- Institute of Biological Engineering Annual Conference Indianapolis, IN.
- Chicago Biomedical Consortium 9th annual Symposium Chicago, IL.
- Gordon Research Conference for Analytical Biosensors New London, NH.
- IBC Antibody Engineering Annual Conference San Diego, CA.
- Biodetection Technologies Conference Baltimore, MD.

- Essential Protein Engineering Summit Boston, MA.

ORAL PRESENTATION: 2006

- Characterization of Bovine Uterocalin -46th Annual Bovine Mastitis Researcher Conference Chicago, IL.

TEACHING EXPERIENCE: 2008-2013

- Microbiology Laboratory Bios 351 (2 semesters)
- Cell Biology Laboratory Bios 223 (5 semesters)
- Mentor for four undergraduate students

AWARDS 2014

- Teaching Excellence Award in Cell Biology Laboratory

VOLUNTEER EXPERIENCE: 2006-2014

- Science Fair Judge at Undergraduate Research Symposiums and High School Programs
- 20th Annual Chicago Cares Serve-a-thon
- Organizer for High School Field Trips to UIC
- Volunteer for National Special Olympics